

STRUCTURE AND SOLVATION IN NICKEL CATION COMPLEXES
DETERMINED BY INFRARED PHOTODISSOCIATION SPECTROSCOPY

by

RICHARD SHERIDAN WALTERS

(Under the Direction of Michael A. Duncan)

ABSTRACT

Nickel cation complexes, $\text{Ni}^+(\text{H}_2\text{O})_n$ and $\text{Ni}^+(\text{C}_2\text{H}_2)_n$, are produced in a laser vaporization pulsed nozzle source, size-selected, and studied by infrared photodissociation spectroscopy. Beginning with $n = 3$, the ion-molecule complexes fragment by ligand elimination in the region of the OH and CH stretching fundamentals, respectively. Rare gas atoms are attached to the small complexes ($n = 1-3$) to enhance photodissociation, and these mixed clusters fragment by losing the rare gas atoms. Dissociation is more efficient on resonance, thus monitoring the fragment ion yield as a function of laser wavelength produces the infrared photodissociation (IRPD) spectrum of the complex that has been size-selected. Vibrational bands shifted away from the free molecule fundamentals in both systems are attributed to the nickel cation-ligand interactions. The structures of the small complexes ($n = 1-4$) are determined by comparing the experimental vibrational spectra to the predictions of Density Functional Theory (DFT). New red-shifted bands appearing at specific cluster sizes are attributed the onset of the second solvation sphere. Therefore, coordination numbers are determined for these gas

phase metal ion systems. For the hydrated nickel ions, the free OH stretches are no longer observed by $n = 7$, indicating complex hydrogen-bonded networks have formed. In the IRPD spectra of the larger $\text{Ni}^+(\text{H}_2\text{O})_n$ complexes, the separation between dangling OH vibrations suggest that inductive forces from the nickel cation continue to perturb the water monomers, even at the largest cluster size studied ($n = 30$). Comparison of IRPD spectra to DFT results confirms that π -complexes are formed for the $\text{Ni}^+(\text{C}_2\text{H}_2)_n$ complexes. Jahn-Teller effects are observed for the $n > 2$ cluster ions. Condensation reaction products are investigated with theory for the $n = 4$ and 5 complexes and found to be more stable than the unreacted species. The vibrational spectrum of the $\text{Ni}^+(\text{C}_2\text{H}_2)_4$ complex is consistent with an unreacted structure where all four acetylenes are intact and π -bonded to the nickel cation. The spectroscopy of the $n = 5, 6$ complexes seems to be consistent with the simple solvation of the $n = 4$ core. However, absolute structures cannot be assigned due to congestion in the CH region.

INDEX WORDS: Spectroscopy, Organometallics, Metal ion solvation, Metal ion- π complexes, Ion chemistry, Condensation reactions, Jahn-Teller, Infrared, Photodissociation, Density Functional Theory

STRUCTURE AND SOLVATION IN NICKEL CATION COMPLEXES
DETERMINED BY INFRARED PHOTODISSOCIATION SPECTROSCOPY

by

RICHARD SHERIDAN WALTERS

B.S., University of North Carolina at Wilmington, 1998

A Dissertation Submitted to the Graduate Faculty of The University of Georgia in
Partial Fulfillment of the Requirements for the Degree

DOCTOR OF PHILOSOPHY

ATHENS, GEORGIA

2005

© 2005

Richard Sheridan Walters

All Rights Reserved

STRUCTURE AND SOLVATION IN NICKEL CATION COMPLEXES
DETERMINED BY INFRARED PHOTODISSOCIATION SPECTROSCOPY

by

RICHARD SHERIDAN WALTERS

Major Professor: Michael A.
Duncan

Committee: Paul v.R. Schleyer
Charles R. Kutal
Henning Meyer

Electronic Version Approved:

Maureen Grasso
Dean of the Graduate School
The University of Georgia
May 2005

DEDICATION

I would first like to thank the Maker, the Prime Mover, through which all things are possible. Thank you for turning the crank and providing the initial energy to get this ball rolling. You have created a fascinating universe full of intricate details I never seem to tire of exploring. As a scientist, I find it hard not to observe the divine and be humbled by it. From the smallest of things to the very large, from the inanimate to life itself, your presence is there. Even though it maybe difficult to quantify or categorize, it exists and I thank you for it.

Never in my wildest dreams did I imagine becoming a chemist, which is perhaps the reason why it took so long for me to reach this point. I suppose some know at an early stage in life what they will aspire to; unfortunately I did not belong to that group of individuals. To put it bluntly and at the risk of being vulgar, I did not know my ass from my elbow for a significant period of time. Therefore, I would like to dedicate half this document to my parents, the best parents a man could have. Your patience must be limitless; I should know...I tried to find them.

The other half is reserved for my wife, Elizabeth. Words cannot describe how much you mean to me and how important you are in my life. I can weather any storm that blows my way as long as you are by my side. I love you. And for the boy-advice: strive to be kind, polite, and diligent, then trust in yourself and in that which cannot be observed and you will be rewarded.

ACKNOWLEDGEMENTS

It goes without saying that the gentleman most responsible for the information presented here is Professor Duncan. Mike has a unique and amazing ability to make the difficult seem easy by transforming the abstract into the mundane. He is both an accomplished scientist and an excellent communicator, and I feel privileged that he is my mentor and friend. We've had good days in the laboratory and better ones on the golf course. When he is not unraveling the mysteries of molecular spectroscopy, he is defying the laws of Newtonian physics on the tee box. How do you hit the golf ball so long and (sometimes) straight with that nasty-looking swing of yours? All joking aside, thank you Mike for the fun and informative years.

I have had the privilege of working with a number of fine and intelligent postdocs, each of which have made a lasting impression. Much thanks to Dr. Gilles Gregoire for his help with the OPO, the after-hour camaraderie, and letting me crash his flat on my Paris trip; many blessings to you, Claire and the new addition to your family. I would also like to thank Dr. Nick Walker for his friendship and the thought-provoking conversations we had while working together. Nick is one of the finest, most descent individuals I have ever met and I am a better person from knowing him. And to Deniz, the crazy Dutchman-one day Gonzaga will win it all.

In my five years at UGA I have had the pleasure of getting to know a number Duncan lab members who have helped me along the way. A special thanks to Dinesh for being a good friend and lab partner. I enjoyed the time spent bouncing ideas off

one another. May we never work on nickel cation again, Amen! The brothers Jaeger and I have had some fine times in the lab, after hours, and chasing the round-ball across rolling hills. Tim has always helped lighten the load...(that's 'Lock and Load' to you Tim). I would also like to thank Chris and Karen Molek for the fine food after the boy was born and their friendship. And to Brian...you know the Big Ten can't compete with SEC football. Finally I come to Joe Velasquez, a connoisseur of the many finer things in life. I am sorry our times did not overlap more, should we blame Frank or Condon? I will miss our conversations and do not envy your position. If you get anything done besides fixing broken (a.k.a. Continuum) lasers, consider yourself blessed. Good luck to all of you.

I wouldn't be much of a friend if I didn't thank Archer Smith. Aside from my wife, Elizabeth, my closest comrade for the past five years has been Arch. We've both worked hard and played hard, and I am glad to call you my friend. Good luck in San Francisco, I know we will keep in touch. Last but certainly not least I would like to thank Greg Greives. When I first arrived at graduate school I knew I wanted to join the Duncan group to work with molecular beams and pulsed lasers. What I didn't know was that I would end up learning the details from an exceptional teacher. Greg is an intelligent and extremely patient individual, two qualities that will serve him well in his academic pursuits. The work presented in the following pages would not have been accomplished without his help, thanks Greg.

TABLE OF CONTENTS

	Page
CHAPTER	
I INTRODUCTION	1
II EXPERIMENTAL.....	42
III STRUCTURE AND SOLVATION DYNAMICS IN HYDRATED NICKEL CATION COMPLEXES	60
IV VIBRATIONAL SPECTROSCOPY OF NICKEL CATION- ACETYLENE COMPLEXES: A STUDY OF METAL ION-II BONDING.....	105
V INVESTIGATIONS OF INTRACLUSTER CHEMISTRY IN NICKEL CATION-ACETYLENE COMPLEXES	156
VI CONCLUSIONS.....	202

CHAPTER I

INTRODUCTION

Molecules containing metal ions are ubiquitous throughout the terrestrial, stellar and interstellar environments. These complexes play fundamental roles in traditional organometallic chemistry, catalysis, biological processes, and atmospheric and astrophysical chemistry. Unsaturated hydrocarbons bound to transition metal clusters,^{1,2} pure metal³ and metal oxide surfaces^{4,5} have been studied extensively in the past, as these systems are key to understanding the details of heterogeneous catalytic processes that produce a variety of substances available for human consumption. The active sites of proteins contain metal clusters that dictate their structure and function,^{6,7} and selective metal ion transport through cell membranes is thought to be caused by the delicate balance between electrostatic and covalent forces at play in metal ion solvation.^{8,9} Meteor ablation into the earth's stratosphere deposits copious quantities of metal ions, which then drive many atmospheric chemical reactions.¹⁰⁻¹² The brilliant display recently observed from the impact of Shoemaker-Levy 9 on the planet Jupiter¹³ included light emitted from metal ions formed during or directly after the impact event. Pure metals and metal aggregates, such as metal-carbides and metal-polyatomic aromatic hydrocarbon (PAH) complexes, are thought to be seed material for condensation reactions in the stellar and interstellar media.¹⁴⁻¹⁷ Probing physical phenomena at the metal ion-molecule interface is therefore vital to

our understanding of the aforementioned processes. Gas phase metal ion-molecular complexes produced, isolated and examined under vacuum serve as tractable models to study the details of metal ion-ligand bonding and the dynamics of metal ion solvation. Physical measurements of these complexes are essential to test the validity of current quantum chemical calculations, some of which are known to have problems computing the potential energy surfaces of open-shell radical species.¹⁸ This work focuses on the infrared spectroscopic study of the nickel cation bound to water and acetylene molecules to elucidate their various structures, determine coordination numbers, and observe the solvation dynamics in these gas phase systems. The experimental spectra are compared to the results of density functional theory (DFT) which provide key insights into the nature of the chemical interactions in these novel metal ion complexes.

The generation of gas phase ions has a rich history dating back more than fifty years, therefore, the following paragraphs are not intended as a complete description of this area, but will only touch on the advantages and limitations of specific ion sources as they relate to the present study. Electron impact ionization (EI) has been used extensively in the past to produce molecular and radical ions from volatile materials.^{19,20} Although this process is quite efficient for some systems, weakly bound electrostatic and van der Waals complexes are difficult to produce by this technique due to extensive fragmentation. Even for the strongly bound systems, high electron voltages are usually required to produce the large ion quantities necessary for further study. The higher energies can fragment the ions of interest or heat them internally, which is undesirable in spectroscopy experiments. Hot sources may

produce ions in many different excited states, leading to broad optical spectra that contain a limited amount of discreet information. An alternative to EI is the ‘soft’ chemical ionization (CI) method, which takes advantage of charge transfer processes during collisions.^{21,22} Although CI produces less fragmentation, it is often limited to systems where the energetics and ionization energies are already known.

Additionally, the collisions can excite the ions of interest into specific states. While this has led to a rich area of research into the dynamics and kinetics of these processes, it often obscures the spectroscopy of the ions in their ground state.

Electron impact ionization has also been used in conjunction with pulsed gas valves to take advantage of the resulting supersonic expansion.²³⁻²⁸ It is well known that when a high-pressure gas expands into a lower pressure regime, the gas molecules ‘cool’ as their internal energies are converted to translational energies. Therefore many groups have incorporated pulsed molecular beam valves to cool the ions generated by electron impact ionization. In some cases, ionization occurs downstream, which warms the ions back up. Recent advances have been made to focus the electron beam in the throat of the expansion, taking more advantage of the cooling process.²³⁻²⁸ However, ions produced this way are still within the evaporative ensemble limit, that is, they cool by evaporating off rare gas atoms or molecular units until their internal energies are less than the cluster’s dissociation energy. EI and CI processes also share a common disadvantage which is pertinent to the present study. Both sources are limited to materials that have high vapor pressures or low melting points, therefore the generation of transition metal ions is not possible with the two techniques, unless there is a volatile metal complex precursor.

One method for producing gas phase ions from high refractory materials is to use electrical discharge sources.^{20,22} These sources can produce metal atom and clusters of metals in a continuous beam of ions. However, the instantaneous ion densities are somewhat low and their internal energies are high, making spectroscopic measurements difficult. A number of groups have incorporated a discharge source with a pulsed nozzle source to produce ions and then cool them in the supersonic expansion.²⁹⁻³¹ Spectroscopic analysis of ions produced this way have shown that the cooling process is rather mild and the ions retain a considerable amount of internal energy. Also, discharge sources are limited to substances that are highly conductive. While this is not a problem for transition metals, other substances, like semiconductor and carbon cluster ions (another area of interest in our research group), cannot be efficiently generated with electrical discharge sources.

Gas phase metal ions can also be produced using electrospray sources, which are efficient at producing multiply charged species.³²⁻³⁴ Briefly, ions are produced in solution and then injected through a charged capillary into the vacuum chamber. The highly charged droplets that are formed evaporate by coulomb repulsion leaving the charged chemical species behind. The advantage of this technique is that it can produce metal ions in their nascent condensed phase oxidation states. All the ion sources described previously typically produce singly charged species because small, highly charged ions generated directly in vacuum environments fragment into two or more singly charged species. The advantage of electrospray is that the multiply charged ions are first produced in solution, where solvent molecules can stabilize

them. Unfortunately ions produced by electrospray are internally excited, making them unattractive candidates for spectroscopic studies.

Matrix Assisted Laser Desorption Ionization (MALDI) is a method used to generate large molecules in the gas phase.³⁵⁻³⁷ This source produces ions with very little fragmentation and is commonly used for mass spectrometry studies on biomolecules. The molecules are embedded in a matrix and put under vacuum where the sample is irradiated with a low fluence laser. The matrix absorbs the light and the molecules of interest are desorbed and ionized without extensive fragmentation. Another laser-based technique uses a high powered pulsed laser focused onto a solid target, which ignites a plasma and vaporizes the material directly without the need for heating.³⁸⁻⁴² The laser vaporization source was initially used to study neutral metal clusters, but virtually any solid material capable of igniting a plasma can be studied, including semiconductors and amorphous carbon or graphite. Because neutral species were first generated with the laser ablation method, photoionization or EI was used to ionize the clusters for mass spectrometry studies. As described previously, downstream ionization typically heats the clusters internally, causing their optical spectra to be broad and obscure.

While MALDI and laser vaporization sources have an advantage over other ionization methods by producing virtually any gas phase molecular species, they suffer from the same limitation in that the ions are internally heated when they are produced. Coupling the laser vaporization technique with a pulsed nozzle source has recently been shown to produce internally cold metal ion complexes in the gas phase.^{38-50, 67-72} Metal ion-ligand species are also easily formed by introducing the

ligand molecules in the expansion gas. Another advantage of the laser ablation-pulsed nozzle source is that it produces relatively large ion densities. The production of large quantities of internally cold ions makes the laser vaporization-pulsed nozzle cluster source an ideal method for generating metal ion complexes for spectroscopic studies.

Gas phase metal cluster ions and metal ion-ligand complexes have been studied extensively in the past using a number of different mass spectrometry techniques.³⁸⁻⁵⁰ The earlier work focused on their thermodynamics and reactivities.³⁸⁻⁴⁶ More recently, equilibrium mass spectrometry,⁴⁷ collision-induced dissociation,⁴⁸ and radiative association measurements^{49,50} have been employed to determine binding energies and coordination numbers for a variety of different systems. Paralleling advances made on the experimental front, quantum chemical calculations have improved and a number of groups have studied metal-containing complexes with theory.⁵¹⁻⁵⁸ Fixed frequency photodissociation studies of metal ion complexes provide information on fragmentation pathways, stable core complexes and, sometimes, photochemistry and charge transfer processes.^{42, 59, 60} However, mass spectrometry and photodissociation experiments do not reveal any structural information of these novel metal-containing molecules. Optical spectroscopy is necessary to obtain the structural information.

In general, absorption measurements are problematic for gas phase complexes due to the low sample densities inherent to molecular beams. Therefore, direct absorption spectroscopy is often not possible and a variety of ‘action’ spectroscopies using high intensity laser sources are employed instead.⁶¹ These

include Laser-Induced Florescence (LIF) spectroscopy,⁶² Photoelectron Spectroscopy (PES),^{63,64} Photoionization spectroscopy of neutrals,⁶⁵⁻⁶⁹ Resonance Enhanced Photodissociation (REPD) electronic spectroscopy,⁷⁰⁻⁷⁷ Mass Analyzed Threshold Ionization (MATI) spectroscopy⁷⁸ and Zero Electron Kinetic Energy (ZEKE) photoelectron spectroscopy.⁷⁹⁻⁸⁴ The majority of these studies have been in the ultraviolet and visible (UV-Vis) region for two reasons: the spectroscopy of metal atoms attached to rare gas atoms or small molecules have transitions very near the well known metal atomic bands, and these transitions are accessible with tunable dye lasers and Optical Parametric Oscillator (OPO) laser systems.

The early studies on metal ion complexes using electronic REPD spectroscopy focused on the main group metals that have strong $P \leftarrow S$ transitions. Our group,⁷⁰⁻⁷¹ Fuke and coworkers,⁷² as well as Kleiber and coworkers⁷³ have used this technique to study Mg^+ and Ca^+ bound to small molecules such as N_2 , CO_2 , H_2O , C_2H_2 , C_2H_4 and CH_3OH . Farrar and coworkers⁷⁴ and the Velagrakis group⁷⁵ have made similar measurements on strontium complexes. Electronic spectroscopy of Al^+ -ligand complexes has recently been accomplished using vacuum UV generation to access the $P \leftarrow S$ aluminum atomic transition.⁷³ Brucat and coworkers⁷⁶ and, more recently, the Metz group⁷⁷ have applied electronic photodissociation spectroscopy to study transition metal ion-molecule complexes. Optical excitation of the transition metal ions correspond to excitation to higher electronic states which involve d-orbital electrons.

Although much information has been gained from these electronic studies, they are not without their limitations. Most transition metal complexes as well as

molecules containing multiple ligands cannot be studied by electronic spectroscopy as these clusters predissociate upon excitation. Predissociation leads to broad, featureless spectra that contain no discrete vibrational information. Also, excitation with a high energy photon can lead to photochemistry in some of these systems which is interesting to observe, but also obscures the spectroscopy. Therefore, excited state structures and energies have been determined for a few metal ions complexed to rare gas atoms or small molecules, but structural information on these complexes in their electronic ground states is limited. MATI and ZEKE spectroscopies of metal-ligand complexes, which accurately measure the IPs of the neutral species, have also revealed some ground state information on the ions.⁷⁸⁻⁸⁴ Our group used these techniques to study the Al^+Ar ⁷⁸ and $\text{Al}^+\text{H}_2\text{O}$ ⁷⁹ complexes and Blake and coworkers have studied $\text{Na}^+\text{H}_2\text{O}$ this way.⁸² More recently, Yang and coworkers have extended these experiments to a variety of metal-ligand complexes.⁸⁴ But ZEKE and MATI spectroscopies are also limited because only the low frequency metal-ligand vibrations can be observed for the ions. It is clear then that infrared spectroscopy is necessary to obtain ground state structural information on transition metal ion complexes as well as species containing multiple ligands.

Infrared photodissociation (IRPD) spectroscopy of metal-ligand complexes was first shown to be possible using line-tunable CO_2 lasers.⁸⁵⁻⁹¹ These earlier studies were severely limited due to the narrow spectral range of the laser source (9-11 μm). Recent advances in infrared lasers have provided tunable light sources that cover wider spectral regions. Free electron lasers have been developed which produce tunable light in the fingerprint region (200-1800 cm^{-1}). Our group has used the

intense output of a free electron laser to acquire vibrational information on neutral metal-carbides and metal-oxides via thermionic emission.⁹² This light source has also been applied to Infrared Resonance Enhanced Multiphoton Photoassociation (IR-REMPD) experiments. Our group⁹³ and Meijer and coworkers⁹⁴ have used this technique to study various metal ion-ligand complexes. Recently, Maitre and coworkers have used a similar laser to study Fe^+ complexed to small hydrocarbon molecules and ether this way.⁹⁵ However, free electron lasers are expensive to operate and the spectral resolution of the output is rather broad, usually greater than 20 cm^{-1} .

Benchtop Optical Parametric Oscillator and Amplifier (OPO/OPA) systems have recently been developed, which produce tunable IR light in the $2050 - 4500\text{ cm}^{-1}$ region. Many groups have used an OPO/OPA laser to study pure molecular complexes via Infrared Photodissociation (IRPD) spectroscopy.^{27, 96-102} Lisy and coworkers were the first to apply this technique to molecules containing alkali and alkali earth metal ions,¹⁰³ and the Inokuchi group has studied similar complexes this way.¹⁰⁴ These groups use an oven source to produce the gas phase metal complexes, which is limited to low melting metals. Our group was the first to apply IRPD spectroscopy to transition metal ion complexes.¹⁰⁵⁻¹⁰⁹ The coupling of an IR OPO/OPA system to a laser vaporization source has proven to be a powerful technique, and we have used it to acquire the vibrational spectra of a variety of metal ions complexed to carbon dioxide,¹⁰⁵ nitrogen,¹⁰⁶ water,¹⁰⁷ acetylene¹⁰⁸ and benzene.¹⁰⁹ The main advantage of IRPD is that excitation occurs from the ground state, which allows structural information to be directly determined. Additionally,

the low energy IR photons do not, in general, initiate any photochemistry. Therefore, multiple ligand complexes can be studied and coordination numbers can be determined for the gas phase metal ion systems.

Infrared photodissociation studies are not without their limitations however.¹¹⁰ The ion-molecule complexes must dissociate on the timescale of the experiment in order to acquire their IRPD spectra. Energy absorbed in the ligand vibrational coordinates is transferred to the M⁺-ligand coordinate, the weakest chemical bond, via intramolecular vibrational redistribution (IVR). If the absorbed energy is greater than the metal ion-ligand bond strength, the complex will fragment by ligand elimination. Relatively large complexes have many different modes for the energy to transfer into, which leads to longer lifetimes. Therefore, the larger complexes might not dissociate on the experimental timescale, preventing the acquisition of their IRPD spectra. Conversely, IRPD spectroscopy of the smaller complexes is difficult because their binding energies are, in general, greater than the energy of a single IR photon and they have lower state densities.¹¹⁰ Strongly-bound complexes might dissociate if they absorb multiple IR photons, but multiphoton absorption is inefficient for the small complexes due to the loss of resonance at higher vibrational levels.⁸⁶ As more ligands are attached to the metal cation, dissociation energies decrease, but the interactions may still be greater than the energy of a single IR photon. Eventually all the sites around the metal ion will fill and additional ligands must attach to existing ligands in the second solvation layer. The solvent molecules are expected to have binding energies similar to the pure molecular dimers. In most cases, the excitation

energy is greater than the solvent bond energies and the complexes dissociate efficiently via a one photon process.¹¹⁰

In order to acquire the IRPD spectra of the smaller, more strongly bound complexes, we employ the rare gas ‘tagging’ technique. The Y. T. Lee group was one of the first to enhance infrared photodissociation by attaching weakly bound messenger molecules (H_2 or N_2).⁹⁶ It is now more common to attach rare gas (RG) atoms to the complexes of interest, and many groups have utilized this technique to study pure molecular clusters.^{27, 97-102} Our group¹⁰⁵⁻¹¹⁰ and others^{103, 104} have used this technique to study the more strongly bound metal ion-molecule complexes. For these systems, the rare gas atoms normally bind to the metal cation by a charge-induced dipole interaction which is much weaker than the metal ion-ligand bond. Therefore, the tagged complexes have lower binding energies and higher state densities than the corresponding pure complexes and are easier to dissociate. Vibrational excitation is transferred to the M^+ -RG coordinate via IVR and the tagged complexes dissociate by losing the rare gas atoms. Because the RG atoms are bound to the metal ion and do not, in general, interact with the chromophore, the IRPD action spectra of the tagged complexes provide the best possible approximation to the IR absorption spectra of the corresponding pure complexes.

The work presented here focuses on the IRPD spectroscopy of $Ni^+-(water)_n$ and $Ni^+-(acetylene)_n$ complexes as prototypical studies of gas phase metal ion solvation and metal ion- π complexes. The rare gas tagging technique is employed in order to acquire the spectra of the small cluster ions. Vibrational excitation for $Ni^+(H_2O)_n$ and $Ni^+(C_2H_2)_n$ occurs in the region of the O-H and C-H stretching

fundamentals,¹¹¹ respectively. Spectral shifts are observed and attributed to the nickel ion-ligand interaction. Comparison of experimental spectra to density functional theory (DFT) provides significant insight into the nature of these interactions and the structures of the smaller complexes are determined. Fragmentation patterns and the onset of surface IR bands indicate when the nickel coordination sites are filled for these gas phase systems.

References

- (1) Heck, R. F. *Organotransition Metal Chemistry*; Academic Press: New York, 1974.
- (2) Jolly, P. W.; Wilke, G. *The Organic Chemistry of Nickel*; John Wiley: New York, 1974.
- (3) Somorjai, G. A. *Introduction to Surface Chemistry and Catalysis*; John Wiley: New York, 1994.
- (4) Henrich, V.E.; Cox, P.A. *The Surface Science of Metal Oxides*, Royal Society of Chemistry, Cambridge, 1994.
- (5) *The Surface Science of Metal Oxides*, Faraday Discussions of the Royal Society of Chemistry, Cambridge, 1999.
- (6) *Iron-Sulfur Proteins*; Academic Press: San Diego, 1999.
- (7) a) Walters, E. M.; Johnson, M. K. *Photosynthesis Research* **2004**, 79, 249.
b) Jameson, G. N. L.; Walters, E. M.; Manieri, W.; Schuermann, P.; Johnson, M. K.; Huynh, B. H. *J. Am. Chem. Soc.* **2003**, 125, 1146.
- (8) a) Ma, J.C.; Dougherty, D.A. *Chem. Rev.* **1997**, 97, 1303. b) Dougherty, D.A. *Science* **1996**, 271, 163.
- (9) Krumpf, R.A.; Dougherty, D.A. *Science*. **1993**, 261, 1708.
- (10) Plane, J.M.C.; *Int. Rev. Phys. Chem.* **1991**, 10, 55.
- (11) a) Gardner, J.A.; Viereck, R.A.; Murad, E.; Knecht, D.J., Pike, C.P.; Broadfoot, A.L.; Anderson, E.R. *Geophys. Res. Lett.* **1995**, 22, 2119. b) McNeil, W.J.; Lai, S.T., Murad, E. *J. Geophys. Res.* **1996**, 101, 5251. c) Viereck, R.A.; Murad, E.; Lai, S.T.; Knecht, D.J.; Pike, C.P.; Gardner, J.A.;

- Broadfoot, A.L.; Anderson, E.R.; McNeil, W.J. *Adv. Space Res.* **1996**, *18*, 61.
- d) McNeil, W.J.; Lai, S.T.; Murad, E. *J. Geophys. Res.* **1998**, *103*, 10899.
- (12) Lyons, J.R. *Science*. **1995**, *267*, 648.
- (13) Noll, K.S.; McGrath, M.A.; Trafton, L.M.; Atreya, S.K.; Caldwell, J.J, et al. *Science*. **1995**, *267*, 1307.
- (14) Millar, T.J.; Williams, D.A., eds. *Dust and Chemistry in Astronomy*, Institute of Physics, London, 1993.
- (15) Henning, T.; *Chem. Soc. Rev.* **1998**, *27*, 315.
- (16) a) Chaudret, B.; Le Beuze, A.; Rabaa, H.; Saillard, J.Y.; Serra, G. *New J. Chem.* **1991**, *15*, 791. b) Serra, G.; Chaudret, B.; Saillard, J.Y.; Le Beuze, A.; Rabaa, H.; Ristorcelli, I.; Klotz A. *Astron. Astrophys.*, **1992**, *260*, 489. c) Marty, P.; Serra, G.; Chaudret, B.; Ristorcelli, I. *Astron. Astrophys.* **1994**, *282*, 916. d) Klotz, A; Marty, P.; Boissel, P.; Serra, G.; Chaudret, B.; Daudey, J.P. *Astron. Astrophys.* **1995**, *304*, 520. e) Klotz, A; Marty, P.; Boissel, P.; De Caro, D.; Serra, G.; Mascetti, J.; De Parseval, P.; Derouault, J.; Duadey, J.P.; Chaudret, B. *Planet. Space Sci.* **1996**, *44*, 957
- (17) Patrie, S.; Becker, H.; Baranov, V.; Bohme, D.K. *Astrophys. J.* **1997**, *476*, 191.
- (18) Cramer, C. J. *Essentials of Computational Chemistry*, John Wiley, London, 2002.
- (19) Massey, H.S.W. *Electron Collisions with Molecules and Photoionization*, Oxford University Press, Oxford, 1969.

- (20) Johnstone, R.A.W.; Rose, M. E. *Mass Spectrometry for Chemists and Biochemists*, Cambridge University Press, 1996.
- (21) Setser, D.W., ed. *Reactive Intermediates in the Gas Phase*, Academic, New York, 1979.
- (22) Blausen, B.D., ed. "Chemical Reactions in Electrical Discharges" *Advances in Chemistry Series No. 80*, Am. Chem. Soc., 1969.
- (23) a) Johnson, M.A.; Alexander, M.L.; Lineberger, W.C. *Chem. Phys. Lett.* **1984**, *112*, 285. b) Johnson, M.A.; Lineberger, W.C. *Tech. Chem. (Tech. Study Ion-Mol. React.)* **1988**, *20*, 591. c) Vorsa, V.; Campagnola, P.J.; Nandi, S.; Larsson, M.; Lineberger, W.C. *J. Chem. Phys.* **1995**, *105*, 2298. d) Vorsa, V.; Nandi, S.; Campagnola, P.J.; Larsson, M.; Lineberger, W.C. *J. Chem. Phys.* **1997**, *106*, 1402. e) Sanov, A.; Sanford, T.; Nandi, S.; Lineberger, W.C. *J. Chem. Phys.* **1999**, *111*, 664.
- (24) a) Hendricks, J.H.; de Clercq, H.L.; Lyapustina, S.A.; Bowen, K.H. *J. Chem. Phys.* **1997**, *107*, 2962. b) Lee, G.H; Arnold, S.T.; Eaton, J.G.; Bowen, K.H. *Chem. Phys. Lett.* **2000**, *321*, 333.
- (25) a) Klapstein, Dieter; Leutwyler, Samuel; Maier, John P. *Chem. Phys. Lett.* **1981**, *84*, 534. b) King, M. A.; Klapstein, D.; Kroto, H. W.; Maier, J. P.; Nixon, J. F. *J. Mol. Struct.* **1982**, *80*, 23. c) Ruchti, T.; Rohrbacher, A.; Speck, T.; Connelly, J.P.; Bieske, E.J.; Maier J.P. *Chem. Phys.* **1996**, *209*, 169. d) Speck, Thomas; Linnartz, Harold; Maier, John P. *J. Chem. Phys.* **1997**, *107*, 8706. e) Linnartz, Harold; Speck, Thomas; Maier, J. P. *Chem.*

- Phys. Lett.* **1998**, 288, 504. f) Dopfer, Otto; Roth, Doris; Maier, John P. *J. Am. Chem. Soc.* **2002**, 124, 494.
- (26) a) Xu, C.; Burton, G.R.; Taylor, T.R.; Neumark, D.M. *J. Chem. Phys.* **1997**, 107, 3428. b) Asmis, K.R.; Taylor, T.R.; Xu, C.; Neumark, D.M. *J. Chem. Phys.* **1998**, 109, 4389. c) Lehr, L.; Zanni, M.T.; Frischkorn, C.; Weinkauf, R.; Neumark, D.M. *Science*. **1999**, 284, 635. d) Lenzer, T.; Furlanetto, M.R.; Pivonka, N.L.; Neumark, D. *J. Chem. Phys.* **1999**, 110, 6714. e) Greenblatt, B.J.; Zanni, M.T.; Neumark, D.M. *J. Chem. Phys.* **1999**, 111, 10566. f) Greenblatt, B.J.; Zanni, M.T.; Neumark, D.M. *J. Chem. Phys.* **2000**, 112, 601. g) Zanni, M.T.; Frischkorn, C.; Davis, A.V.; Neumark, D.M. *J. Phys. Chem. A* **2000**, 104, 2527.
- (27) a) Ayotte, P.; Bailey, C.G.; Kim, J.; Johnson, M.A. *J. Chem. Phys.* **1998**, 108, 444. b) Ayotte, P.; Weddle, G.H.; Kim, J.; Johnson, M.A. *J. Am. Chem. Soc.* **1998**, 120, 12361. c) Ayotte, P.; Weddle, G.H.; Bailey, C.G.; Johnson, M.A.; Vila, F.; Jordan, K.D. *J. Chem. Phys.* **1999**, 110, 6268. d) Ayotte, P.; Weddle, G.H.; Johnson, M.A. *J. Chem. Phys.* **1999**, 110, 7129. e) Ayotte, P.; Kim, J.; Kelley, J.A.; Nielson, S.B.; Johnson, M.A. *J. Am. Chem. Soc.* **1999**, 121, 6950. f) Ayotte, P.; Nielson, S.B.; Weddle, G.H.; Johnson, M.A.; Xantheas, S.S. *J. Phys. Chem. A* **1999**, 103, 10665. g) Nielson, S.B.; Ayotte, P.; Kelley, J.A.; Weddle, G.H.; Johnson, M.A. *J. Chem. Phys.* **1999**, 111, 10464.
- (28) a) Johnson, M.S.; Kuwata, K.T.; Wong, C.K.; Okumura, M. *Chem. Phys. Lett.* **1996**, 260, 551. b) Choi, J.H.; Kuwata, K.T.; Cao, Y.B.; Okumura, M. *J. Phys. Chem. A* **1998**, 102, 503.

- (29) a) Corderman, R.R.; Lineberger, W.C. *Annu. Rev. Phys. Chem.* **1979**, *30*, 347.
 b) Neumark, D.M.; Lykke, K.R.; Anderson, T.; Lineberger, W.C. *J. Chem. Phys.* **1985**, *83*, 4364. c) Leopold, D.; Ho, J.; Lineberger, W.C. *J. Chem. Phys.* **1987**, *86*, 1715. d) Ervin, K.M.; Ho, J.; Lineberger, W.C. *ibid.* **1989**, *91*, 5974. e) Ho, J.; Ervin, K.M.; Lineberger, W.C. *ibid.* **1990**, *93*, 6987.
- (30) a) a) Woods, R. Claude; Dixon, Thomas A.; Saykally, Richard J.; Szanto, Peter G. *Phys. Rev. Lett.* **1975**, *35*, 1269. b) Rosenbaum, Neil H.; Owrutsky, Jeffrey C.; Tack, Leslie M.; Saykally, Richard J. *J. Chem. Phys.* **1986**, *84*, 5308. c) Hovde, David C.; Saykally, Richard J. *J. Chem. Phys.* **1987**, *87*, 4332. d) Coe, J.V.; Saykally, R.J. in *Ion and Cluster Ion Spectroscopy and Structure*, Maier, J.P., ed., Elsevier, Amsterdam, **1989**, 131. e) Petek, H.; Nesbitt, D. J.; Owrutsky, J. C.; Gudeman, C. S.; Yang, X.; Harris, D. O.; Moore, C. B.; Saykally, R. J. *J. Chem. Phys.* **1990**, *92*, 3257. f) Michael, E. A.; Keoshian, C. J.; Anderson, S. K.; Saykally, R. J. *J.Mol. Spec.* **2001**, *208*, 219.
- (31) a) Linnartz, H.; Motylewski, T.; Vaizert, O.; Maier, J. P.; Apponi, A. J.; McCarthy, M. C.; Gottlieb, C. A.; Thaddeus, P. *J. Mol. Spec.* **1999**, *197*, 1.
 b) Tulej, M.; Guethe, F.; Schnaiter, M.; Pachkov, M. V.; Kirkwood, D. A.; Maier, J. P.; Fischer, G. *J. Phys. Chem. A* **1999**, *103*, 9712. c) Pfluger, D.; Motylewski, T.; Linnartz, H.; Sinclair, W. E.; Maier, J. P. *Chem. Phys. Lett.* **2000**, *329*, 29. d) Birza, P.; Motylewski, T.; Khoroshev, D.; Chirokolava, A.; Linnartz, H.; Maier, J. P. *Chem. Phys.* **2002**, *283*, 119. e) Schmidt, T. W.; Ding, H.; Boguslavskiy, A. E.; Pino, T.; Maier, J. P. *J. Phys. Chem. A* **2003**,

- 107, 6550. f) Khoroshev, Dmitriy; Araki, Mitsunori; Kolek, Przemyslaw; Birza, Petre; Chirokolava, Andrei; Maier, John P. *J. Mol. Spec.* **2004**, 227, 81.
- (32) a) Dzidic, I.; Kebarle, P. *J. Phys. Chem.* **1970**, 74, 1466. b) Kabarle, P. *Ann. Rev. Phys. Chem.* **1977**, 28, 445. c) Ikonomou, M.G.; Sunner, J.; Kebarle, P. *J. Phys. Chem.* **1988**, 92, 6308. d) Jayaweera, P.; Blades, A.T.; Ikonomou, M.G.; Kebarle, P. *J. Am. Chem. Soc.* **1990**, 112, 2452. e) Blades, A.T.; Jayaweera, P.; Ikonomou, M.G.; Kebarle, P. *Int. J. Mass Spectrom. Ion Proc.* **1990**, 101, 325. f) Peschke, M.; Blades, A.T.; Kebarle, P. *J. Phys. Chem. A* **1998**, 102, 9978. g) Nielsen, S.B.; Masella, M.; Kebarle, P. *J. Phys. Chem. A* **1999**, 103, 9891. h) Peschke, M.; Blades, A.T.; Kebarle, P. *J. Am. Chem. Soc.* **2000**, 122, 1492. i) Peschke, M.; Blades, A.T.; Kebarle, P. *Adv. Met. Semicond. Clusters.* **2001**, 5, 77.
- (33) a) Yamashita, M.; Fenn, J.B. *J. Phys. Chem.* **1984**, 88, 4451. b) Whitehouse, C.M.; Dreyer, R.N.; Yamashita, M. Fenn, J.B. *Anal. Chem.* **1985**, 57, 675. c) Fenn, J.B.; Mann, M.; Meng, C.K.; Wong, S.F.; Whitehouse, C.M. *Science.* **1989**, 246, 64. d) Fenn, J.B.; Mann, M.; Meng, C.K.; Wong, S.F.; Whitehouse, C.M. *Mass. Spectrom. Rev.* **1990**, 9, 37. e) Zhan, D.; Rosell, J.; Fenn, J.B. *J. Am. Soc. Mass Spectrom.* **1998**, 9, 1241.
- (34) a) Burns, T.D.; Spence, T.G.; Mooney, M.A.; Posey, L.A. *Chem. Phys. Lett.* **1996**, 258, 669. b) Spence, T.G.; Burns, T.D.; Posey, L.A. *J. Phys. Chem. A.* **1997**, 101, 139. c) Spence, T.G.; Burns, T.D.; Guckenberger, G.B.; Posey, L.A. *J. Phys. Chem. A.* **1997**, 101, 1081. d) Spence, T.G.; Trotter, B.T.;

- Burns, T.D.; Posey, *J. Phys. Chem. A* **1998**, *102*, 6101. e) Spence, T.G.; Trotter, B.T.; Posey, *J. Phys. Chem. A* **1998**, *102*, 7779. f) Spence, T.G.; Trotter, B.T.; Posey, *Int. J. Mass Spectrom.* **1998**, *177*, 187. g) Posey, L.A. *Adv. Met. Semicond. Clusters* **2001**, *5*, 145.
- (35) a) Ding, C.F.; Wang, X.B.; Wang, L.S. *J. Phys. Chem. A* **1998**, *102*, 8633. b) Li, X.; Wu, H.; Wang, X.B.; Wang, L.S. *Phys. Rev. Lett.* **1998**, *81*, 1909. c) Wang, L.S.; Ding, C.F.; Wang, X.B.; Nicholas, J.B. *Phys. Rev. Lett.* **1998**, *81*, 2667. d) Wang, X.B.; Ding, C.F.; Wang, L.S. *Phys. Rev. Lett.* **1998**, *81*, 3351. e) Wang, L.S.; Ding, C.F.; Wang, X.B.; Barlow, S.E. *Rev. Sci. Instrum.* **1999**, *70*, 1957. f) Wang, X.B.; Wang, L.S. *Nature* **1999**, *400*, 245. g) Li, X.; Wang, L.S. *J. Chem. Phys.* **1999**, *111*, 8389. h) Wang, X.B.; Wang, L.S. *Phys. Rev. Lett.* **1999**, *83*, 3402. i) Wang, X.B.; Ferris, K.; Wang, L.S. *J. Phys. Chem. A* **2000**, *104*, 25. j) Wang, L.S.; Wang, X.B. *J. Phys. Chem. A* **2000**, *104*, 1978. k) Wang, X.B.; Wang, L.S. *J. Am. Chem. Soc.* **2000**, *122*, 2339.
- (36) a) Karas, M.; Hillenkamp, F. *Int. J. Mass Spectrom. Ion Processes* **1987**, *78*, 53. b) Karas, M., et al. *Mass Spectrom. Rev.* **1991**, *10*, 335. c) Karas, M.; Hillenkamp, F. *Org. Mass. Spectrom.* **1993**, *28*, 1476. d) Bahr, U.; Karas, M.; Hillenkamp, F. *Fres. J. Anal. Chem.* **1994**, *348*, 783
- (37) a) Beavis, R.C.; Chait, B.T. *Rapid Commun. Mass Sp.* **1989**, *3*, 432. b) Beavis, R.C.; Chait, B.T. *Org. Mass. Spectrom.* **1992**, *27*, 156. c) Beavis, R.C. *Org. Mass. Spectrom.* **1992**, *27*, 653.
- (38) a) Tanaka, K., et al. *Rapid Commun. Mass Sp.* **1988**, *2*, 151. b) Tanka, K. *Angew. Chem. Int. Edit.* **2003**, *42*, 3861.

- (39) a) Dietz, T.G.; Duncan, M.A.; Powers, D.E.; Smalley, R.E. *J. Chem. Phys.* **1981**, *74*, 6511. b) Zheng, L.S.; Brucat, P.J.; Pettiette, C.L.; Yang, S.; Smalley, R.E. *J. Chem. Phys.* **1985**, *83*, 4273. c) Brucat, P.J.; Zheng, L.S.; Pettiette, C.L.; Yang, S.; Smalley, R.E. *J. Chem. Phys.* **1986**, *84*, 3078. d) Zheng, L.S.; Carner, C.M.; Brucat, P.J.; Yang, S.H.; Pettiette, C.L.; Craycraft, M.J.; Smalley, R.E. *J. Chem. Phys.* **1986**, *85*, 1681. e) Chesnovsky, O.; Yang, S.H.; Pettiette, C.L.; Craycraft, M.J.; Liu, Y.; Smalley, R.E. *Chem. Phys. Lett.* **1987**, *138*, 119. f) Yang, S.; Taylor, K.J.; Craycraft, M.J.; Conceicao, J.; Pettiette, C.L.; Chesnovsky, O.; Smalley, R.E. *Chem. Phys. Lett.* **1988**, *144*, 431. g) Chesnovsky, O.; Taylor, K.J.; Conceicao, J.; Smalley, R.E. *Phys. Rev. Lett.* **1990**, *64*, 1785. h) Jin, C.; Taylor, K.J.; Conceicao, J.; Smalley, R.E. *Chem. Phys. Lett.* **1990**, *175*, 17.
- (40) a) Heath J. R.; Cooksy A. L.; Gruebele M. H.; Schmittenmaer C. A.; Saykally R. J. *Science* **1989**, *244*, 564. b) Heath, J. R.; Sheeks, R. A.; Cooksy, A. L.; Saykally, R. J. *Science* **1990**, *249*, 895. c) Van Orden, A.; Giesen, T. F.; Provencal, R. A.; Hwang, H. J.; Saykally, R. J. *J. Chem. Phys.* **1994**, *101*, 10237. d) Van Orden, Alan; Saykally, Richard J. *Chem. Rev.* **1998**, *98*, 2313. e) Casaes, Raphael; Provencal, Robert; Paul, Joshua; Saykally, Richard J. *J. Chem. Phys.* **2002**, *116*, 6640.
- (41) a) Rohlfing, E. A.; Cox, D. M.; Kaldor, A. *Chem. Phys. Lett.* **1983**, *99*, 161. b) Rohlfing, E. A.; Cox, D. M.; Kaldor, A. *J. Phys. Chem.* **1984**, *88*, 4497. c) Rohlfing, E. A.; Cox, D. M.; Kaldor, A. *J. Chem. Phys.* **1984**, *81*, 3322. d) Trevor, D. J.; Whetten, R. L.; Cox, D. M.; Kaldor, A. *J. Am. Chem. Soc.*

- 1985**, *107*, 518. e) Cox, D. M.; Trevor, D. J.; Reichmann, K. C.; Kaldor, A. *J. Am. Chem. Soc.* **1986**, *108*, 2457. f) Trevor, D. J.; Cox, D. M.; Reichmann, K. C.; Brickman, R. O.; Kaldor, A. *J. Phys. Chem.* **1987**, *91*, 2598. g) Cox, D. M.; Reichmann, K. C.; Trevor, D. J.; Kaldor, A. *J. Chem. Phys.* **1988**, *88*, 111. h) Eberhardt, W.; Fayet, P.; Cox, D. M.; Fu, Z.; Kaldor, A.; Sherwood, R.; Sondericker, D. *Phys. Rev. Lett.* **1990**, *64*, 780. i) Heiz, U.; Sherwood, R.; Cox, D. M.; Kaldor, A.; Yates, J. T., Jr. *J. Phys. Chem.* **1995**, *99*, 8730.
- (42) a) Jacobson, D.B.; Freiser, B.S. *J. Am. Chem. Soc.* **1984**, *106*, 3900. b) Jacobson, D.B.; Freiser, B.S. *J. Am. Chem. Soc.* **1984**, *106*, 4623. c) Phelps, D.K.; Gord, J.R.; Freiser, B.S.; Weaver, M.J. *J. Phys. Chem.* **1991**, *95*, 4338. d) Huang, Y.; Freiser, B.S. *J. Am. Chem. Soc.* **1991**, *113*, 9418. e) Yeh, C.S.; Byun, Y.G.; Afzaal, S.; Kan, S.Z.; Lee, S.; Freiser, B.S.; Hay, P.J. *J. Am. Chem. Soc.* **1995**, *117*, 4042. f) Rufus, D.; Ranatunga, A.; Freiser, B.S. *Chem. Phys. Lett.* **1995**, *233*, 319. g) Jiao, C.Q.; Freiser, B.S. *J. Phys. Chem.* **1995**, *99*, 10723. h) Freiser, B.S. *Organometallic Ion Chemistry*. Kluwer, Dordrecht, 1996.
- (43) a) Tonkyn, R.; Weisshaar, J.C. *J. Phys. Chem.* **1986**, *90*, 2305. b) Tonkyn, R.; Weisshaar, J.C. *J. Am. Chem. Soc.* **1986**, *108*, 71280. c) Sappey, A.D.; Harrington, J.E.; Weisshaar, J.C. *J. Chem. Phys.* **1988**, *88*, 5243. d) Ritter, D.; Weisshaar, J.C. *J. Phys. Chem.* **1989**, *93*, 1576. e) Sanders, L.; Hanton, S.D.; Weisshaar, J.C. *J. Chem. Phys.* **1990**, *92*, 3485. f) Weisshaar, J.C. *Acc. Chem. Res.* **1993**, *26*, 213. g) Blomberg, M.; Yi, S.S.; Noll, R.J.;

- Weisshaar, J.C. *J. Phys. Chem. A* **1999**, *103*, 7254. h) Reichert, E.L.; Weisshaar, J.C. *J. Phys. Chem. A* **2002**, *106*, 5563.
- (44) a) Leuchtner, R. E.; Harms, A. C.; Castleman, A. W., Jr. *J. Chem. Phys.* **1990**, *92*, 6527. b) Guo, B. C.; Kerns, K. P.; Castleman, A. W., Jr. *Science* **1992**, *255*, 1411. c) Guo, B. C.; Castleman, A. W., Jr. *J. Am. Chem. Soc.* **1992**, *114*, 6152. d) Cartier, S. F.; May, B. D.; Castleman, A.W., Jr. *J. Am. Chem. Soc.* **1994**, *116*, 5295. e) Kerns, K. P.; Guo, B. C.; Deng, H. T.; Castleman, A. W., Jr. *J. Am. Chem. Soc.* **1995**, *117*, 4026. f) Kerns, K. P.; Guo, B. C.; Deng, H. T.; Castleman, A. W. Jr. *J. Phys. Chem.* **1996**, *100*, 16817. g) Vann, W. D.; Wagner, R. L.; Castleman, A. W. Jr. *J. Phys. Chem. A* **1998**, *102*, 1708. h) Zemski, K. A.; Justes, D. R.; Castleman, A. W., Jr. *J. Phys. Chem. B* **2002**, *106*, 6136.
- (45) a) Beyer, M.; Berg, C.; Görlitzer, H.W.; Schindler, T.; Achatz, U.; Albert, G.; Niedner-Schatteburg, G.; Bondybey, V.E. *J. Am. Chem. Soc.* **1996**, *118*, 7386. b) Beyer, M.; Achatz, U.; Berg, C.; Joos, S.; Niedner-Schatteburg, G.; Bondybey, V.E. *J. Phys. Chem. A* **1999**, *103*, 671. c) Bondybey, V.E.; Beyer, M.K. *Int. Rev. Phys. Chem.* **2002**, *21*, 277. d) Fox, B.S.; Balteanu, I.; Balaj, O.P.; Liu, H.; Beyer, M.K; Bondybey, V.E. *Phys. Chem. Chem. Phys.* **2002**, *4*, 2224. e) Berg C.; Achatz, U.; Beyer, M.; Joos, S.; Albert, G.; Schindler, T.; Niedner-Schatteburg, G.; Bondybey, V.E. *Int. J. Mass Spectrom.* **1997**, *167*, 723. f) Berg, C.; Beyer, M.; Achatz, U.; Joos, S.; Niedner-Schatteburg, G.; Bondybey, V.E. *Chem. Phys.* **1998**, *239*, 379.

- (46) a) Schalley, C.; Schroeder, D.; Schwarz, H. *Organometallics* **1995**, *14*, 316.
 b) Schwarz, J.; Heinemann, C.; Schwarz, H. *J. Phys. Chem.* **1995**, *99*, 11405.
 c) Schalley, C.A.; Wesendrup, R.; Schroeder, D.; Schwarz, H. *Organometallics* **1996**, *15*, 678. d) Schroeter, K.; Schalley, C.A.; Wesendrup, R.; Schroeder, D.; Schwarz, H. *Organometallics* **1997**, *16*, 986.
 e) Schroeder, D.; Kretzschmar, I.; Schwarz, H.; Rue, C.; Armentrout, P.B. *Inorg. Chem.* **1999**, *38*, 3474. f) Jackson, P.; Harvey, J.N.; Schroeder, D.; Schwarz, H. *Int. J. Mass Spectrom.* **2001**, *204*, 233. g) Schwarz, H. *Ang. Chem., Int. Ed.* **2003**, *42*, 4442.
- (47) a) Kemper, P.R.; Hsu, M.T.; Bowers, M.T. *J. Phys. Chem.* **1991**, *95*, 10600.
 b) Bushnell, J.E.; Kemper, P.R.; Maitre, P.; Bowers, M.T. *J. Am. Chem. Soc.* **1994**, *116*, 9710. c) Bushnell, J.E.; Kemper, P.R.; Bowers, M.T. *J. Phys. Chem.* **1995**, *99*, 15602. d) Kemper, P.R.; Weis, P.; Bowers, M.T. *Int. J. Mass Spectrom. Ion Proc.* **1997**, *160*, 17. e) Weis, P.; Kemper, P.R.; Bowers, M.T., *J. Phys. Chem. A* **1997**, *101*, 8207. f) Kemper, P.R.; Bushnell, J.; Bowers, M.T.; Gellene, G.I. *J. Phys. Chem. A* **1998**, *102*, 8590. g) Zhang, Q.; Kemper, P. R.; Shin, S. K.; Bowers, M. T. *Int. J. Mass Spectrom.* **2001**, *204*, 281. f) Zhang, Q.; Kemper, P.R.; Bowers, M.T. *Int. J. Mass Spectrom.* **2001**, *210*, 265. h) Manard, M.J.; Kemper, P.R.; Carpenter, C.J.; Bowers, M.T. *Int. J. Mass Spectrom.* **2005**, *241*, 99. i) Manard, M.J.; Kemper, P.R.; Bowers, M.T. *Int. J. Mass Spectrom.* **2005**, *241*, 109.
- (48) a) Aristov, N.; Armentrout, P. B. *J. Am. Chem. Soc.* **1986**, *108*, 1806. b) Georgiadis, R.; Armentrout, P. B. *Int. J. Mass Spectrom. Ion Proc.* **1989**, *89*,

227. c) Fisher, E. R.; Armentrout, P. B. *J. Phys. Chem.* **1990**, *94*, 1674. d) Chen, Y.M.; Armentrout, P.B., *Chem. Phys. Lett.* **1993**, *210*, 123. e) Clemmer, D. E.; Chen, Y.-M.; Aristov, N.; Armentrout, P. B. *J. Phys. Chem.* **1994**, *98*, 7538. f) Dalleska, N. F.; Honma, K.; Sunderlin, L. S.; Armentrout, P. B. *J. Am. Chem. Soc.* **1994**, *116*, 3519. g) Meyer, F.; Khan, F. A.; Armentrout, P. B. *J. Am. Chem. Soc.* **1995**, *117*, 9740. h) Sievers, M. R.; Jarvis, L. M.; Armentrout, P. B. *J. Am. Chem. Soc.* **1998**, *120*, 1891. i) Sievers, M. R.; Chen, Y.-M.; Haynes, C. L.; Armentrout, P. B. *Int. J. Mass Spectrom.* **2000**, *195*, 149. j) Shoeib, T.; Milburn, R.K.; Koyanagi, G.K.; Lavrov, V.V.; Bohme, D.K.; Siu, K.W.M.; Hopkinson, A.C. *Int. J. Mass Spectrom.* **2000**, *201*, 87. k) Koizumi, H.; Larson, M.; Muntean, F.; Armentrout, P. B. *Int. J. Mass Spectrom.* **2003**, *228*, 221.
- (49) Ho, Y.P.; Yang, Y.C.; Klippenstein, S.J.; Dunbar, R.C., *J. Phys. Chem. A* **1997**, *101*, 3338. Petrie, S.; Dunbar, R.C. *J. Phys. Chem. A* **2000**, *104*, 4480. Petrie, S. *J. Phys. Chem.* **2002**, *106*, 7034.
- (50) Schroeder, D.; Hrušák, J.; Hertwig, R.; Koch, W.; Schwerdtfeger, P.; Schwarz, H. *Organometallics* **1995**, *14*, 312. b) Stoeckigt, D.; Hrušák, J.; Schwarz, H. *Int. J. Mass Spectrom. Ion Proc.* **1995**, *149*, 1. c) Schroeder, D.; Schwarz, H.; Hrušák, J.; Pyykkoe, P. *Inorg. Chem.* **1998**, *37*, 624.
- (51) a) Sodupe, M.; Bauschlicher, C.W., Jr. *J. Phys. Chem.* **1991**, *95*, 8640. b) Bauschlicher, C.W., Jr.; Partridge, H.; Langhoff, S.R. *J. Phys. Chem.* **1992**, *96*, 3273. Sodupe, M.; Bauschlicher, C.W., Jr.; Langhoff, S.R. *J. Phys. Chem.* **1992**, *96*, 5350. Sodupe, M.; Bauschlicher, C.W.; Langhoff, S.R.; Partridge,

- H., *J. Phys. Chem.* **1992**, 96, 2118. Partridge, H.; Bauschlicher, C.W., Jr.; Langhoff, S.R. *J. Phys. Chem.* **1992**, 96, 5350. Bauschlicher, C.W., Jr.; Sodupe, M.; Partridge, H. *J. Chem. Phys.* **1992**, 96, 4453. Partridge, H.; Bauschlicher, C.W., Jr. *Chem. Phys. Lett.* **1992**, 195, 494. Sodupe, M.; Bauschlicher, C.W., Jr.; Partridge, H. *Chem. Phys. Lett.* **1992**, 192, 185. Bauschlicher, C.W., Jr. *Chem. Phys. Lett.* **1993**, 201, 11. Sodupe, M.; Bauschlicher, C.W., Jr. *Chem. Phys.* **1994**, 185, 163. Maitre, P.; Bauschlicher, C.W., Jr. *Chem. Phys.* **1994**, 225, 467. Bauschlicher, C.W., Jr.; Partridge, H. *Chem. Phys. Lett.* **1995**, 239, 241. Sodupe, M.; Branchadell, V.; Rosi, M.; Bauschlicher, C.W., Jr. *J. Phys. Chem. A* **1997**, 101, 7854. Heineman, C.; Koch, W.; Partridge, H. *Chem. Phys. Lett.* **1998**, 286, 131. Rodriguez, Santiago, L.; Bauschlicher, C.W., Jr. *Spectrochim. Acta A* **1999**, 55, 457.
- (52) a) Hrušák, J.; Stöckigt, D.; Schwarz, H. *Chem. Phys. Lett.* **1994**, 221, 518. b) Hertwig, R.H.; Koch, W.; Schroeder, D.; Schwarz, H.; Hrusak, J.; Schwerdtfeger, P. *J. Phys. Chem.* **1996**, 100, 12253. c) Dunbar, R.C.; Klippenstein, S.J.; Hrusak, J.; Stöckigt, D.; Schwarz, H. *J. Am. Chem. Soc.* **1996**, 118, 5277. d) Stöckigt, D. *J. Phys. Chem.* **1997**, 101, 3800.
- (53) a) Reinhard, B. M.; Niedner-Schatteburg, G. *J. Phys. Chem. A*, **2002**, 106, 7988. b) Reinhard, B. M.; Niedner-Schatteburg, G. *Phys. Chem. Chem. Phys.* **2002**, 4, 1471. c) Reinhard, B. M.; Niedner-Schatteburg, G. *J. Chem. Phys.* **2003**, 118, 3571.
- (54) a) Yang, C.N.; Klippenstein, S.J. *J. Phys. Chem.* **1999**, 103, 1094. b) Klippenstein, S.J.; Yang, C.N. *Int. J. Mass Spectrom.* **2000**, 201, 253.

- (55) a) Frenking, G.; Frohlich, N. *Chem. Rev.* **2000**, 100, 717. b) Nechaev, M. S.; Rayon, V. M.; Frenking, G. *J. Phys. Chem. A* **2004**, 108, 3134.
- (56) a) Kirschner, K.N.; Ma, B.; Bowen, J.P.; Duncan, M.A. *Chem. Phys. Lett.* **1998**, 295, 204. b) Weslowski, S.S.; King, R. A.; Schaefer, H.F.; Duncan, M.A. *J. Chem. Phys.* **2000**, 113, 701.
- (57) a) Hoffman, B.C.; Schaefer, H.F. *Int. J. Mass Spectrom.* **1999**, 185, 961.
- (58) a) Watanabe, H.; Iwata, S.; Hashimoto, K.; Misaizu, F.; Fuke, K. *J. Am. Chem. Soc.* **1995**, 117, 755. b) Watanabe, H.; Iwata, S. *J. Phys. Chem.* **1997**, 101, 487. c) Watanabe, H.; Iwata, S. *J. Chem. Phys.* **1998**, 108, 10078. d) Fuke, K.; Hashimoto, K.; Iwata, S. *Adv. Chem. Phys.* **1999**, 110, 431.
- (59) a) LaiHing, K.; Cheng, P. Y.; Taylor, T. G.; Willey, K. F.; Peschke, M.; Duncan, M. A. *Anal. Chem.* **1989**, 61, 1458. b) Willey, K. F.; Cheng, P. Y.; Taylor, T. G.; Bishop, M. B.; Duncan, M. A. *J. Phys. Chem.* **1990**, 94, 1544. c) Cornett, D. S.; Peschke, M.; LaiHing, K.; Cheng, P. Y.; Willey, K. F.; Duncan, M. A. *Rev. Sci. Instr.* **1992**, 63, 2177. d) Pilgrim, J. S.; Duncan, M. A. *J. Am. Chem. Soc.* **1993**, 115, 4395. e) Pilgrim, J. S.; Duncan, M. A. *J. Am. Chem. Soc.* **1993**, 115, 6958. f) Pilgrim, J. S.; Duncan, M. A. *J. Am. Chem. Soc.* **1993**, 115, 9724. g) Pilgrim, J. S.; Brock, L. R.; Duncan, M. A. *J. Phys. Chem.* **1995**, 99, 544. h) France, M. R.; Buchanan, J. W.; Robinson, J. C.; Pullins, S. H.; Tucker, J. L.; King, R. B.; Duncan, M. A. *J. Phys. Chem. A* **1997**, 101, 6214. i) Buchanan, J. W.; Reddic, J. E.; Grieves, G. A.; Duncan, M. A. *J. Phys. Chem. A* **1998**, 102, 6390. j) Foster, N. R.; Grieves, G. A.; Buchanan, J. W.; Flynn, N. D.; Duncan, M. A. *J. Phys. Chem. A* **2000**,

- 104, 11055. k) Grieves, G. A.; Buchanan, J. W.; Reddic, J. E.; Duncan, M. A. *Int. J. Mass Spectrom.* **2001**, 204, 223. l) Walker, N. R.; Grieves, G. A.; Jaeger, J. B.; Walters, R. S.; Duncan, M. A. *Int. J. Mass Spectrom.* **2003**, 228, 285. m) Jaeger, T. D.; Duncan, M. A. *J. Phys. Chem. A* **2004**, 108, 11296. n) Pillai, E. D.; Molek, K. S.; Duncan, M. A. *Chem. Phys. Lett.* **2005**, 405, 247. o) Ticknor, B. W.; Duncan, M. A. *Chem. Phys. Lett.* **2005**, 405, 214.
- (60) a) Hoshino, K.; Kurikawa, T.; Takeda, H.; Nakajima, A.; Kaya, K., *J. Phys. Chem.* **1995**, 99, 3053. b) Judai, K.; Hirano, M.; Kawamata, H.; Yabushita, S.; Nakajima, A.; Kaya, K., *Chem. Phys. Lett.* **1997**, 270, 23. c) Yasuike, T.; Nakajima, A.; Yabushita, S.; Kaya, K., *J. Phys. Chem. A* **1997**, 101, 5360. d) Kurikawa, T.; Takeda, H.; Hirano, M.; Judai, K.; Arita, T.; Nagao, S.; Nakajima, A.; Kaya, K., *Organometallics* **1999**, 18, 1430. e) Nakajima, A.; Kaya, K., *J. Phys. Chem. A*, **2000**, 104, 176. f) Miyajima, K.; Nakajima, A.; Yabushita, S.; Knickelbein, M.B.; Kaya, K. *J. Am. Chem. Soc.* **2004**, 126, 13202.
- (61) Berkowitz, J. *Photoabsorption, Photoionization and Photoelectron Spectroscopy*, Academic, New York, 1979.
- (62) a) Pasternack, L.; Dagdigian, P.J. *J. Chem. Phys.* **1977**, 67, 3854. b) Chen, J.; Dagdigian, P.J. *J. Phys. Chem.* **1992**, 96, 1284. c) Hwang, E.; Dagdigian, P.J. *J. Chem. Phys.* **1995**, 102, 2426. d) Yang, X.; Dagdigian, P.J.; Alexander, M.H. *J. Chem. Phys.* **1998**, 108, 3522. e) Yang, X.; Gerasimov, I.; Dagdigian, P.J. *Chem. Phys.* **1998**, 239, 207. f) Lei, J.; Dagdigian, P.J.

- Chem. Phys. Lett.* **1999**, *304*, 317. g) Gerasimov, I.; Lei, J.; Dagdigian, P.J. *J. Phys. Chem. A* **1999**, *103*, 5910. i) Tan, X.; Dagdigian, P.J. *J. Phys. Chem. A* **2001**, *105*, 11009. j) Lie, J.; Dagdigian, P.J. *J. Chem. Phys.* **2001**, *114*, 2137.
- (63) a) Bondybey, V.E.; Heaven, M.; Miller, T.A. *J. Chem. Phys.* **1983**, *78*, 3593. b) Cai, M.F.; Miller, T.A.; Bondybey, V.E. *Chem. Phys. Lett.* **1989**, *158*, 475. c) Ellis, A.M.; Robles, E.S.J.; Miller, T.A. *J. Chem. Phys.* **1991**, *94*, 1752. d) Robles, E.S.J.; Ellis, A.M.; Miller, T.A. *J. Phys. Chem.* **1992**, *96*, 3247. e) Robles, E.S.J.; Ellis, A.M.; Miller, T.A. *J. Phys. Chem.* **1992**, *96*, 8791. f) Panov, S.I.; Williamson, J.M.; Miller, T.A. *J. Chem. Phys.* **1995**, *102*, 7359.
- (64) a) Negishi, Y.; Kawamata, H.; Hayakawa, F.; Nakajima, A.; Kaya, K. *Chem. Phys. Lett.* **1998**, *294*, 370. b) Kurikawa, T.; Negishi, Y.; Hayakawa, F.; Nagao, S.; Miyajima, K.; Nakajima, A.; Kaya, K. *J. Am. Chem. Soc.* **1998**, *120*, 11766. c) Lee, G.H.; Huh, S.H.; Park, Y.C.; Hayakawa, F.; Negishi, Y.; Nakajima, A.; Kaya, K. *Chem. Phys. Lett.* **1999**, *299*, 309. d) Palpant, B.; Otake, A.; Hayakawa, F.; Negishi, Y.; Lee, G.H.; Nakajima, A.; Kaya, K. *Phys. Rev. B* **1999**, *60*, 4509. e) Nakajima, A.; Kaya, K. *J. Phys. Chem. A* **2000**, *104*, 176. f) Pramann, A.; Nakamura, Y.; Nakajima, A.; Kaya, K. *J. Phys. Chem. A* **2001**, *105*, 7534. g) Duncan, M.A.; Knight, A.M.; Negeshi, Y.; Nagoa, S.; Nakamura, Y.; Kato, A.; Nakajima, A.; Kaya, K. *J. Phys. Chem. A* **2001**, *105*, 10093. h) Pramann, A.; Koyasu, K.; Nakajima, A.; Kaya, K. *J. Chem. Phys.* **2002**, *116*, 6521. i) Ohara, M.; Koyasu, K.; Nakajima, A.; Kaya, K. *Chem. Phys. Lett.* **2003**, *371*, 490.

- (65) Gardner, J.M.; Lester, M.I. *Chem. Phys. Lett.* **1987**, *137*, 301.
- (66) a) Knickelbein, M.B.; Yang, S.; Riley, S.J. *J. Chem. Phys.* **1990**, *93*, 94. b) Yang, S.; Knickelbein, M.B. *J. Chem. Phys.* **1990**, *93*, 1533. c) Knickelbein, M.B. *Chem. Phys. Lett.* **1992**, *192*, 129. d) Knickelbein, M. *J. Chem. Phys.* **1995**, *102*, 1. e) Koretsky, G.M.; Knickelbein, M.B. *J. Chem. Phys.* **1997**, *107*, 10555. f) Koretsky, G. M.; Kerns, K. P.; Nieman, G. C.; Knickelbein, M. B.; Riley, S. J. *J. Phys. Chem. A* **1999**, *103*, 1997. g) Knickelbein, M.B. *Phys. Rev. A* **2003**, *67*, 013202/1. h) Hosoya, N.; Takegami, R.; Suzumura, J.; Yada, K.; Koyasu, K.; Miyajima, K.; Mitsui, M.; Knickelbein, M.B.; Yabushita, S.; Nakajima, A. *J. Phys. Chem. A* **2005**, *109*, 9.
- (67) a) Niles, S.; Prinslow, D.A.; Wight, C.A.; Armentrout, P.B. *J. Chem. Phys.* **1990**, *93*, 6186. b) Niles, S.; Armentrout, P.B.; Wight, C.A. *Chem. Phys.* **1992**, *165*, 143. c) Niles, S.; Prinslow, D.A.; Wight, C.A.; Armentrout, P.B. *J. Chem. Phys.* **1992**, *97*, 3115. d) Russon, L.M.; Heidecke, S.A.; Birke, M.K.; Conceicao, J.; Morse, M.D.; Armentrout, P.B. *J. Chem. Phys.* **1994**, *100*, 4747.
- (68) a) Willey, K. F.; Cheng, P. Y.; Yeh, C. S.; Robbins, D. L.; Duncan, M. A. *J. Chem. Phys.* **1991**, *95*, 6249. b) Yeh, C. S.; Robbins, D. L.; Pilgrim, J. S.; Duncan, M. A. *Chem. Phys. Lett.* **1993**, *206*, 509. c) Brock, L. R.; Pilgrim, J. S.; Duncan, M. A. *Chem. Phys. Lett.* **1994**, *230*, 93. d) Pilgrim, J. S.; Duncan, M. A. *Chem. Phys. Lett.* **1995**, *232*, 335. e) Brock, L. R.; Knight, A. M.; Reddic, J. E.; Pilgrim, J. S.; Duncan, M. A. *J. Chem. Phys.* **1997**, *106*, 6268. f) Berry, K. R.; Duncan, M. A. *Chem. Phys. Lett.* **1997**, *279*, 44. g)

- Stangassinger, A.; Knight, A. M.; Duncan, M. A. *J. Phys. Chem. A* **1999**, *103*, 1547.
- (69) a) Kirkwood, D.A.; Winkel, J.F.; Stace, A.J. *Chem. Phys. Lett.* **1995**, *247*, 332. b) Woodward, C.A.; Dobson, M.P.; Stace, A.J. *J. Phys. Chem.* **1996**, *100*, 5605. c) Dobson, M.P.; Stace, A.J. *Chem. Comm.* **1996**, *13*, 1533. d) Walker, N.R.; Firth, S.; Stace, A.J. *Chem. Phys. Lett.* **1998**, *292*, 125. e) Kirkwood, D.A.; Stace, A.J. *J. Am. Chem. Soc.* **1998**, *120*, 12316. f) Walker, N.R.; Wright, R.R.; Stace, A.J. *J. Am. Chem. Soc.* **1999**, *121*, 4837. g) Walker, N.R.; Wright, R.R.; Barran, P.E.; Stace, A.J. *Organometallics* **1999**, *18*, 3569. h) Walker, N.R.; Dobson, M.P.; Wright, R.R.; Barran, P.E.; Murrell, J.N.; Stace, A.J. *J. Am. Chem. Soc.* **2000**, *122*, 11138. i) Wright, R.R.; Walker, N.R.; Firth, S.; Stace, A.J. *J. Phys. Chem. A* **2001**, *105*, 54. j) Walker, N.R.; Wright, R.R.; Barran, P.E.; Murrell, J.N.; Stace, A.J. *J. Am. Chem. Soc.* **2001**, *123*, 4223. k) Stace, A. J. *J. Phys. Chem. A* **2002**, *106*, 7993. l) Puskar, L.; Barran, P.E.; Duncombe, B.J.; Chapman, D.; Stace, A.J. *J. Phys. Chem. A* **2005**, *109*, 273. m) Stace, A.J. *Adv. Met. Semicond. Clusters* **2001**, *5*, 121.
- (70) a) Willey, K.F.; Yeh, C.S; Robbins, D.L.; Pilgrim, J.S.; Duncan, M.A. *J. Chem. Phys.* **1992**, *97*, 8886. b) Yeh, C. S.; Willey, K. F.; Robbins, D. L.; Pilgrim, J. S.; Duncan, M. A. *Chem. Phys. Lett.* **1992**, *196*, 233. c) Pilgrim, J. S.; Yeh, C. S.; Duncan, M. A. *Chem. Phys. Lett.* **1993**, *210*, 322. d) Pilgrim, J. S.; Yeh, C. S.; Berry, K. R.; Duncan, M. A. *J. Chem. Phys.* **1994**, *100*, 7945. e) Scurlock, C. T.; Pilgrim, J. S.; Duncan, M. A. *J. Chem. Phys.* **1995**,

- 103, 3293. f) Yeh, C. S.; Pilgrim, J. S.; Willey, K. F.; Robbins, D. L.; Duncan, M. A. *Int. Rev. Phys. Chem.* **1994**, *13*, 231. g) Yeh, C. S.; Willey, K. F.; Robbins, D. L.; Duncan, M. A. *J. Phys. Chem.* **1992**, *96*, 7833. h) Willey, K. F.; Yeh, C. S.; Robbins, D. L.; Duncan, M. A. *Chem. Phys. Lett.* **1992**, *192*, 179. i) Yeh, C.S.; Willey, K.F.; Robbins, D.L.; Duncan, M.A. *J. Chem. Phys.* **1993**, *98*, 1867. j) Robbins, D.L.; Brock, L.R.; Pilgrim, J.S.; Duncan, M.A. *J. Chem. Phys.* **1995**, *102*, 1481. k) France, M.R.; Pullins, S.H.; Duncan, M.A. *Chem. Phys.* **1998**, *239*, 447. l) Reddic, J.E.; Duncan, M.A. *Chem. Phys. Lett.* **1999**, *312*, 96. m) Reddic, J.E.; Duncan, M.A. *J. Chem. Phys.* **1999**, *110*, 9948.
- (71) a) Scurlock, C.T.; Pullins, S.H.; Reddic, J.E.; Duncan, M.A. *J. Chem. Phys.* **1996**, *104*, 4591. b) Pullins, S.H.; Scurlock, C.T.; Reddic, J.E.; Duncan, M.A. *J. Chem. Phys.* **1996**, *104*, 7518. c) Velasquez, J.; Kirschner, K.N.; Reddic, J.E.; Duncan, M.A. *Chem. Phys. Lett.* **2001**, *343*, 613. d) Reddic, J.E.; Duncan, M.A. *J. Chem. Phys.* **2000**, *112*, 4974. e) Scurlock, C.T.; Pullins, S.H.; Duncan, M.A. *J. Chem. Phys.* **1996**, *105*, 3579. f) Kirschner, K.N.; Ma, B.; Bowen, J.P.; Duncan, M.A. *Chem. Phys. Lett.* **1998**, *295*, 204. g) Pullins, S.H.; Reddic, J.E.; France, M.R.; Duncan, M.A. *J. Chem. Phys.* **1998**, *108*, 2725. h) Weslowski, S. S.; King, R. A.; Schaefer, H. F.; Duncan, M. A. *J. Chem. Phys.* **2000**, *113*, 701. i) France, M. R.; Pullins, S. H.; Duncan, M. A. *J. Chem. Phys.* **1998**, *108*, 7049. j) France, M. R.; Pullins, S. H.; Duncan, M. A. *J. Chem. Phys.* **1998**, *109*, 8842.

- (72) a) Misaizu, F.; Sanekata, M.; Tsukamoto, K.; Fuke, K.; Iwata, S. *J. Phys. Chem.* **1992**, *96*, 8259. b) Sanekata, M.; Misaizu, F.; Fuke, K.; Iwata, S.; Hashimoto, K.; *J. Am. Chem. Soc.* **1995**, *117*, 747. c) Watanabe, H.; Iwata, S. *J. Phys. Chem.* **1996**, *100*, 3377. d) Sanekata, M.; Misaizu, F.; Fuke, K. *J. Chem. Phys.* **1996**, *104*, 9768. e) Fuke, K.; Hashimoto, K.; Takasu, R. *Adv. Met. Semicond. Clusters* **2001**, *5*, 1. f) Yoshida, S.; Okai, N.; Fuke, K. *Chem. Phys. Lett.* **2001**, *347*, 93.
- (73) Cheng, Y.C.; Chen, J.; Ding, L.N.; Wong, T.H.; Kleiber, P.D.; Liu, D.-K. *J. Chem. Phys.* **1996**, *104*, 6452. Chen, J.; Cheng, Y.C.; Kleiber, P.D. *J. Chem. Phys.* **1997**, *106*, 3884. Chen, J.; Wong, T.H.; Kleiber, P.D. *Chem. Phys. Lett.* **1997**, *279*, 185. Kleiber, P.D.; Chen, J. *Int. Rev. Phys. Chem.* **1998**, *17*, 1. Chen, J.; Wong, T.H.; Cheng, Y.C.; Montgomery, K.; Kleiber, P.D. *J. Chem. Phys.* **1998**, *108*, 2285. Chen, J.; Wong, T.H.; Kleiber, P.D.; Wang, K.H. *J. Chem. Phys.* **1999**, *110*, 11798.
- (74) a) Shen, M.H.; Winniczek, J.W.; Farrar, J.M. *J. Phys. Chem.* **1987**, *91*, 6447. b) Shen, M.H.; Farrar, J.M. *J. Phys. Chem.* **1989**, *93*, 4386. c) Shen, M.H.; Farrar, J.M. *J. Chem. Phys.* **1991**, *94*, 3322. d) Donnelly, S.G.; Farrar, J.M. *J. Chem. Phys.* **1993**, *98*, 5450. e) Qian, J.; Midey, A.J.; Donnelly, S.G.; Lee, J.I.; Farrar, J.M. *Chem. Phys. Lett.* **1995**, *244*, 414.
- (75) Luder, C.; Velegrakis, M. *J. Chem. Phys.* **1996**, *105*, 2167. Luder, C.; Prekas, D.; Vourliotaki, A.; Velegrakis, M. *Chem. Phys. Lett.* **1997**, *267*, 149. Fanourgakis, G.S.; Farantos, S.C.; Luder, C.; Velegrakis, M.; Xantheas, S.S. *J. Chem. Phys.* **1998**, *109*, 108. Prekas, D.; Feng, B.H.; Velegrakis, M.; J.

- Chem. Phys.* **1998**, *108*, 2712. Xantheas, S.; Fanourgakis, G.S.; Farantos, S.C.; Velagakis, M. **1998**, *108*, 46.
- (76) Asher, R.L.; Bellert, D.; Buthelezi, T.; Lessen, D.; Brucat, P.J. *Chem. Phys. Lett.* **1995**, *234*, 119. Buthelezi, T.; Bellert, D.; Lewis, V.; Brucat, P.J. *Chem. Phys. Lett.* **1995**, *246*, 145. Buthelezi, T.; Bellert, D.; Lewis, V.; Brucat, P.J. *Chem. Phys. Lett.* **1995**, *242*, 627. Bellert, D.; Buthelezi, T.; Lewis, V.; Dezfulian, K.; Brucat, P.J. *Chem. Phys. Lett.* **1995**, *240*, 495. Asher, R.L.; Bellert, D.; Buthelezi, T.; Brucat, P.J. *J. Phys. Chem.* **1995**, *99*, 1068. Bellert, D.; Buthelezi, Dezfulian, K.; T.; Hayes, T.; Brucat, P.J. *Chem. Phys. Lett.* **1996**, *260*, 458. Bellert, D.; Buthelezi, T.; Hayes, T.; Brucat, P.J. *Chem. Phys. Lett.* **1997**, *277*, 27. Hayes, T.; Bellert, D.; Buthelezi, T.; Brucat, P.J. *Chem. Phys. Lett.* **1997**, *264*, 220. Hayes, T.; Bellert, D.; Buthelezi, T.; Brucat, P.J. *Chem. Phys. Lett.* **1998**, *287*, 22. Bellert, D.; Buthelezi, T.; Brucat, P.J. *Chem. Phys. Lett.* **1998**, *290*, 316.
- (77) Husband, J.; Aguirre, F.; Thompson, C.J.; Laperle, C.M.; Metz, R.B. *J. Phys. Chem. A* **2000**, *104*, 2020. Thompson, C.J.; Husband, J.; Aguirre, F.; Metz, R.B. *J. Phys. Chem. A* **2000**, *104*, 8155. Thompson, C.J.; Aguirre, F.; Husband, J.; Metz, R.B. *J. Phys. Chem. A* **2000**, *104*, 9901. Faherty, K.P.; Thompson, C.J.; Aguirre, F.; Michen, J.; Metz, R.B. *J. Phys. Chem. A* **2001**, *105*, 10054.
- (78) Willey, K. F.; Yeh, C. S.; Duncan, M. A. *Chem. Phys. Lett.* **1993**, *211*, 156.
- (79) a) Gantefor, G. F.; Cox, D. M.; Kaldor, A. *J. Chem. Phys.* **1990**, *93*, 8395. b) Gantefor, G. F.; Cox, D. M.; Kaldor, A. *J. Chem. Phys.* **1992**, *96*, 4102.

- (80) a) Panov, S.I.; Powers, D.E.; Miller, T.A. *J. Chem. Phys.* **1998**, *108*, 1335. b) Barckholtz, T.A.; Powers, D.E.; Miller, T.A.; Bursten, B.E. *J. Am. Chem. Soc.* **1999**, *121*, 2576.
- (81) a) Agreiter, J. K.; Knight, A. M.; Duncan, M. A. *Chem. Phys. Lett.* **1999**, *313*, 162.
- (82) a) Wang, K.; Rodham, D.A.; McKoy, V.; Blake, G.A. *J. Chem. Phys.* **1998**, *108*, 4817. b) Rodham, D.A.; Blake, G.A. *Chem. Phys. Lett.* **1997**, *264*, 522.
- (83) Linton, C.; Simard, B.; Loock, H.P.; Wallin, S.; Rothschof, G.K.; Gunion, R.F.; Morse, M.D.; Armentrout, P.B. *J. Chem. Phys.* **1999**, *111*, 5017.
- (84) a) Yang, D.S.; Hackett, P.A. *J. Electron Spectros.* **2000**, *106*, 153. b) Rothschof, G.K.; Perkins, J.S.; Li, S.; Yang, D.S. *J. Phys. Chem. A* **2000**, *104*, 8178. c) Rothschof, G.K.; Li, S.; Perkins, J.S.; Yang, D.S. *J. Chem. Phys.* **2001**, *115*, 4565. d) Li, S.; Rothschof, G.K.; Pillai, E.D.; Sohnlein, B.R.; Wilson, B.M.; Yang, D.S. *J. Chem. Phys.* **2001**, *115*, 7968. e) Pederson, D.B.; Zgierski, M.Z.; Anderson, S.; Rayner, D.M.; Simard, B.; Li, S.; Yang, D.S. *J. Phys. Chem. A* **2001**, *105*, 11462. f) Li, S.; Rothschof, G.K.; Yang, D.S. *J. Chem. Phys.* **2002**, *116*, 6589. g) Rothschof, G.K.; Li, S.; Yang, D.S. *J. Chem. Phys.* **2002**, *117*, 8800. h) Li, S.; Rothschof, G.K.; Fuller, J.F.; Yang, D.S. *J. Chem. Phys.* **2003**, *118*, 8636. i) Miyawaki, J.; Yang, D.S.; Sugawar, K.I. *Chem. Phys. Lett.* **2003**, *372*, 627. j) Li, S.; Sohnlein, B.R.; Rothschof, G.K.; Fuller, J.F.; Yang, D.S. *J. Chem. Phys.* **2003**, *119*, 5406. k) Li, S.; Fuller, J.F.; Sohnlein, B.R.; Yang, D.S. *J. Chem. Phys.* **2003**, *119*, 8882. l) Wang, X.; Yang, D.S. *J. Phys. Chem. A* **2004**, *108*, 6449.

- (85) a) Bloembergen, N.; Cantrell, C.D.; Larssen, D.M. *Springer Ser. Opt. Sci.* **1976**, 3, 162. b) McDowell, R.S.; Galbraith, H.W.; Krohn, B.J.; Cantrell, C.D.; Hinkley, E. D. *Opt. Comm.* **1976**, 17, 178.
- (86) Letokhov, V.S.; *Multiphoton Processes*, Proceedings of International Conference, **1978**, 331.
- (87) Marcus, R.A.; Noid, D.W.; Koszykowski, M.L. *Springer Ser. Chem. Phys.* **1978**, 3, 298.
- (88) Kung, A.H.; Dai, H.L.; Berman, M.R.; Moore, C.B. *Springer Ser. Opt. Sci.* **1979**, 21, 309.
- (89) King, D.S. *Adv. Chem. Phys.* **1982**, 50, 105.
- (90) Thorne, L.R.; Beauchamp, J.L. *Gas Phase Ion Chemistry*, **1984**, 3, 41.
- (91) a) Knickelbein, M.B.; Menezes, W.J.C. *Phys. Rev. Lett.* **1992**, 69, 1046. b) Menezes, W.J.C.; Knickelbein, M.B. *J. Chem. Phys.* **1993**, 98, 1856. c) Knickelbein, M.B. *J. Chem. Phys.* **1993**, 99, 2377. Knickelbein, M.B. *Chem. Phys. Lett.* **1995**, 239, 11. Knickelbein, M.B. *J. Chem. Phys.* **1996**, 104, 3217. Koretsky, G.M.; Knickelbein, M.B. *Chem. Phys. Lett.* **1997**, 267, 485.
- (92) a) van Heijnsbergen, D.; von Helden, G.; Duncan, M.A.; van Roij, A.J.A.; Meijer, G. *Phys. Rev. Lett.* **1999**, 83, 4983. b) von Helden, G.; van Heijnsbergen, D.; Duncan, M.A.; Meijer, G. *Chem. Phys. Lett.* **2001**, 333, 350. c) von Helden, G.; Kirilyuk, A.; van Heijnsbergen, D.; Sartakov, B.; Duncan, M.A.; Meijer, G. *Chem. Phys.* **2000**, 262, 31. d) van Heijnsbergen, D.; Duncan, M.A.; Meijer, G.; von Helden, G. *Chem. Phys. Lett.* **2001**, 349,

220. e) van Heijnsbergen, D.; Demyk, K.; Duncan, M.A.; Meijer, G.; von Helden, G. *Phys. Chem. Chem. Phys.* **2003**, *5*, 2515.
- (93) van Heijnsbergen, D.; Jaeger, T.D.; von Helden, G.; Meijer, G.; Duncan, M.A. *Chem. Phys. Lett.* **2002**, *364*, 345. van Heijnsbergen, D.; von Helden, G.; Meijer, G.; Maitre, P.; Duncan, M.A. *J. Am. Chem. Soc.* **2002**, *124*, 1562. Jaeger, T.D.; Fielicke, A.; von Helden, G.; Meijer, G.; Duncan, M.A. *Chem. Phys. Lett.* **2004**, *392*, 409. Jaeger, T.D.; van Heijnsbergen, D.; Klippenstein, S.J.; von Helden, G.; Meijer, G.; Duncan, M.A. *J. Am. Chem. Soc.* **2004**, *126*, 10981.
- (94) von Helden, G.; Holleman, I.; Knippels, G.M.H.; van der Meer, A.F.G.; Meijer, G. *Phys. Rev. Lett.* **1997**, *79*, 5234. von Helden, G.; Holleman, I.; Meijer, G.; Sartakov, B. *Opt. Express* **1999**, *4*, 46. van Heijnsbergen, D.; von Helden, G.; Meijer, G. *J. Phys. Chem. A* **2003**, *107*, 1671. Fielicke, A.; Meijer, G.; von Helden, G. *J. Am. Chem. Soc.* **2003**, *125*, 3659. Fielicke, A.; Meijer, G.; von Helden, G. *Eur. Phys. J. D.* **2003**, *24*, 69. Fielicke, A.; Meijer, G.; von Helden, G.; Simard, B.; Denommee, S.; Rayner, D. *J. Am. Chem. Soc.* **2003**, *125*, 11184. Fielicke, A.; Mitric, R.; Meijer, G.; Bonacic-Koutecky, V.; von Helden, G. *J. Am. Chem. Soc.* **2003**, *125*, 15716. Fielicke, A.; von Helden, G.; Meijer, G. *J. Phys. Chem. B* **2004**, *108*, 14591. Fielicke, A.; Kirilyuk, A.; Ratsch, C.; Behler, J.; Scheffler, M.; von Helden, G.; Meijer, G. *Phys. Rev. Lett.* **2004**, *93*, 023401/1. Oomens, J.; Moore, D.T.; von Helden, G.; Meijer, G.; Dunbar, R.C. *J. Am. Chem. Soc.* **2004**, *126*, 724.

- (95) Lemaire, J.; Boissel, P.; Heninger, M.; Mauclaire, G.; Bellec, G.; Mestdag, H.; Simon, A.; Le Caer, S.; Ortega, J.M.; Glotin, F.; Maitre, P. *Phys. Rev. Lett.* **2002**, *89*, 273002/1. Lemaire, J.; Boissel, P.; Heninger, M.; Mestdag, H.; Mauclaire, G.; Le Caer, S.; Ortega, J.M.; Maitre, P. *Spectra Anal.* **2003**, *32*, 28. Le Caer, S.; Heninger, M.; Lemaire, J.; Boissel, P.; Maitre, P.; Mestdag, H. *Chem. Phys. Lett.* **2004**, *385*, 273. Simon, A.; Jones, W.; Ortega, J.M.; Boissel, P.; Lemaire, J.; Maitre, P. *J. Am. Chem. Soc.* **2004**, *126*, 11666.
- (96) a) Okumura, M.; Yeh, L.I.; Lee, Y.T. *J. Chem. Phys.* **1985**, *83*, 3705. b) Okumura, M.; Yeh, L.I.; Lee, Y.T. *J. Chem. Phys.* **1988**, *88*, 79. c) Yeh, L.I.; Okumura, M.; Meyers, J.D.; Price, J.M.; Lee, Y.T. *J. Chem. Phys.* **1989**, *91*, 7319. d) Yeh, L.I.; Lee, Y.T.; Hougen, J.T. *J. Mol. Spectrosc.* **1994**, *164*, 473. e) Crofteon, M.W.; Price, J.M.; Lee, Y.T. *Springer Ser. Chem. Phys.* **1994**, *56*, 44. f) Boo, D.W.; Liu, Z.F.; Suits, A.G.; Tse, J.S.; Lee, Y.T. *Science* **1995**, *269*, 57. g) Wu, C.C.; Jiang, J.C.; Boo, D.W.; Lin, s.H.; Lee, Y.T. Chang, H.C.; *J. Chem. Phys.* **2000**, *112*, 176. h) Wu, C.C.; Jian, J.C.; Hahndorf, I.; Choudhuri, C.; Lee, Y.T.; Chang, H.C. *J. Phys. Chem. A* **2000**, *104*, 9556.
- (97) a) Buck, U.; Huisken, F.; Lauenstein, C.; Meyer, H.; Sroka, R. *J. Chem. Phys.* **1987**, *87*, 6276. b) Buck, U.; Gu, X.; Lauenstein, C.; Rudolph, A. *J. Phys. Chem.* **1988**, *92*, 5561. c) Buck, U.; Gu, X.; Lauenstein, C.; Rudolph, A. *J. Chem. Phys.* **1990**, *92*, 6017. d) Buck, U.; Gu, X.; Krohne, R.; Lauenstein, C. *Chem. Phys. Lett.* **1990**, *174*, 247. e) Sun, H.; Watts, R.O.; Buck, U. *J.*

- Chem. Phys.* **1992**, *96*, 1810. f) Buck, U. *J. Phys. Chem.* **1994**, *98*, 5190-200. g) Buck, U.; Ettischer, I.; Melzer, M.; Buch, V.; Sadlej, J. *Phys. Rev. Lett.* **1998**, *80*, 2578. h) Brudermann, J.; Melzer, M.; Buck, U.; Kazimirski, J.K.; Sadlej, J.; Bush, V. *J. Chem. Phys.* **1999**, *110*, 10649. i) Buck, U.; Huiskens, F. *Chem. Rev.* **2000**, *100*, 3863. j) Brudermann, J.; Buck, U.; Buch, V. *J. Phys. Chem. A* **2002**, *106*, 453. k) Steinbach, C.; Andersson, P.; Kazimirski, J.K.; Buck, U.; Buch, V.; Beu, T.A. *J. Phys. Chem. A* **2004**, *108*, 6165.
- (98) a) Linnartz, H.; Speck, T.; Maier, J.P. *Chem. Phys. Lett.* **1998**, 288, 504. b) Dopfer, O.; Nizkorodov, S.A.; Meuwly, M.; Bieske, E.J.; Maier, J.P. *Chem. Phys. Lett.* **1996**, *260*, 545. c) Ruchti, T.; Speck, T.; Connelly, J.P.; Bieskes, E.J.; Linnartz, H.; Maier, J.P. *J. Chem. Phys.* **1995**, *105*, 2592. d) Meuwly, M.; Nizkorodov, S.A.; Maier, J.P.; Bieske, E.J. *J. Chem. Phys.* **1996**, *104*, 3876. e) Bieske, E.J.; Dopfer, O. *Chem. Rev.* **2000**, *100*, 3963. f) Roth, D.; Dopfer, O.; Maier, J.P. *Phys. Chem. Chem. Phys.* **2000**, *2*, 5013. g) Dopfer, O.; Roth, D.; Maier, J.P. *J. Phys. Chem. A* **2000**, *104*, 11702. h) Dopfer, O.; Roth, D.; Maier, J.P. *J. Chem. Phys.* **2001**, *114*, 7081. i) Dopfer, O.; Roth, D.; Maier, J.P. *J. Am. Chem. Soc.* **2002**, *124*, 494. j) Dopfer, Roth, D.; O.; Maier, J.P. *Int. J. Mass. Spectrom.* **2002**, *218*, 281. k) Linnartz, H.; Verdes, D.; Maier, J.P. *Science*, **2002**, *297*, 1166. l) Olkhov, R.V.; Nizkorodov, S.A.; Dopfer, O. *Chem. Phys.* **1998**, *239*, 393.
- (99) Tanabe, S.; Ebata, T.; Fujii, M.; Mikami, N. *Chem. Phys. Lett.* **1993**, *215*, 347. b) Ebata, T.; Fujii, A.; Mikami, N. *Int. Rev. Phys. Chem.* **1998**, *17*, 331.

- c) Fujii, A.; Fujimaki, E.; Ebata, T.; Mikami, N. *J. Am. Chem. Soc.* **1998**, *120*, 13256. d) Ebata, T.; Iwasaki, A.; Mikami, N. *J. Phys. Chem. A* **2000**, *104*, 7974. e) Ebata, T.; Kayano, M.; Sato, S.; Mikami, N. *J. Phys. Chem. A* **2001**, *105*, 8623. f) Fujii, A.; Ebata, T.; Mikami, N. *J. Phys. Chem. A* **2002**, *106*, 8554. g) Miyazaki, M.; Fujii, A.; Ebata, T.; Mikami, N. *Science* **2004**, *304*, 1134. h) Abou El-Nasr, E.; Fujii, A.; Yahagi, T.; Ebata, T.; Mikami, N. *J. Phys. Chem. A* **2005**, *109*, 2498.
- (100) a) Huiskens, F.; Pertsch, T. *J. Chem. Phys.* **1987**, *86*, 106. b) Huiskens, F.; Pertsch, T. *Chem. Phys.* **1988**, *126*, 213. c) Huiskens, F.; Stemmler, M. *Chem. Phys.* **1989**, *132*, 351. d) Huiskens, F.; Kaloudis, M.; Kulckes, A. *J. Chem. Phys.* **1996**, *104*, 17. e) Huiskens, F.; Mohammad-Pooran, S.; Werhahn, O. *Chem. Phys.* **1998**, *239*, 11.
- (101) a) Carney, J.R.; Hagemeister, F.C.; Zweir, T.S. *J. Chem. Phys.* **1998**, *108*, 3379. b) Gruenloh, C.J.; Carney, J.R.; Arrington, C.A.; Zweir, T.S.; Frederick, S.Y.; Jordan, K.D. *Science* **1997**, *276*, 1678. c) Zweir, T.S. *Annu. Rev. Phys. Chem.* **1996**, *47*, 205. d) Frost, R.K.; Hagemeister, F.C.; Schleppnbach, D.; Zweir, T.S.; Jordan, K.D. *J. Chem. Phys.* **1996**, *105*, 2605. e) Pribble, R.N.; Garrett, A.W.; Haber, K.; Zweir, T.S. *J. Chem. Phys.* **1995**, *103*, 531. f) Pribble, R.N.; Zweir, T.S. *Science*, **1994**, *265*, 75.
- (102) a) Halberstadt, N.; Brechignac, P.; Beswick, J. A.; Shapiro, M. *J. Chem. Phys.* **1986**, *84*, 170. b) Becucci, M.; Lakin, N. M.; Pietraperzia, G.; Castellucci, E.; Brechignac, Ph.; Coutant, B.; Hermine, P. *J. Chem. Phys.* **1999**, *110*, 9961. c) Lopez-Tocon, I.; Otero, J. C.; Becucci, M.; Pietraperzia,

- G.; Castellucci, E.; Brechignac, P. *Chem. Phys.* **2001**, 269, 29. d) Becucci, M.; Pietraperzia, G.; Castellucci, E.; Brechignac, P. *Chem. Phys. Lett.* **2004**, 390, 29.
- (103) a) Lisy, J.M. *Cluster Ions*, Ng. C; Baer, T.; Powis, I. (Eds.) Wiley, Chichester, 1993. b) Weinheimer, C.J.; Lisy, J.M. *Int. J. Mass Spectrom Ion Process* **1996**, 159, 197. c) Weinheimer, C.J.; Lisy, J.M. *J. Phys. Chem.* **1996**, 100, 15303. d) Weinheimer, C.J.; Lisy, J.M. *J. Chem. Phys.* **1996**, 105, 2938. e) Lisy, J.M. *Int. Rev. Phys. Chem.* **1997**, 16, 267. f) Cabarcos, O.M.; Weinheimer, C.J.; Lisy, J.M. *J. Chem. Phys.* **1998**, 108, 5151. g) Cabarcos, O.M.; Weinheimer, C.J.; Lisy, J.M.; Xantheas, S.S. *J. Chem. Phys.* **1999**, 110, 5. h) Cabarcos, O.M.; Weinheimer, C.J.; Lisy, J.M.; Xantheas, S.S. *J. Chem. Phys.* **1999**, 110, 9516. i) Vaden, T.D.; Forinash, B.; Lisy, J.M. *J. Chem. Phys.* **2002** 117, 4628.
- (104) a) Inokuchi, Y.; Ohshimo, K.; Misaizu, F.; Nishi, N. *Chem. Phys. Lett.* **2004**, 390, 140. b) Inokuchi, Y.; Ohshimo, K.; Misaizu, F.; Nishi, N. *J. Phys. Chem. A*, **2004**, 108, 5034.
- (105) a) Gregoire, G.; Velasquez, J.; Duncan, M. A. *Chem. Phys. Lett.* **2001**, 349, 451. b) Gregoire, G.; Duncan, M. A. *J. Chem. Phys.* **2002**, 117, 2120. c) Gregoire, G.; Brinkmann, N. R.; van Heijnsbergen, D.; Schaefer, H. F.; Duncan, M. A. *J. Phys. Chem. A* **2003**, 107, 218. d) Walters, R. S.; Brinkmann, N. R.; Schaefer, H. F.; Duncan, M. A. *J. Phys. Chem. A* **2003**, 107, 7396. e) Walker, N. R.; Grieves, G. A.; Walters, R. S.; Duncan, M. A. *Chem. Phys. Lett.* **2003**, 380, 230. f) Walker, N. R.; Walters, R. S.; Grieves,

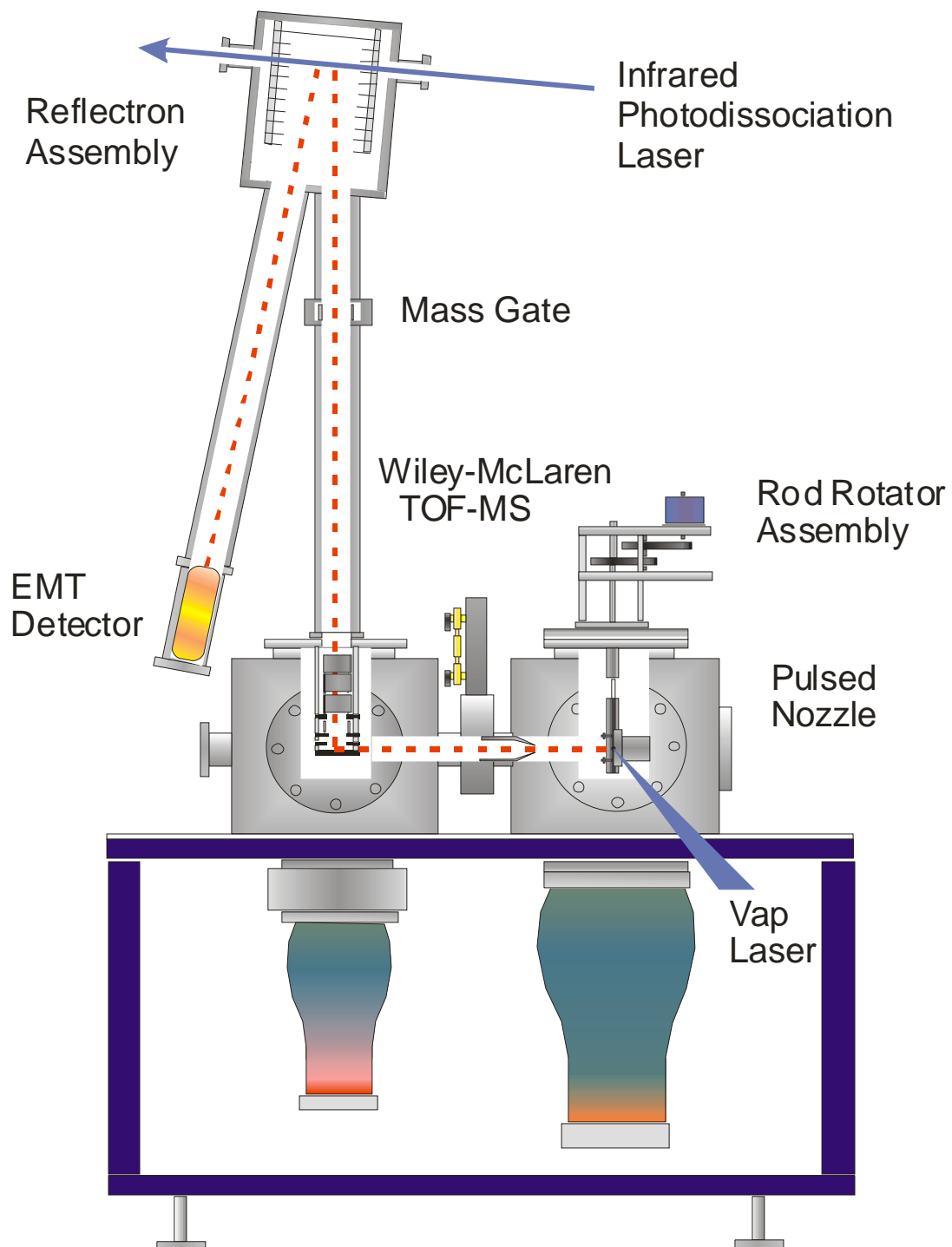
- G. A.; Duncan, M. A. *J. Chem. Phys.* **2004**, *121*, 10498. g) Walker, N. R.; Walters, R. S.; Duncan, M. A. *J. Chem. Phys.* **2004**, *120*, 10037. h) Jaeger, J. B.; Jaeger, T. D.; Brinkmann, N. R.; Schaefer, H. F.; Duncan, M. A. *Can. J. Chem.* **2004**, *82*, 934.
- (106) Pillai, E. D.; Jaeger, T. D.; Duncan, M. A. *J. Phys. Chem. A* **2005**, *109*, 3521.
- (107) a) Walker, N.R.; Walters, R.S.; Pillai, E.D.; Duncan, M.A. *J. Chem. Phys.* **2003**, *119*, 10471. b) Walters, R.S.; Duncan, M.A. *Austr. J. Chem.* **2004**, *57*, 1145. c) Tsai, B.M.; Jordan, K.D.; Walters, R.S.; Duncan, M.A. *J. Phys. Chem. A*, submitted. d) Walters, R. S.; Pillai, E.D.; Duncan, M. A. *J. Phys. Chem. A*, to be submitted.
- (108) a) Walters, R. S.; Jaeger, T. D.; Duncan, M. A. *J. Phys. Chem. A* **2002**, *106*, 10482. b) Walters, Richard S.; Schleyer, Paul v. R.; Corminboeuf, Clemence; Duncan, Michael A. *J. Am. Chem. Soc.* **2005**, *127*, 1100. c) Walters, R. S.; Pillai, E. D.; Schleyer, P. v. R.; Duncan, M. A. *J. Am. Chem. Soc.*, to be submitted. d) Walters, R. S.; Pillai, E. D.; Schleyer, P. v. R.; Duncan, M. A. *J. Am. Chem. Soc.*, to be submitted.
- (109) a) Jaeger, T. D.; Pillai, E. D.; Duncan, M. A. *J. Phys. Chem. A* **2004**, *108*, 6605. b) Jaeger, T. D.; Duncan, M. A. *J. Phys. Chem. A* **2005**, *109*, 3311. c) Jaeger, J. B.; Pillai, E. D.; Jaeger, T. D.; Duncan, M. A. *J. Phys. Chem. A* **2005**, *109*, 2801.
- (110) Duncan, Michael A. *Int. Rev. Phys. Chem.* **2003**, *22*, 407.
- (111) Shimanouchi, T. Molecular Vibrational Frequencies. *Chemistry Webbook*, 69 ed., NIST Standard Reference Database, 2001.

CHAPTER II

EXPERIMENTAL

Metal ion complexes are generated with a laser vaporization pulsed nozzle cluster source and analyzed with a Reflectron Time-of-Flight (RTOF) mass spectrometer. Figure 2.1. shows a diagram of the molecular beam apparatus, and this machine has been described elsewhere in the literature.¹⁻⁴ The second (532 nm) or third (355 nm) harmonic of a Nd:YAG laser is focused onto a metal sample rod that is both translating and rotating to provide fresh metal surface for each laser shot. Laser powers vary from 2 mJ/pulse to 20 mJ/pulse. Metal is vaporized at the ablation focal point and a plasma is ignited. Ion-molecule complexes produced in the plasma are entrained into a molecular beam generated by a General Valve, Series 9 pulsed nozzle (1 mm orifice). Typical nozzle operating parameters are 40-60 psig backing pressures and 180-380 μ sec pulse durations, but these conditions can be varied to optimize ion production. The vaporization laser and the pulsed nozzle are operated at a 10 Hz repetition rate. The source vacuum chamber is pumped by a Varian VHS-10 diffusion pump capable of removing 5300 L of helium per second, and typical source operating pressures range from 10^{-5} to 10^{-6} torr. Although the laser plasma is overall neutral, it contains cationic, neutral and anionic species. Therefore, the laser vaporization cluster source is capable of producing a variety of metal containing clusters in different oxidation states for spectroscopic study.

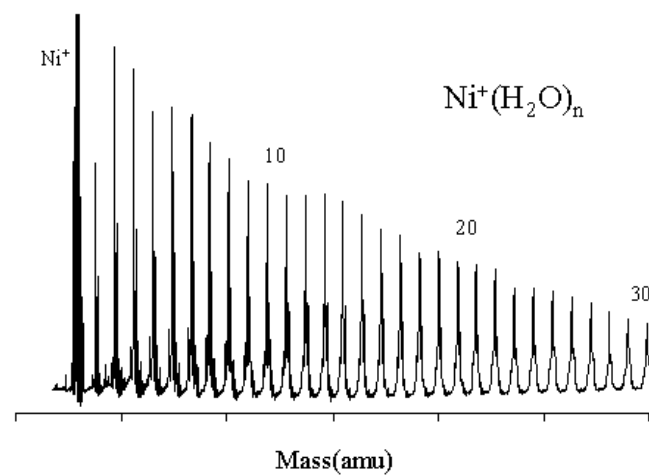
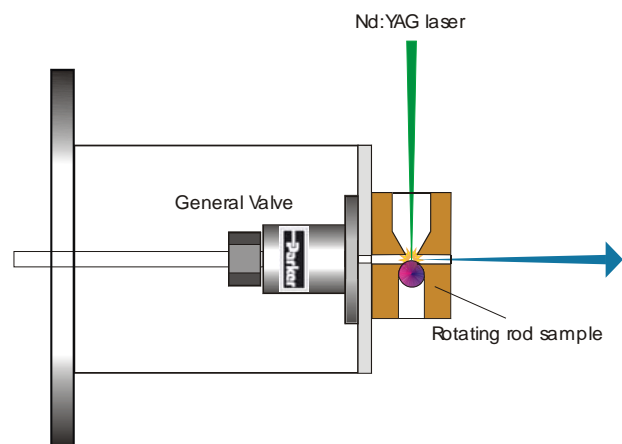
Figure 2.1 Molecular Beam Apparatus with Reflectron Time-of-Flight Mass Spectrometer



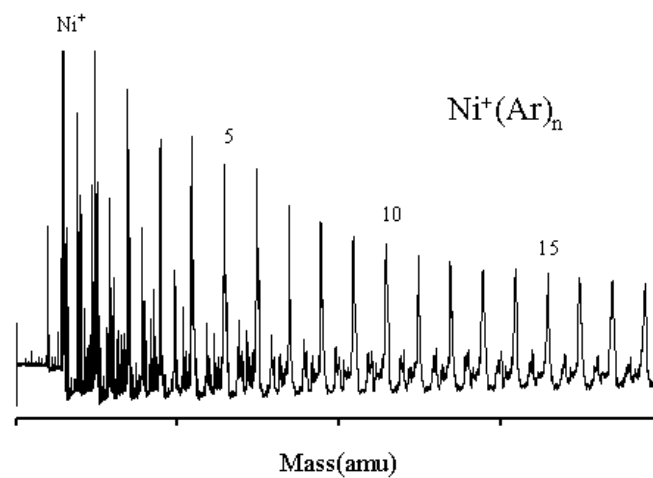
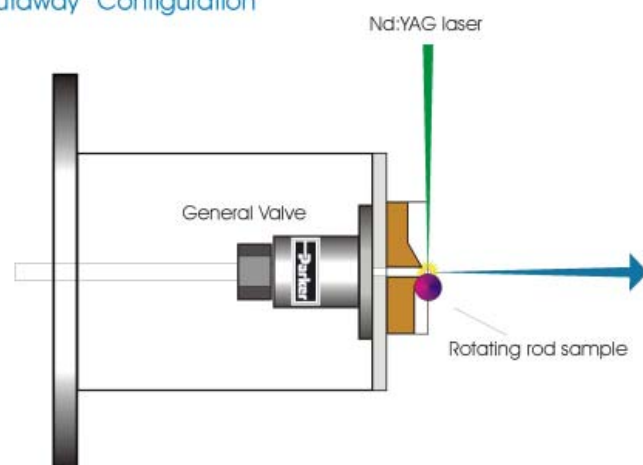
The form of the rod holder influences the cluster distribution produced in the laser vaporization source. Utilizing a regular rod holder (2 mm diameter) equipped with a 1 -2 inch growth channel (2 mm diameter) provides a collisional region where recombination produces complexes containing multiple metal atoms.⁵ Strongly bound complexes, such as metal-oxides and metal-carbides, are easily produced in this set-up. The ‘cutaway’ design¹⁻⁴ is used in conjunction with argon or neon expansions in order to produce the more weakly bound electrostatic and van der Waals complexes. In this configuration, a regular rod holder has been cut in half to expose the metal sample to vacuum and remove the collisional activation channel. This design typically produces ion-molecule complexes that contain a single metal atom and is extremely efficient at producing internally cold molecules. The $\text{Ni}^+(\text{C}_2\text{H}_2)_n$ and all the rare gas tagged complexes presented in this work were generated using the cutaway rod holder. However, this design was not efficient at producing the $\text{Ni}^+(\text{H}_2\text{O})_n$ complexes. In order to generate the hydrated nickel ions, a regular rod holder was used which was modified by boring out the gas channel to ~ 5 mm. Incorporating the modified design with a helium expansion produces $\text{Ni}^+(\text{H}_2\text{O})_n$ out to $n = 50$ or more. Figure 2.2 shows the two source configurations and the ion distributions generated from them. The multiplet of peaks observed at each cluster size is due to natural isotopes of nickel (58, 60, 62 amu). The cutaway design is efficient at producing $\text{Ni}^+(\text{Ar})_n$ and $\text{Ni}^+(\text{H}_2\text{O})\text{Ar}_n$, but complexes containing multiple water molecules are not observed. The other minor mass peaks in the $\text{Ni}^+(\text{Ar})_n$ mass spectrum are due to atmospheric impurities (i.e. $\text{Ni}^+(\text{N}_2)\text{Ar}_n$ and $\text{Ni}^+(\text{CO}_2)\text{Ar}_n$).

Figure 2.2 Laser Vaporization Cluster Sources: Regular Rod Holder and the
 ‘Cutaway’ Configuration

Laser Vaporization Cluster Source



Laser Vaporization Cluster Source "Cutaway" Configuration

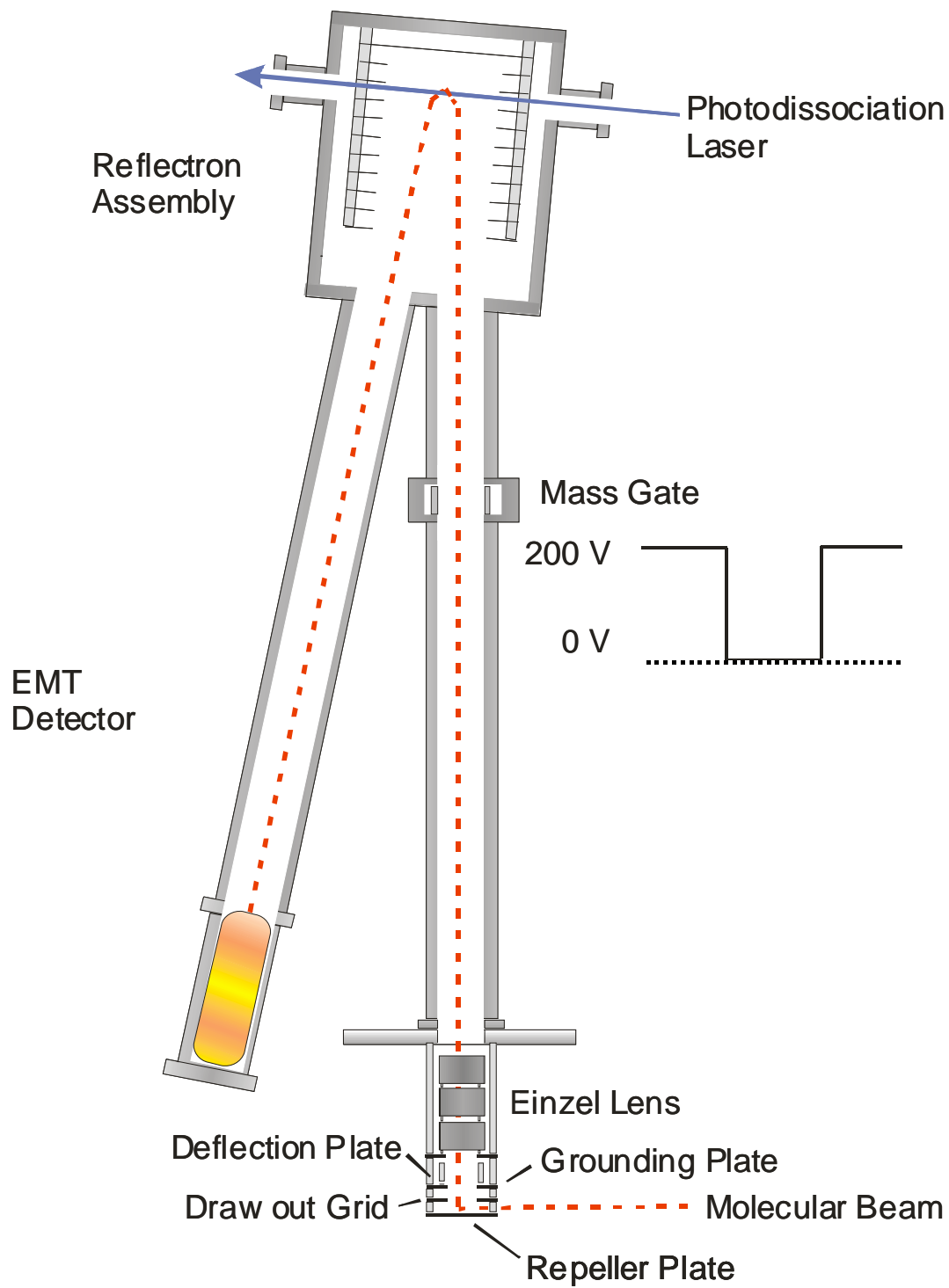


Both designs produce the ion-molecule complexes directly in the laser plasma. As stated before, ions that are first produced and then expanded have lower internal energies than molecules that are ionized downstream. Therefore, ions directly out of the jet are more attractive for spectroscopic examination. Ion-molecule complexes in the expansion are skimmed into the differentially pumped mass spectrometer vacuum chamber. A conical skimmer with a 3 mm aperture (Beam Dynamics, Inc.) is used to collimate the ion beam by deflecting the off-axis molecules. Once skimmed, the ions enter the two stage Wiley-McLaren type time-of-flight mass spectrometer,⁶ where they are pulsed extracted into the first drift region of the reflectron. A schematic of the RTOF instrument is shown in Figure 2.3. The repeller plate (REP) and draw out grid (DOG) are kept at ground until the ion packet enters the extraction region and then rapidly pulsed to high voltages. Fast response high voltage pulsers (Behlke Corporation HTS-50, 50 nsec rise time) are used to charge the REP and DOG, and typical voltages used are 1000 volts and 900 volts, respectively. This accelerates the ions down the first flight tube with approximately 1 keV energy. Because the ions are uniformly accelerated perpendicular to their translational velocities, the ions separate in time and space according to their mass defined by the following equation:

$$\text{Kinetic Energy} = 1/2 * \text{Mass} * \text{Velocity}^2$$

Low mass and high mass ions have different trajectories, therefore a deflection plate and an Einzel lens are used to focus the ions on the detector using adjustable DC voltages. Typical voltages are 0 - 50 volts for the deflector and ~400 volts for the

Figure 2.3 The Reflectron Time-of-Flight Mass Spectrometer

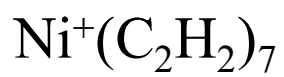


Einzel lens. Before entering the reflectron region the ions are size-selected by using another set of pulsed voltages (mass gate). For this set up, a static DC field is generated between two plates which deflects away any unwanted low mass ions. The plates are then pulsed to ground to allow the ions of interest to pass into the reflectron field and pulsed back up to high voltage to reject any higher mass ions. Typical mass gate pulses are 200 - 400 volts with ~ 10 nsec rise/fall times (Avtech AVR series).

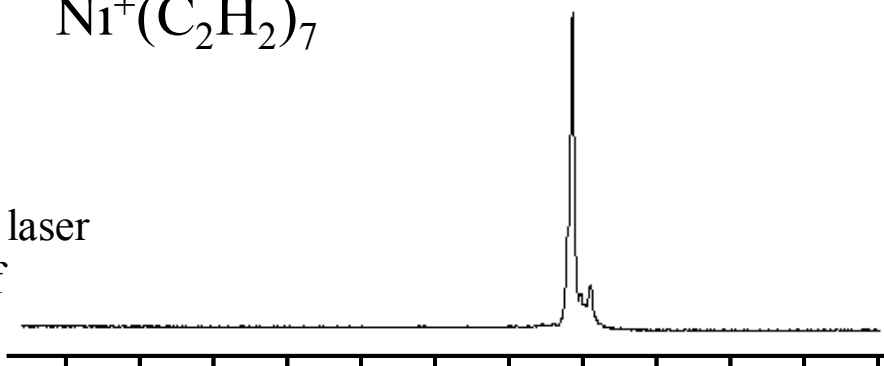
Once selected, the ions of interest enter the reflectron field.⁷ The reflectron stack is constructed of twelve stainless steel frames separated by 1.5 cm ceramic spacers. The first plate is grounded and the next ten plates are connected to a high voltage divider set of resistors (200 k Ω each). Applying a DC voltage to the back plate produces a static electrical field gradient that turns the ions and reaccelerates them down the second flight tube to the detector. Typical voltages for maximum mass resolution are 1.25 - 1.35 keV. The reflectron not only improves mass resolution, it also provides a convenient place to overlap the ion packet with the IR OPO laser. The ions are excited at the turning point and if photodissociation occurs, parent and fragment ions separate in time and space when reaccelerated in the second stage of the reflectron. Ion signals are detected using an electron multiplier tube (EMT, Hamamatsu R595) and recorded with a digital oscilloscope (LeCroy Waverunner series). Data are transferred to a PC through an IEEE interface.

Figure 2.4 illustrates the mass selection and photodissociation processes. The upper trace shows a mass spectrum of $\text{Ni}^+(\text{C}_2\text{H}_2)_7$ that has been size-selected from the distribution. If the cluster ions absorb the IR radiation and photodissociate, new ions appear in the mass spectrum as shown in the middle trace. A difference mass

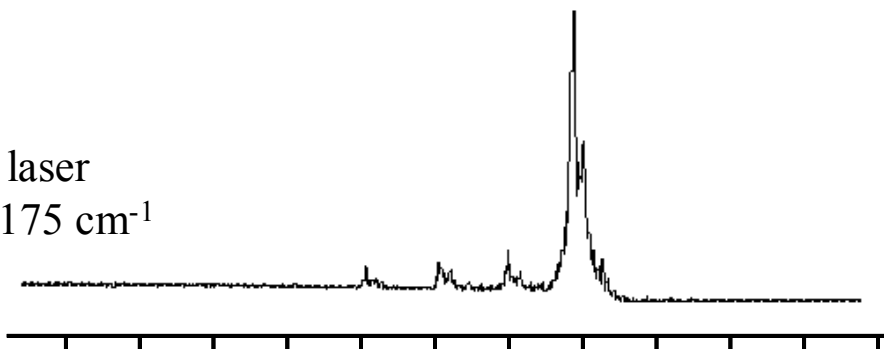
Figure 2.4 Mass Selection and Photodissociation Mass Spectra.



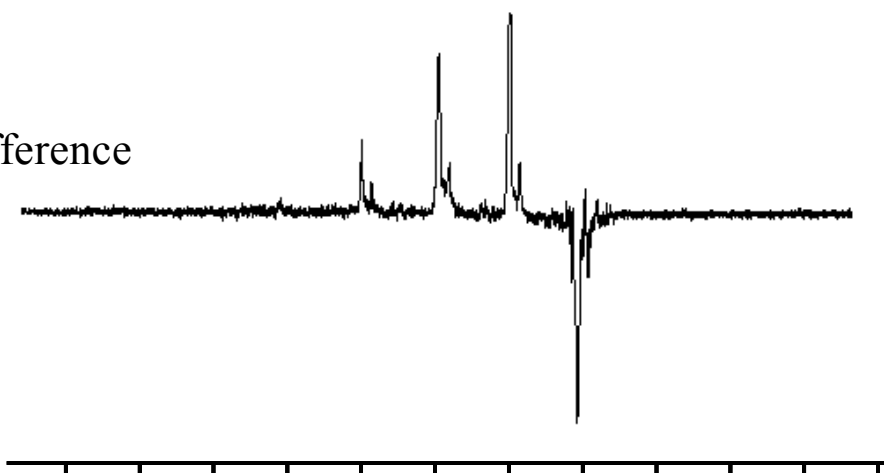
IR laser
off



IR laser
 $\sim 3175\text{ cm}^{-1}$



difference



cluster size

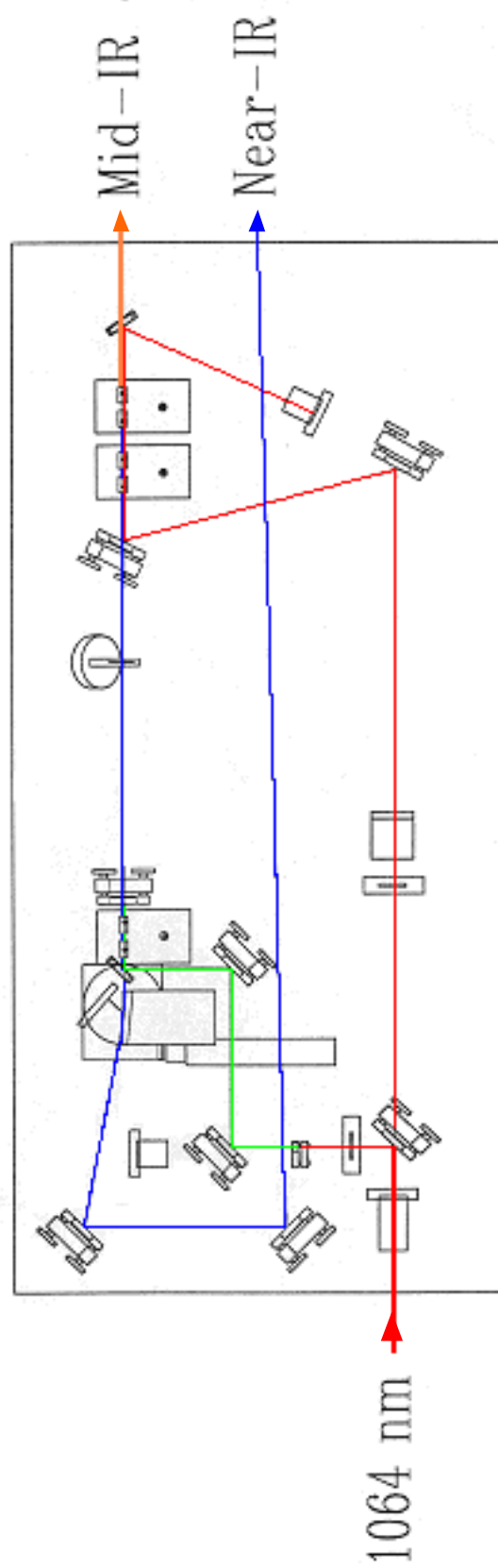
spectrum is then generated by subtracting the ion yields from two mass spectra recorded with the IR laser on and off. The lower trace of Figure 2.4 shows the difference mass spectrum for the $\text{Ni}^+(\text{C}_2\text{H}_2)_7$ complex at 3175 cm^{-1} . The negative-going peak represents depletion of the parent ion ($n = 7$) that was size-selected, and the positive peaks are the daughter ions produced by the photodissociation process. Fragmentation is more efficient on resonance, therefore, monitoring the fragment ion yield as a function of IR laser wavelength produces the vibrational ‘action’ spectrum of the ion that has been mass-selected. As stated previously, ion densities are too low for absorption measurements and spectroscopic studies must be made by monitoring an action that occurs after the absorption event. In this case we are detecting dissociation caused by the absorption of infrared radiation. This type of detection scheme is highly sensitive as it provides a zero noise background.

A schematic of the infrared OPO/OPA system (*LaserVision*) is shown in Figure 2.5. The pump laser is either a Continuum 9010 or 8010 injection-seeded Nd:YAG which provides 550-600 mJ/pulse of horizontally polarized 1064 nm light. The pump beam is split as it enters the OPO/OPA with 33% sent through a doubling crystal (KTP) and the other 67% sent through a delay line to the amplifier section. The doubled light (532 nm) passes through the grating tuned oscillator section where two angle tuned KTP crystals split the incident light into the signal and the idler beams according to the following relationship:

$$\omega_{\text{pump}} = \omega_{\text{signal}} + \omega_{\text{idler}}$$

$$\omega_{\text{signal}} \neq \omega_{\text{idler}} \text{ and } \omega_{\text{signal}} > \omega_{\text{idler}}$$

Figure 2.5 *LaserVision* Optical Parametric Oscillator / Amplifier System



where ω is the frequency in cm^{-1} of the photons.⁸ These crystals produce a signal output from 710-880 nm ($\sim 14,000 - 11,300 \text{ cm}^{-1}$) and an idler output from 1.35-2.12 μm ($\sim 7,400 - 4,700 \text{ cm}^{-1}$). The idler from the oscillator then passes into the amplifier section where it is recoupled with the 1064 nm light from the delay line. Four KTA crystals in the amplifier utilize difference frequency generation between the idler and the 1064 nm to provide light from 2050-4500 cm^{-1} ($\sim 5.0 - 2.2 \mu\text{m}$) with pulse energies from 1-30 mJ/pulse and a linewidth of 0.3 - 0.8 cm^{-1} . This light is then sent through the reflectron region to photodissociate the complex of interest. Typical spectra are recorded with 0.5 - 1.0 cm^{-1} step sizes and averaged over 30-50 laser shots. A number of small molecules have fundamental vibrations within the region covered by the IR-OPO laser.⁹ Therefore, we have already used it to acquire the vibrational spectra of a variety of metal ions complexed to carbon dioxide,¹⁰ nitrogen,¹¹ water,¹² acetylene¹³ and benzene,¹⁴ and the work presented here is a continuation of these studies.

References

- (1) LaiHing, K.; Cheng, P. Y.; Taylor, T. G.; Willey, K. F.; Peschke, M.; Duncan, M. A. *Anal. Chem.* **1989**, *61*, 1458.
- (2) Cornett, D. S.; Peschke, M.; LaiHing, K.; Cheng, P. Y.; Willey, K. F.; Duncan, M. A. *Rev. Sci. Instr.* **1992**, *63*, 2177.
- (3) Yeh, C. S.; Pilgrim, J. S.; Willey, K. F.; Robbins, D. L.; Duncan, M. A. *Int. Rev. Phys. Chem.* **1994**, *13*, 231.
- (4) Duncan, Michael A. *Int. Rev. Phys. Chem.* **2003**, *22*, 407.
- (5) a) Dietz, T.G.; Duncan, M.A.; Powers, D.E.; Smalley, R.E. *J. Chem. Phys.* **1981**, *74*, 6511. b) Zheng, L.S.; Brucat, P.J.; Pettiette, C.L.; Yang, S.; Smalley, R.E. *J. Chem. Phys.* **1985**, *83*, 4273. c) Brucat, P.J.; Zheng, L.S.; Pettiette, C.L.; Yang, S.; Smalley, R.E. *J. Chem. Phys.* **1986**, *84*, 3078.
- (6) Wiley, W.C.; McLaren, I.H. *Rev. Sci. Instrum.* **1955**, *26*, 1150.
- (7) a) Mamyrin, B.A.; Karataev, V.I.; Shmikk, D.V.; Zagulin, V.A. *Zh. Eksp. Teor. Fiz.* **1973**, *64*, 82. b) Boesl, U.; Neusser, H.J.; Weinkauf, R.; Schlag, E.W. *J. Phys. Chem.* **1982**, *86*, 4857.
- (8) Demtroder, W. *Laser Spectroscopy* Springer-Verlag: Berlin, 1996.
- (9) Shimanouchi, T. *Molecular Vibrational Frequencies*; 69th ed.; Chemistry WebBook, NIST Standard Reference Database (<http://webbook.nist.gov>), 2001
- (10) a) Gregoire, G.; Velasquez, J.; Duncan, M. A. *Chem. Phys. Lett.* **2001**, *349*, 451. b) Gregoire, G.; Duncan, M. A. *J. Chem. Phys.* **2002**, *117*, 2120. c) Gregoire, G.; Brinkmann, N. R.; van Heijnsbergen, D.; Schaefer, H. F.;

- Duncan, M. A. *J. Phys. Chem. A* **2003**, *107*, 218. d) Walters, R. S.; Brinkmann, N. R.; Schaefer, H. F.; Duncan, M. A. *J. Phys. Chem. A* **2003**, *107*, 7396. e) Walker, N. R.; Gieves, G. A.; Walters, R. S.; Duncan, M. A. *Chem. Phys. Lett.* **2003**, *380*, 230. f) Walker, N. R.; Walters, R. S.; Gieves, G. A.; Duncan, M. A. *J. Chem. Phys.* **2004**, *121*, 10498. g) Walker, N. R.; Walters, R. S.; Duncan, M. A. *J. Chem. Phys.* **2004**, *120*, 10037. h) Jaeger, J. B.; Jaeger, T. D.; Brinkmann, N. R.; Schaefer, H. F.; Duncan, M. A. *Can. J. Chem.* **2004**, *82*, 934.
- (11) Pillai, E. D.; Jaeger, T. D.; Duncan, M. A. *J. Phys. Chem. A* **2005**, *109*, 3521.
- (12) a) Walker, N. R.; Walters, R. S.; Pillai, E. D.; Duncan, M. A. *J. Chem. Phys.* **2003**, *119*, 10471. b) Walters, Richard S.; Duncan, Michael A. *Austr. J. Chem.* **2004**, *57*, 1145. c) Tsai, Brad M.; Jordan, Kenneth D.; Walters, Richard S.; Duncan, Michael A. *J. Phys. Chem. A*, submitted.
- (13) a) Walters, R. S.; Jaeger, T. D.; Duncan, M. A. *J. Phys. Chem. A* **2002**, *106*, 10482. b) Walters, Richard S.; Schleyer, Paul v. R.; Corminboeuf, Clemence; Duncan, Michael A. *J. Am. Chem. Soc.* **2005**, *127*, 1100.
- (14) a) Jaeger, T. D.; Pillai, E. D.; Duncan, M. A. *J. Phys. Chem. A* **2004**, *108*, 6605. b) Jaeger, T. D.; Duncan, M. A. *J. Phys. Chem. A* **2005**, *109*, 3311. c) Jaeger, J. B.; Pillai, E. D.; Jaeger, T. D.; Duncan, M. A. *J. Phys. Chem. A* **2005**, *109*, 2801.

CHAPTER III

STRUCTURE AND SOLVATION DYNAMICS IN HYDRATED NICKEL
CATION COMPLEXES¹

¹ Walters, R.S.; Pillai, E.D.; Duncan, M.A. To be submitted to *J. Am. Chem. Soc.*

Abstract

Infrared photodissociation spectroscopy of size-selected nickel cation-water complexes, $\text{Ni}^+(\text{H}_2\text{O})_n$ where $n = 1-25$, is reported. The pure complexes fragment by eliminating intact water molecules, while the $n = 1$ complex tagged with argon dissociates by losing a rare gas atom. All cluster sizes have resonances in the OH region red-shifted from the free molecule vibrations due to the metal interaction. New features appear beginning at $n = 4$ in the $3400 - 3700 \text{ cm}^{-1}$ range due to hydrogen bonding. By $n = 7$, the symmetric OH stretch has all but disappeared and the asymmetric band has split into a doublet, suggesting that all of the water moieties in the $\text{Ni}^+(\text{H}_2\text{O})_7$ and larger complexes are donating at least one of their OH groups to hydrogen-bonding and are included in a more complex network. The doublet near 3700 cm^{-1} is assigned to OH vibrations from acceptor-acceptor-donor (AAD) and acceptor-donor (AD) water monomers in the network. Unlike pure water clusters, nickel cation-water complexes do not form high symmetry structures as there is no evidence for dodecahedron formation in the $\text{Ni}^+(\text{H}_2\text{O})_{20}$ complex. Additionally, the AAD/AD line spacings in the hydrated nickel ions are greater than those in the pure water analogues, indicating that induction from the metal ion extends throughout the hydrogen-bonding network.

Introduction

Metal ion solvation is prevalent throughout the chemical and biological disciplines.¹⁻³ However, understanding the dynamics of the solvation process at the molecular level remains challenging. Metal ion-water clusters serve as tractable models for the study of the metal-water interactions. The gas phase ions are also attractive from an experimental perspective as they can be size-selected, allowing for the solvation process to be systematically studied from a bottoms-up approach. Metal ion-water binding energies have been measured for a variety of metals using mass spectrometry,⁴⁻¹⁹ and these complexes have been investigated with theory.²⁰⁻²⁹ Electronic spectroscopy has been employed in the past which elucidated excited state structures for some of the monohydrated metal ions.³⁰⁻³⁶ Accurate measurements of the ionization potentials of the neutral metal-water clusters have been obtained using ZEKE-PFI spectroscopy, but ground state information of the ions is usually limited to the low frequency metal-ligand vibrations.^{35,36} Recent advances in infrared photodissociation spectroscopy have begun to shed light on the geometric structures and coordination in metal ion-water complexes in their ground electronic configurations.³⁷⁻⁴⁰ In the present work, we report on the mass-selected infrared spectroscopy of $\text{Ni}^+(\text{H}_2\text{O})_n$ complexes in the size range of $n = 1-30$. Spectra are acquired in the OH stretching region and provide detailed information on the structure of these complexes and the dynamics of the solvation process.

Geometric and electronic structures of metal ion-water clusters has been theoretically investigated by a number of groups.²⁰⁻²⁹ In a benchmark study, Bauschlicher calculated ground state electronic structure and binding energies for the

monohydrated-first row transition metal ions using the Modified Coupled Pair (MCP) functional.²⁰ In a more recent paper, Klippenstein and Yang studied the same complexes with density functional theory (DFT) and reported harmonic frequencies for the OH vibrations.²⁴ The metal cation-water bond is determined to be primarily electrostatic with some partial covalent interaction for the transition metals. The metal ion withdraws charge from the water, mostly out of its lone pair orbitals. Because the lone pairs have some bonding character, this interaction weakens the binding in water and shifts the OH vibrations to lower frequency. Paralleling the advances made on the theoretical front, sophisticated experiments have been developed to accurately measure the energetics and structural details of hydrated metals. A number of mass spectrometry techniques have been used in the past, such as equilibrium measurements, radiative association studies and collision-induced dissociation experiments to determine metal-water bond energies.⁷⁻¹⁹ Most of this work has focused on the singly charged species as they are easier to produce in the gas phase, but recent experiments are beginning to study multiply charged complexes.^{14-19,34} The multiply charged species are attractive as they are more direct analogues of metals in the condensed phase.

Direct absorption spectroscopy of gas phase ions is problematic due to the low sample densities, therefore a number of different action spectroscopies have been used in the past to study metal ion-water clusters. Electronic photodissociation spectroscopy has been employed to probe the excited states of the singly charged alkaline earth metals, which excite the metal-based $P \leftarrow S$ transitions.³⁰⁻³² Brucat and coworkers have also used this technique to study $V^+(H_2O)$ by excitation into low-

lying electronic states corresponding to different d orbital configurations.³⁰ Recently, Metz and coworkers used the same technique to study $\text{Co}^{2+}(\text{H}_2\text{O})_n$ complexes.^{34a} However, electronic studies on other transition metals and complexes containing multiple waters are often not possible due to predissociation. ZEKE spectroscopy has been performed on some neutral monohydrated metals which accurately measures their ionization potentials.^{35,36} These studies have also provided information on low frequency vibrations for the cations in their ground state. Recent advances in infrared photodissociation spectroscopy (IRPD) have allowed the ground states of the metal ion-water complexes to be probed in more detail.³⁷⁻⁴⁰ Lisy and coworkers have studied alkali cation-water clusters by IRPD in the OH region,³⁷ and Inokuchi and coworkers have used this technique to study similar complexes.³⁸ Our group has extended this method to complexes containing transition metal cations.^{39,40}

Infrared spectroscopy of metal ions bound to water molecules is both useful and informative as the OH vibrations are intense and shift in particular ways upon complexation. For example, it is known that the free OH vibrations (3657 cm^{-1} , 3756 cm^{-1})⁴¹ shift to lower frequency ($3200 - 3500\text{ cm}^{-1}$) when the OH groups participate in hydrogen bonding.⁴²⁻⁴⁵ Several groups have recently used infrared photodissociation spectroscopy to study anion and protonated water clusters.⁴⁶⁻⁵³ Lisy and coworkers have adapted this technique to observe the solvation dynamics in alkali cation-water complexes.³⁷ Our group and others have incorporated IRPD together with laser vaporization sources to study cation complexes containing metals with higher melting points.³⁸⁻⁴⁰ In the present paper we report on the IRPD

spectroscopy of $\text{Ni}^+(\text{H}_2\text{O})_n$ in the OH stretch region. This is the first spectroscopic study to document the progressive solvation of a transition metal cation.

Experimental

Nickel ion-water complexes are produced in a laser vaporization pulsed nozzle source and analyzed in a time-of-flight mass spectrometer. The source and molecular beam machine have been described previously.^{39,40} Briefly, the nascent ion distribution is produced directly from the source by vaporizing a nickel rod sample with the third harmonic of a Nd:YAG laser (355 nm). For the argon-tagged complex, our specially designed ‘cutaway’ source is used in an argon expansion. We employ a sample rod holder equipped with a short 5 mm diameter growth channel directly after the laser plasma in a helium expansion to produce the larger, multiple water complexes. In each case, water is introduced into the backing gas under ambient conditions and typical backing pressures and pulse durations are 50 psi and 250 μsec , respectively. The ion-molecule complexes are skimmed into the mass spectrometer chamber where they are accelerated into the first drift region of the reflectron. They are then size-selected using pulsed voltages before entering the reflectron grid. Photodissociation is accomplished with the output of an Nd:YAG-pumped optical parametric oscillator / amplifier (OPO/OPA) laser system at the turning point. Parent and fragment ions are reaccelerated down the second stage of the reflectron and detected with an electron multiplier tube (EMT). Photodissociation is more efficient on resonance, thus monitoring the fragment ion yield as a function of laser wavelength produces the IRPD spectra of the ion that has been selected.

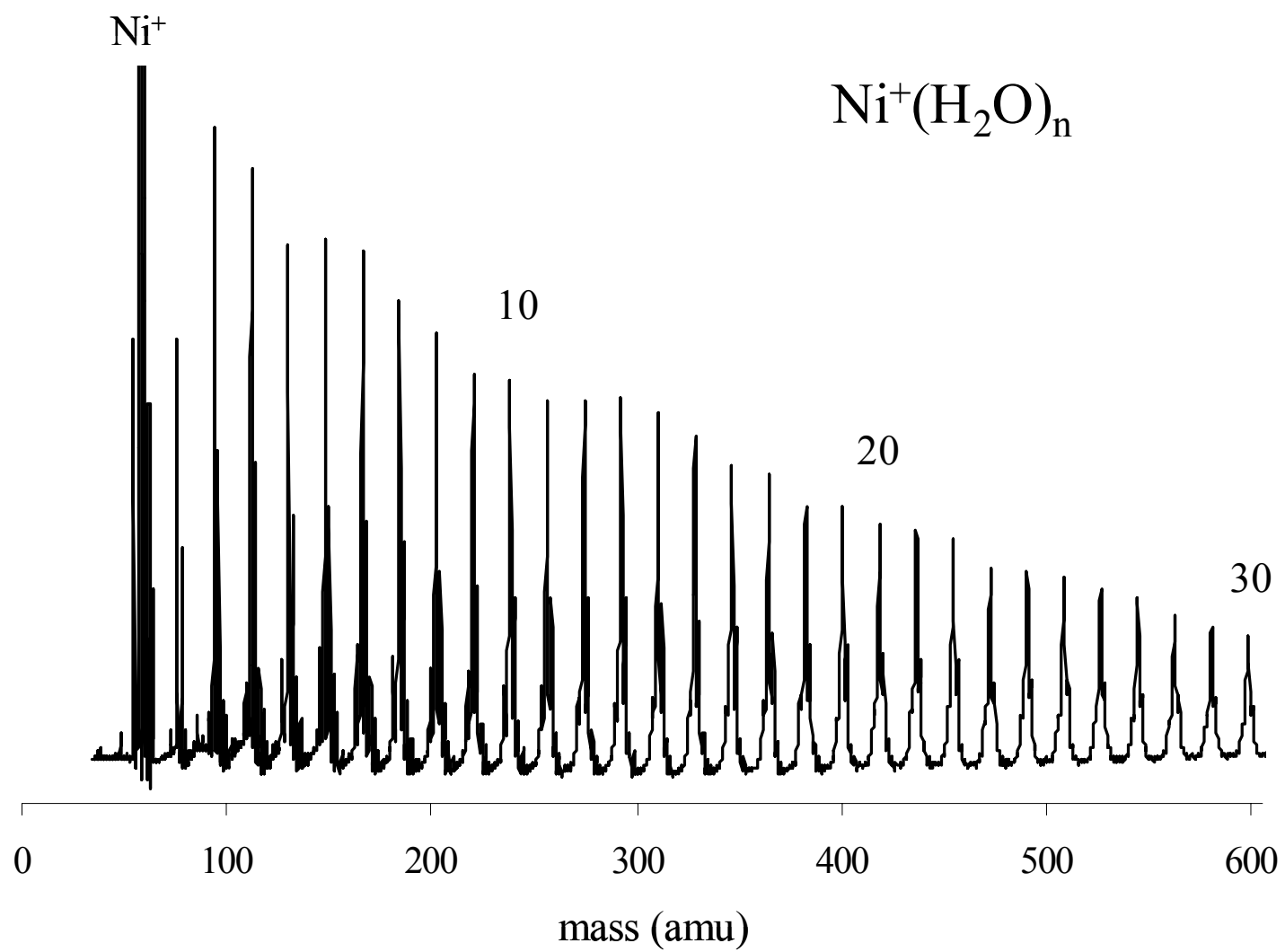
The characteristics of the OPO/OPA laser system has been described previously.⁴⁰ The output range is 2050-4000 cm⁻¹ with typical pulse powers from 2 - 30 mJ. Frequency calibration is accomplished by acquiring the photoacoustic scan of methane. The IRPD spectra of the n = 1 complex has been interpreted with the aid of density functional theory (DFT). Calculations are performed with the Gaussian '03 Windows version⁵⁴ at the B3LYP level⁵⁵ using the 6-311⁺G** basis set for the heavy atoms. The theoretical harmonic frequencies have been empirically scaled by 0.953 to provide a better comparison to the experiment.

Discussion

Figure 3.1 shows the nascent ion distribution of the Ni⁺(H₂O)_n complexes produced from the laser vaporization source utilizing the short growth channel and helium expansion described previously. The multiplet of peaks observed at each cluster size is from the natural isotopes of nickel. They are resolved at low mass, but the cluster ions appear as a single mass peak at larger sizes. The maximum intensity in this distribution and its extent to larger masses can be manipulated by varying a number of different experimental conditions. The partial pressure of water present, pulse duration and backing pressures of the expansion gas, the position and fluence of the focused laser on the metal target, as well as the timing of the vaporization laser relative to the gas pulse are all key variables in optimizing the distribution.

In order to obtain the vibrational spectra of these ion-molecule complexes, we mass-select them individually and excite them with the IR OPO laser in the OH stretch region to attempt photodissociation. No appreciable fragment ion signals were

Figure 3.1 The mass spectrum of $\text{Ni}^+(\text{H}_2\text{O})_n$ cation clusters produced by laser vaporization



detected for the $n = 1, 2$ complexes in this spectral region. This is not surprising as photodissociation is not only dependent on the absorption event but also on whether the molecule has absorbed enough energy to break its weakest bond. In this case, the weakest bond is the M^+-H_2O interaction and we are exciting the OH stretches in the water moiety. Energy absorbed by the chromophore is transferred to the M^+-H_2O coordinate via IVR and if it is greater than the binding, the cluster will fragment by eliminating the water. The dissociation energies of $Ni^+(H_2O)_{1-4}$ have already been measured with collision-induced-dissociation⁸⁻¹⁰ and calculated with theory,²⁰ and these values are listed in Table 3.1. The first two water molecules are strongly bound to the nickel cation and have similar values, whereas the third and fourth waters are relatively weakly attached. Therefore, the fact that we do not observe any substantial fragmentation from the $n = 1, 2$ complexes and yet the $n = 3$ complex fragments efficiently is consistent with the energetics of this system. The ~ 40 kcal/mol required to dissociate the mono- and di-hydrated ions corresponds to $14,000\text{ cm}^{-1}$.

Photodissociation in the OH region would therefore require at least four photons, but multiphoton absorption is inefficient due to the loss of resonance at higher vibrational states. The third and fourth ligands are bound by only 12 kcal/mol ($\sim 4200\text{ cm}^{-1}$).

While this is still greater than a single IR photon near 3700 cm^{-1} , clusters that retain some internal energy from the ion source might dissociate via a one-photon process. Additionally, as more waters are complexed to the nickel cation, the vibrational density of states increases, which enhances multiphoton absorption.

We employ the argon-tagging technique to acquire the vibrational spectra of the $Ni^+(H_2O)_{1,2}$ complexes. A number of groups have used this technique to enhance

Table 3.1 The dissociation energies of $\text{Ni}^+(\text{H}_2\text{O})_n$ ions in kcal/mol.

Complex	Experimental	Theory
$\text{Ni}^+(\text{H}_2\text{O})$	39.7 ^a , 36.5, ^b 43.9 ^c	41.9, ^d 45.0 ^e
$\text{Ni}^+(\text{H}_2\text{O})_2$	38.0, ^b 40.6 ^a , 40.2 ^c	
$\text{Ni}^+(\text{H}_2\text{O})_3$	16.2 ^c	
$\text{Ni}^+(\text{H}_2\text{O})_4$	12.3 ^c	

^aReference 8.

^bReference 9.

^cReference 10.

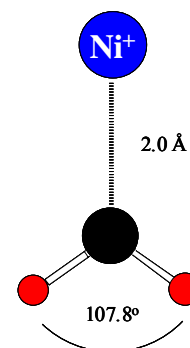
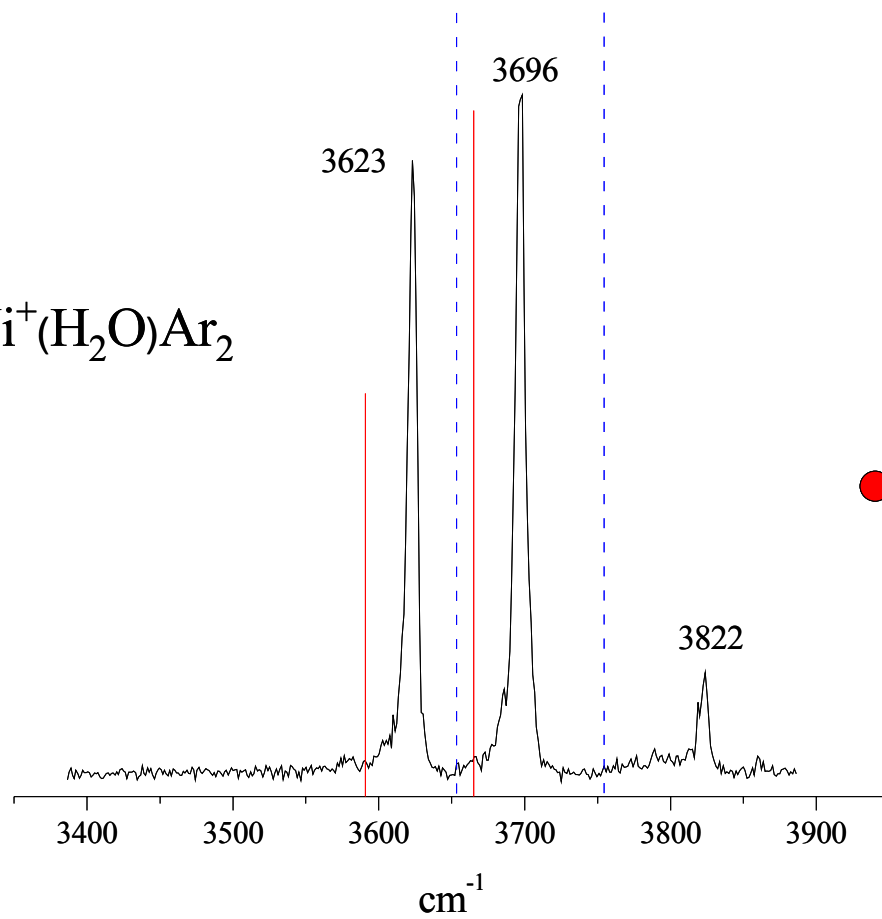
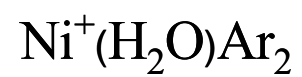
^dReference 20.

^eReference 24.

infrared photodissociation for molecular ions⁴⁶⁻⁵⁰ as well as the more strongly bound metal ion complexes,³⁷⁻⁴⁰ and the details of the method have been described previously.^{39,40} For the $\text{Ni}^+(\text{H}_2\text{O})_n$ complexes, the argon atoms likely bind to the metal ion and do not perturb the chromophores much. Therefore, acquiring the IRPD spectrum in the argon-loss channel for the mixed complex, $\text{Ni}^+(\text{H}_2\text{O})\text{Ar}_2$, is the best possible representation of the IR absorption spectra of the corresponding pure complex.

Figure 3.2 shows the IRPD spectrum of the $\text{Ni}^+(\text{H}_2\text{O})\text{Ar}_2$ complex as it compares to the predicted IR frequencies of the theoretical $\text{Ni}^+(\text{H}_2\text{O})$ complex calculated at the B3LYP level of theory. Its structure is included in the inset. The theoretical harmonic frequencies have been scaled to provide a better match to the experimental spectrum and are represented by red bars. The dashed lines mark the free water OH vibrations. Photo-dissociation of the $\text{Ni}^+(\text{H}_2\text{O})\text{Ar}$ complex was inefficient, and we had to attach two argon atoms to acquire the vibrational spectrum of the monohydrated ion. Two bands are observed in the IRPD spectrum for $\text{Ni}^+(\text{H}_2\text{O})\text{Ar}_2$ at 3623 cm^{-1} and 3696 cm^{-1} . They correspond to the symmetric and asymmetric OH vibrations in $\text{Ni}^+(\text{H}_2\text{O})\text{Ar}_2$, respectively. A small peak attributed to a combination band is observed at 3822 cm^{-1} . The $\text{Ni}^+(\text{H}_2\text{O})\text{Ar}_2$ OH frequencies are shifted from the free stretches by 34 cm^{-1} and 60 cm^{-1} for the symmetric and asymmetric bands, respectively. The DFT calculations for the $\text{Ni}^+(\text{H}_2\text{O})$ complex predict that the water binds to the metal cation primarily by the charge-dipole interaction to form a C_{2v} structure, consistent with previous theoretical work.²⁰⁻²⁹ As stated before, this interaction weakens the bonding the water molecule. This causes the H-O-H angle to

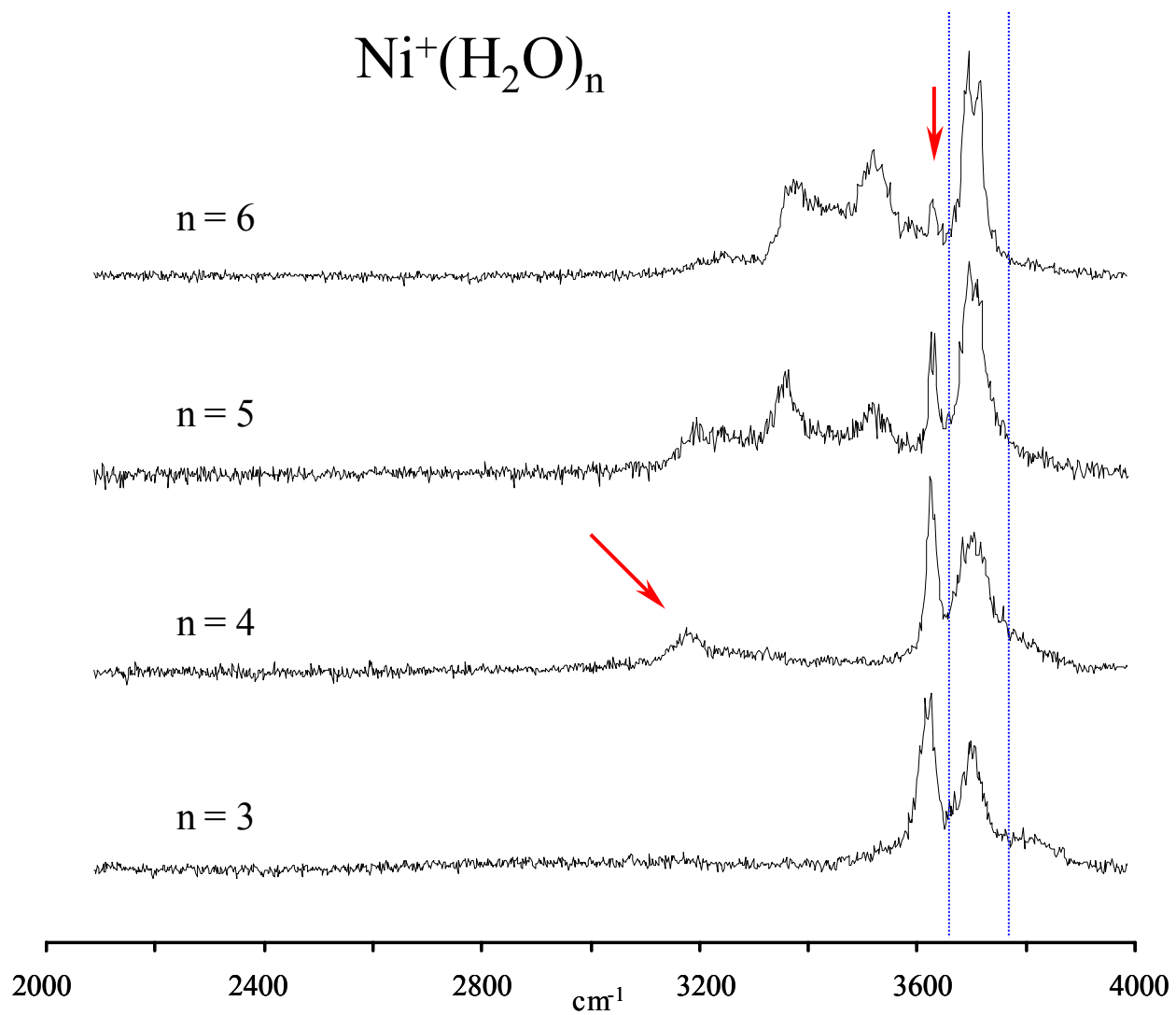
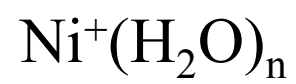
Figure 3.2 The IRPD spectrum of $\text{Ni}^+(\text{H}_2\text{O})\text{Ar}_2$ as it compares to the scaled fundamentals of the $\text{Ni}^+(\text{H}_2\text{O})$ complex calculated with DFT (red bars). The OH vibrations of the free water molecule are represented as dashed lines.



open from 104.5° in the free molecule to 107.8° in the $\text{Ni}^+(\text{H}_2\text{O})$ complex. DFT predicts symmetric and asymmetric OH stretches at 3593 cm^{-1} and 3668 cm^{-1} , respectively. The calculations also reveal that the two argons attach directly to the nickel cation in the $\text{Ni}^+(\text{H}_2\text{O})$ cluster and cause only minor perturbations on its structure. Because binding is distributed to the argons, the $\text{Ni}^+-\text{H}_2\text{O}$ interaction is lessened and the OH vibrations shift back to the blue by $\sim 17\text{ cm}^{-1}$. Therefore, the match between experiment and theory is quite good for band positions and relative intensities.

Unfortunately, we could not acquire the IRPD spectrum of the $\text{Ni}^+(\text{H}_2\text{O})_2$ complex as this complex does not dissociate and was difficult to argon-tag. However, photodissociation was efficient for the pure $\text{Ni}^+(\text{H}_2\text{O})_n$ complexes beginning with $n = 3$. As stated previously and shown in Table 3.1, the dissociation energies for the $n = 3, 4$ complexes are greater than the IR photon energy but only by $\sim 500\text{ cm}^{-1}$. The fact that these clusters photodissociate efficiently when excited near 3700 cm^{-1} likely means that some internal energy is retained from the laser vaporization process. This excess energy, in turn, facilitates fragmentation. The IRPD spectra of $\text{Ni}^+(\text{H}_2\text{O})_{3-6}$ acquired in the $(n-1)$ mass channel are displayed in Figure 3.3. There are two intense modes observed near 3700 cm^{-1} for each cluster size that roughly correspond to the symmetric and asymmetric OH stretches. Beginning with $n = 4$, new red-shifted features appear in the $3400 - 3600\text{ cm}^{-1}$ region, indicating formation of the second solvent sphere. Vibrations in this region are attributed to hydrogen-bonded OH modes⁴²⁻⁴⁵ and they have been observed in the spectroscopy of neutral and ionic water clusters.⁴⁶⁻⁵³ The fact that we observe hydrogen-bonding for the $\text{Ni}^+(\text{H}_2\text{O})_4$ complex

Figure 3.3 The IRPD spectra of $\text{Ni}^+(\text{H}_2\text{O})_{3-6}$ complexes measured in the (n-1) mass channel. The dashed blue lines represent the positions of the symmetric and asymmetric stretches in free water. Red arrows point to hydrogen-bonded OH features and the disappearance of the symmetric stretch.

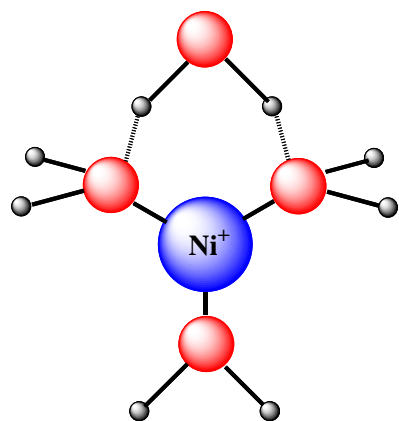


is intriguing. Previous experiments on this system indicate that the fourth water molecule binds directly to the nickel cation.¹⁰ Additionally, nickel is known to prefer a coordination of four in the condensed phase.⁶¹ Our previous work on $\text{Ni}^+(\text{CO}_2)_n$ and $\text{Ni}^+(\text{C}_2\text{H}_2)_n$ indicate that the Ni^+ is four-coordinate in these gas-phase systems,^{56,57} but the $\text{Ni}^+\text{-CO}_2$ and $\text{-C}_2\text{H}_2$ complexes were produced in our ‘cutaway’ source. In order to produce the $\text{Ni}^+(\text{H}_2\text{O})_n$ distribution shown in Figure 3.1, we employ a short collisional activation region just after laser ablation. This set up produces the hydrated nickel ions in great abundance but they are expected to be internally warmer than ion-molecule complexes generated in the ‘cutaway’ configuration. Therefore, it is likely that a subset of the $\text{Ni}^+(\text{H}_2\text{O})_4$ cluster ions are produced in higher energy isomeric form and give rise to the photodissociation signal observed in the hydrogen-bonded region. Clusters with three waters attached to the nickel cation and the fourth water bound in the second solvation layer, the so-called ‘3+1’ structure, would have at least one hydrogen-bond. Figure 3.4 shows the different hydrogen-bonding structural motifs that are possible for the ‘3+1’ isomer. They are discussed in more detail below. Photodissociation of the ‘3+1’ cluster is expected to be more efficient as less energy is required to detach the solvent molecule. Therefore, even a minor population of ‘3+1’ structures would be over-represented in the $n = 4$ IRPD spectrum.

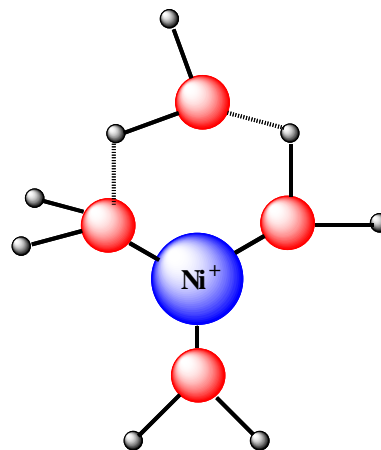
As clustering continues, more signals in the hydrogen-bonding region are observed for the larger complexes. As seen in Figure 3.3, three broad bands are observed in the $n = 5$ IRPD spectrum centered near 3200, 3350, and 3500 cm^{-1} . This suggests that isomers are also present for the $n = 5$ complex. Figure 3.4 illustrates the different hydrogen-bonding structural motifs that are possible in the second solvation

Figure 3.4 The different hydrogen-bonding structural motifs possible for the
‘3+1’ structure.

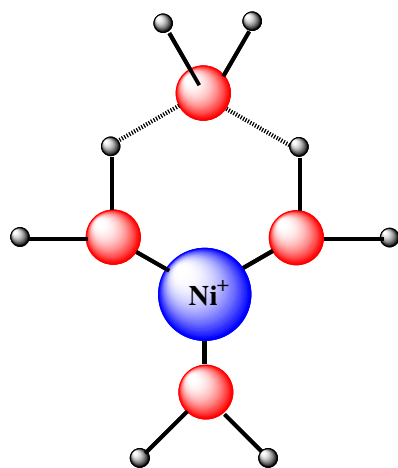
a)



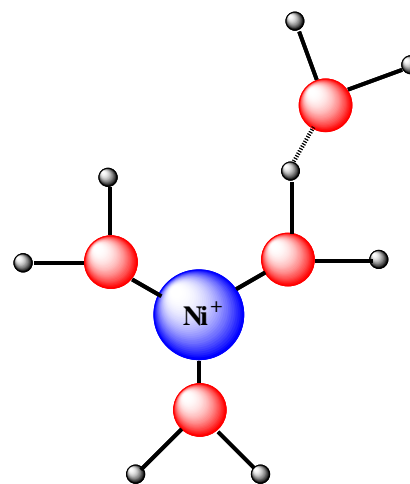
b)



c)



d)



layer. The a) and b) structures are not likely as the metal ion-dipole interaction aligns the core water molecules in such a way that only the hydrogen atoms participate in hydrogen-bonding. Therefore, any solvent likely attaches to existing water by being a single acceptor (A) or double acceptor (AA) molecule, as depicted in the c) and d) structures in Figure 3.4. Only two types of hydrogen-bonding motifs are likely and yet three bands are observed in the hydrogen-bonding region in the $n = 5$ IRPD spectrum. Less stable isomers, such as '4+1' and '3+2' structures, would also have A and AA solvent molecules but their hydrogen-bonded stretches are expected to occur at different frequencies due to induction from the different metal ion cores. Future theoretical work or acquiring the IR spectra of the $n = 3, 4, 5$ complexes tagged with argon will be required to properly assign the bands in the hydrogen-bonded region.

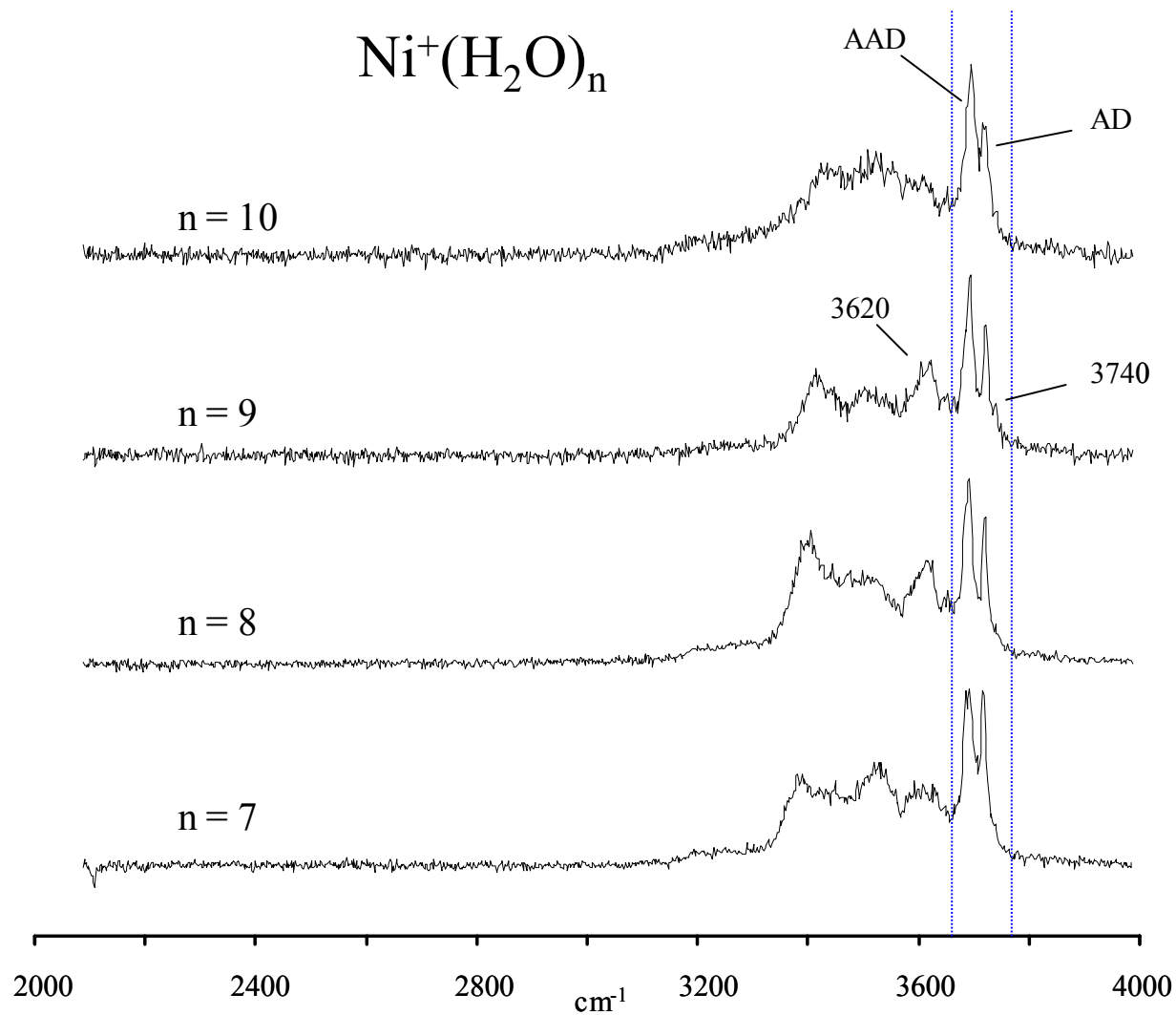
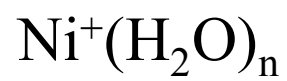
As cluster size increases, two trends are observed in the spectra shown in Figure 3.3, the intensity of the symmetric OH stretch decreases and the broad asymmetric band splits into a closely spaced doublet. In fact these two phenomena are related and have been observed in the protonated, neutral and anionic water clusters.⁴⁶⁻⁵³ Eventually all the water monomers participate in hydrogen-bonding by donating at least one of their hydrogen atoms. Once that occurs, their OH vibrations are no longer analogous to the free molecule symmetric and asymmetric stretches, that is, they contain a single hydrogen that is free to vibrate in vacuum. In a more complex hydrogen-bonding network, any signals observed in the free OH region are due to these so-called 'dangling' OH groups. They correspond to waters in the network that are either single acceptor-single donor (AD) or double acceptor-single donor (AAD) monomers. Therefore, depreciation of the symmetric stretch and the

appearance of a closely spaced doublet centered at 3700 cm^{-1} indicates that the water molecules are participating in hydrogen donation and no longer end chain-like structural motifs.

Figure 3.5 shows the IRPD spectra of the $\text{Ni}^+(\text{H}_2\text{O})_n$ complexes for $n = 7-10$. Surprisingly, the symmetric OH stretch has disappeared completely and the AD / AAD doublet near 3700 cm^{-1} is well resolved by $n = 7$. For the neutral and protonated water systems, the symmetric- and asymmetric-like OH stretches do not disappear until $n = 10$. For the hydrated nickel ions, apparently higher ordered structures such as ring formation and 2-D networks are beginning at $n = 7$. This is unexpected in light of what is already known for the $\text{Ni}^+(\text{H}_2\text{O})_{1-4}$ complexes. Previous CID measurements on these complexes are consistent with structures where the third and fourth water molecule binds directly to the nickel cation.¹⁰ It is therefore difficult to imagine that adding three additional water molecules to the $\text{Ni}^+(\text{H}_2\text{O})_4$ core could produce a structure where only dangling OH groups are present and no open-ended water monomers exist. As stated before, the charge-dipole interaction orients the core water molecules in such a way that the solvent waters are likely H-bond acceptors (A, AA). Acceptor monomers in the second solvation layer would have symmetric and asymmetric OH stretches, but none are observed for $n=7$.

One possible explanation is that clustering of water to the Ni^+ cation occurs asymmetrically. We have seen asymmetric clustering of CO_2 on Mg^+ and Al^+ ,⁵⁸ but this was caused by polarization of their valence s electrons, which is clearly not the case for nickel. A more likely explanation is that the nickel cation is included in hydrogen-bonded ring formations. Rings with five-fold symmetry are observed for

Figure 3.5 The IRPD spectra of $\text{Ni}^+(\text{H}_2\text{O})_{7-10}$ complexes measured in the (n-1) mass channel. The dashed blue lines represent the positions of the symmetric and asymmetric stretches in free water.



pure water clusters, which are the subunits that eventually produce the dodecahedron cages in $(\text{H}_2\text{O})_{20}$ and $\text{H}^+(\text{H}_2\text{O})_{21}$.⁴⁶⁻⁵³ In $\text{H}^+(\text{H}_2\text{O})_n$, the extra proton is included in a five-member ring for the $n = 7$ complex.⁵² A similar structure is feasible for the $\text{Ni}^+(\text{H}_2\text{O})_7$, where the Ni^+ is included in a ring structure. From the IR studies on the pure water clusters,⁴⁶⁻⁵³ ring formation produces a signature doublet near 3600 cm^{-1} . The partially resolved band at 3620 cm^{-1} in the $\text{Ni}^+(\text{H}_2\text{O})_{8,9}$ spectra indicates that hydrogen-bonded rings might be present for these hydrated nickel ions. Careful inspection of all the spectra shown in Figure 3.6 reveals that an asymmetric-like OH vibration might still be present, albeit at low intensity. There is a small shoulder band on the high frequency side of the AD signal at 3740 cm^{-1} for the $n = 7$ complex and this feature is reproduced in the spectra of the larger clusters up to $n = 10$. This weak signal might be an asymmetric stretch from AA-type monomers in the network, which would have both hydrogens free to vibrate. It could also arise from waters attached directly to the nickel cation. The AAD and AD bands in the larger clusters emerge from the broad asymmetric OH signal in the smaller complexes. Due to this vibrational overlap, it is difficult to accurately assign the peaks in the 3700 cm^{-1} region. More work on the $n = 7-10$ complexes will be necessary to determine their structures and prove whether or not ring formation occurs for these hydrated ions.

The IRPD spectra of selected larger $\text{Ni}^+(\text{H}_2\text{O})_n$ complexes are shown in Figure 3.6 for comparison and band positions for all cluster sizes studied are listed in Table 2.2. The spectra of all the $n > 10$ complexes are quite similar as only minor changes are observed. The intensity of the higher frequency AD-type band of the doublet near 3700 cm^{-1} decreases relative to the AAD-type peak as cluster size increases.

Figure 3.6 The IRPD spectra of selected $\text{Ni}^+(\text{H}_2\text{O})_n$ complexes measured in the (n-1) mass channel. The dashed blue lines represent the positions of the symmetric and asymmetric stretches in free water.

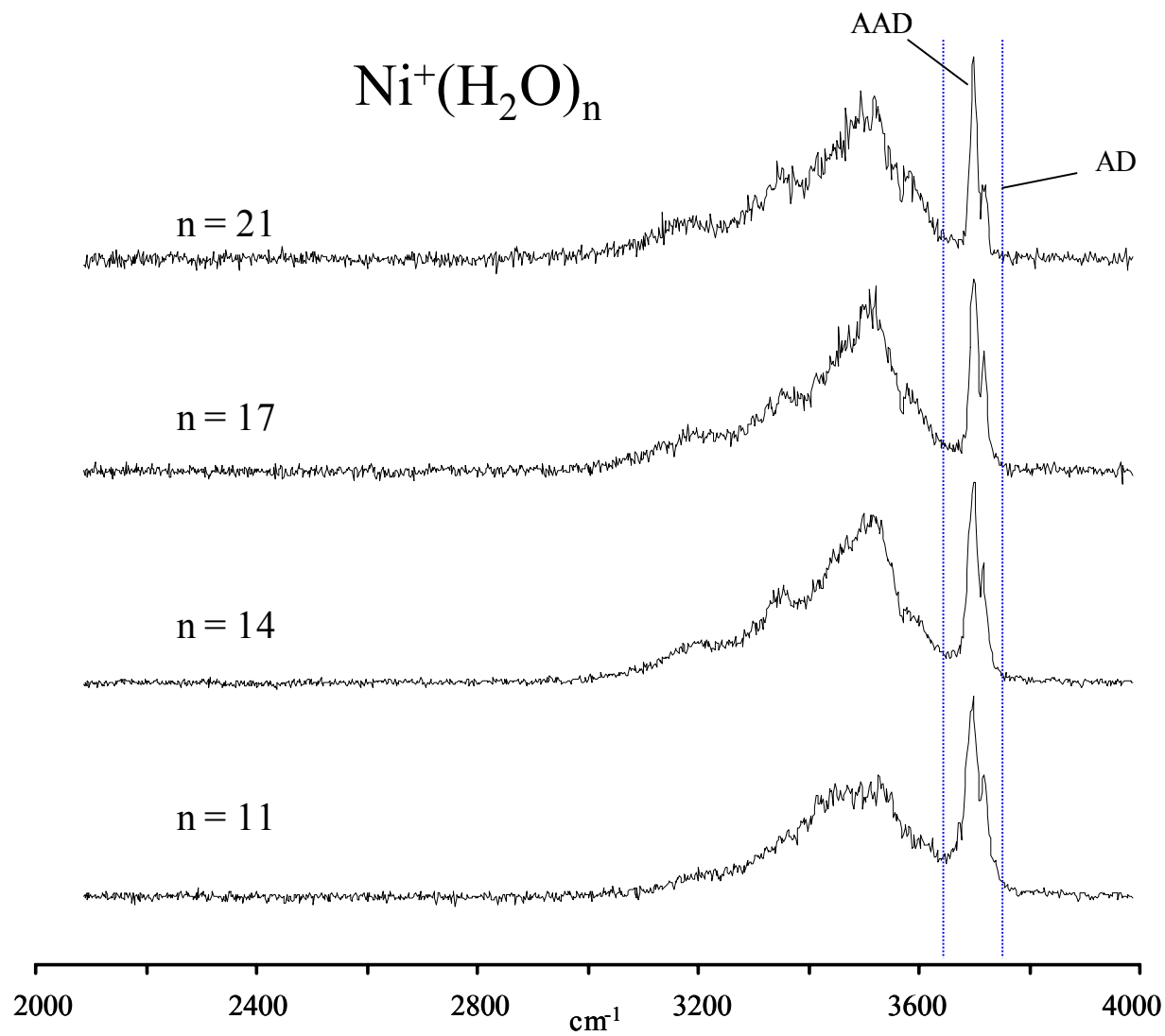
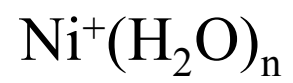


Table 3.2 Band positions of the infrared resonances measured for $\text{Ni}^+(\text{H}_2\text{O})_n$ complexes. All units are cm^{-1} , and measurements are made at band center.

$\text{Ni}^+(\text{H}_2\text{O})\text{Ar}_2$	3623, 3696, 3822
$\text{Ni}^+(\text{H}_2\text{O})_3$	3619, 3700
$\text{Ni}^+(\text{H}_2\text{O})_4$	3185, 3626, 3702
$\text{Ni}^+(\text{H}_2\text{O})_5$	3195, 3357, 3520, 3630, 3705
$\text{Ni}^+(\text{H}_2\text{O})_6$	3380, 3520, 3628, 3694, 3716
$\text{Ni}^+(\text{H}_2\text{O})_7$	3391, 3526, 3615, 3687, 3719
$\text{Ni}^+(\text{H}_2\text{O})_8$	3402, 3620, 3690, 3721
$\text{Ni}^+(\text{H}_2\text{O})_9$	3420, 3520, 3620, 3692, 3722
$\text{Ni}^+(\text{H}_2\text{O})_{10}$	3520, 3695, 3720
$\text{Ni}^+(\text{H}_2\text{O})_{11}$	3500, 3696, 3720
$\text{Ni}^+(\text{H}_2\text{O})_{12}$	3500, 3695, 3719
$\text{Ni}^+(\text{H}_2\text{O})_{13}$	3350, 3500, 3700, 3720
$\text{Ni}^+(\text{H}_2\text{O})_{14}$	3350, 3510, 3701, 3717
$\text{Ni}^+(\text{H}_2\text{O})_{15}$	3200, 3360, 3516, 3698, 3718
$\text{Ni}^+(\text{H}_2\text{O})_{16}$	3514, 3702, 3717
$\text{Ni}^+(\text{H}_2\text{O})_{17}$	3510, 3701, 3719

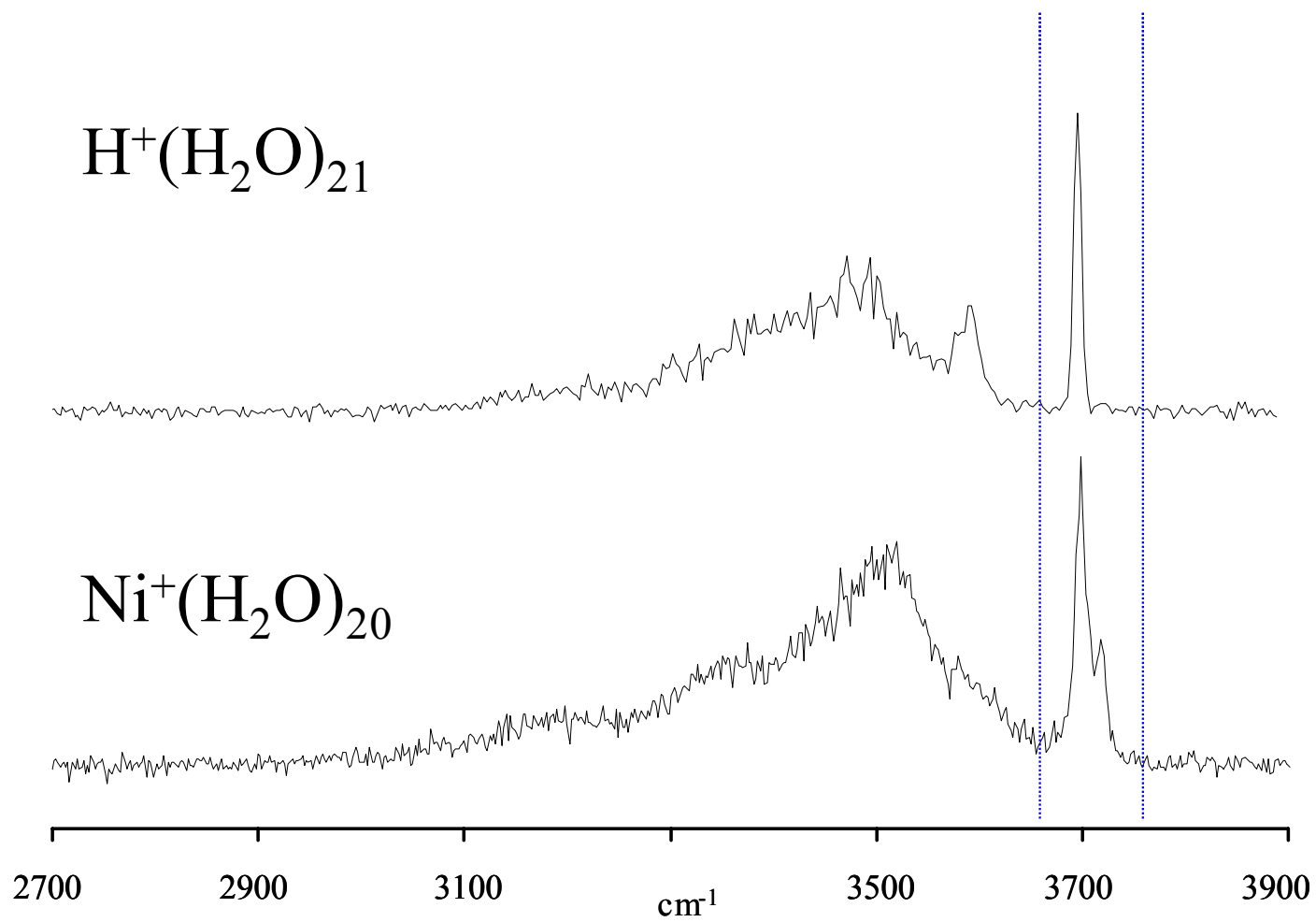
$\text{Ni}^+(\text{H}_2\text{O})_{18}$	3510, 3700, 3718
$\text{Ni}^+(\text{H}_2\text{O})_{19}$	3510, 3698, 3718
$\text{Ni}^+(\text{H}_2\text{O})_{20}$	3513, 3699, 3721
$\text{Ni}^+(\text{H}_2\text{O})_{21}$	3515, 3699, 3721
$\text{Ni}^+(\text{H}_2\text{O})_{22}$	3515, 3700, 3720
$\text{Ni}^+(\text{H}_2\text{O})_{23}$	3509, 3698, 3721
$\text{Ni}^+(\text{H}_2\text{O})_{24}$	3500, 3700, 3720
$\text{Ni}^+(\text{H}_2\text{O})_{25}$	3500, 3699, 3718
$\text{Ni}^+(\text{H}_2\text{O})_{26}$	3500, 3698, 3718
$\text{Ni}^+(\text{H}_2\text{O})_{28}$	xxxx, * 3698, 3718
$\text{Ni}^+(\text{H}_2\text{O})_{30}$	xxxx, * 3698, 3719

*no measurements in the hydrogen bonding region were done for these clusters.

However, the spacing between the modes does not change much even at the largest cluster size studied ($n = 30$). A spectral gap of $\sim 17 \text{ cm}^{-1}$ was observed between the AAD / AD bands in the larger $\text{H}^+(\text{H}_2\text{O})_n$ clusters.⁵² In the hydrated nickel ions, the bands are separated by 20 - 22 cm^{-1} as seen in Table 3.2. This suggests that there is some inductive effect from the nickel cation that permeates throughout the hydrogen-bonded network, even at the $n = 30$ cluster size. An essential yet unanswered question in condensed phase chemistry is: how many water molecules does it take to fully solvate a metal ion? According to the present work, it apparently requires more than thirty in the $\text{Ni}^+(\text{H}_2\text{O})_n$ system. Unfortunately, the spectra do not provide enough information to accurately determine the structures of the larger complexes, but insights can be gained in light of what has already been learned of the protonated water clusters.

Figure 3.7 shows the IRPD spectrum of $\text{Ni}^+(\text{H}_2\text{O})_{20}$ as it compares to the IRPD spectrum of the $\text{H}^+(\text{H}_2\text{O})_{21}$ cluster. The protonated $n = 21$ ‘magic number’ cluster has been studied extensively in the past,^{7,12,52} ever since Kebarle and coworkers first observed its special stability in mass spectrometry measurements.⁷ The various structures postulated for the $\text{H}^+(\text{H}_2\text{O})_{21}$ cluster have all centered on the formation of an $n = 20$ dodecahedron cage with one water located inside. Many questions remain concerning the location of the proton in this cluster, but both experiment and theory agree that its geometry is based on the dodecahedron structural motif.⁵² The main piece of evidence is the observation of a single band in the OH region arising from AAD-type water monomers in a high symmetry arrangement,⁵² as shown in the upper trace of Figure 3.7. Another key observation is the separation of

Figure 3.7 The IRPD spectra of $\text{Ni}^+(\text{H}_2\text{O})_{20}$ as it compares to the IRPD of $\text{H}^+(\text{H}_2\text{O})_{21}$.



the band near 3580 cm^{-1} from the broad envelop in the hydrogen-bonded region which is attributed to ring-based vibrations. The lower trace shows the IRPD spectrum of the $\text{Ni}^+(\text{H}_2\text{O})_{20}$ complex. Unlike the $\text{H}^+(\text{H}_2\text{O})_{21}$ cluster, two bands (AAD and AD) are observed near 3700 cm^{-1} for $\text{Ni}^+(\text{H}_2\text{O})_{20}$. In fact there is no evidence for high symmetry structures for any of the larger hydrated nickel ions studied. The presence of the nickel cation and its strong binding to the core water molecules prevent the symmetric clustering of subsequent waters and, therefore, the formation of the $n = 20$ dodecahedron. Apparently, the nickel cation continues to influence the clustering of water even out to $n = 30$.

Conclusions

Hydrated nickel cation complexes of the form $\text{Ni}^+(\text{H}_2\text{O})_n$ are produced in a laser vaporization pulsed nozzle cluster source, isolated by time-of-flight, and studied with infrared photodissociation spectroscopy. In addition, the IRPD spectrum of $\text{Ni}^+(\text{H}_2\text{O})\text{Ar}_2$ is also obtained, which contains two peaks in the OH region. Comparison of its vibrational spectrum to the predictions of theory confirm that the water molecule attaches to the nickel cation via the charge-dipole interaction to produce a C_{2v} symmetry structure and that the attachment of argon atoms cause only minor perturbations. The charge that is polarized toward the Ni^+ has some bonding character, therefore the binding in the water moiety is weakened and the OH vibrations shift to lower frequency. The IRPD spectrum of the $\text{Ni}^+(\text{H}_2\text{O})\text{Ar}_2$ complex compares favorably to the scaled harmonic frequencies predicted by DFT.

The pure $\text{Ni}^+(\text{H}_2\text{O})_n$ complexes dissociate efficiently beginning with the $n = 3$ complex, indicating that these clusters are internally heated during production, or that the $n = 3, 4$ complexes are efficient multiphoton absorbers. The IRPD spectrum of the $n = 3$ complex has two bands in the free OH region which correspond to symmetric and asymmetric OH vibrations, indicating that all three water molecules are bound to the nickel cation. New red-shifted bands begin to appear by $n = 4$ and are attributed to the onset of hydrogen bonding. Binding of the fourth water molecule to the second solvation layer is inconsistent with previous experiments,¹⁰ indicating isomers are present in the beam. Symmetric- and asymmetric-like OH stretches disappear by $n = 7$ and only AD- and AAD-type modes are observed near 3700 cm^{-1} . This suggests that more complex hydrogen-bonded networks are beginning at a surprisingly early stage of clustering. However, the IRPD spectra of the larger complexes do not provide any evidence of dodecahedron formation near the $n = 20$ size regime, as AD- and AAD-type OH bands are observed for all the larger cluster sizes studied. Comparison of the AD / ADD line spacings in the spectra of the hydrated nickel ions to that in the protonated water spectra suggest that inductive effects are present even out to $n = 30$. Future experiments for these complexes in the H-O-H bending region and more theoretical work will be required to determine the structures of these hydrated metal ions.

References

- (1) Hunt, J. P. *Metal Ions in Aqueous Solution*, W.A. Benjamin and Sons, New York, 1963.
- (2) a) Burgess, J. *Metal Ions in Solution*, John Wiley and Sons, New York, 1978.
b) Burgess, J. *Ions in Solution*, Horwood Publishing, Chichester, UK, 1999.
- (3) Richens, D. T. *The Chemistry of Aqua Ions*, John Wiley, Chichester, 1997.
- (4) Freiser, B. S., ed., *Organometallic Ion Chemistry*, Kluwer, Dordrecht, 1996.
- (5) Duncan, M. A., ed. *Adv. Metal and Semiconductor Clusters*, Elsevier, Amsterdam, 2001, Vol. 5.
- (6) Duncan, M. A. *Int. J. Mass Spectrom.* **2000**, 200, 545.
- (7) Kebarle, P. *Ann. Rev. Phys. Chem.* **1977**, 28, 445.
- (8) Marinelli, P. J.; Squires, R. R. *J. Am. Chem. Soc.* **1989**, 111, 4101.
- (9) a) Magnera, T. M.; David, D. E.; Michl, J. *J. Am. Chem. Soc.* **1989**, 111, 4100. b) Magnera, T. M.; David, D. E.; Stulik, D.; Orth, R. G.; Jonkman, H. T.; Michl, J. *J. Am. Chem. Soc.* **1989**, 111, 5036.
- (10) a) Dalleska, N. F.; Honma, K.; Sunderlin, L. S.; Armentrout, P. B. *J. Am. Chem. Soc.* **1994**, 116, 3519. b) Clemmer, D. E.; Chen, Y.-M.; Aristov, N.; Armentrout, P. B. *J. Phys. Chem.* **1994**, 98, 7538. c) Dalleska, N. F.; Tjelta, B. L.; Armentrout, P. B. *J. Phys. Chem.* **1994**, 98, 4191. d) Rogers, M. T.; Armentrout, P. B. *J. Phys. Chem. A* **1997**, 101, 1238. e) Koizumi, H.; Larson, M.; Muntean, F.; Armentrout, P. B. *Int. J. Mass Spectrom.* **2003**, 228, 221.

- (11) a) Poisson, L.; Lepetit, F.; Mestdagh, J. -M.; Visticot, J. -P. *J. Phys. Chem. A* **2002**, *106*, 5455. b) Poisson, L.; Dukan, L.; Sunlemontier, O.; Lepetit, F.; Reau, F.; Pradel, P.; Mestdagh, J. -M.; Visticot, J. -P. *Int. J. Mass Spectrom.* **2002**, *220*, 111. c) Poisson, L.; Pradel, P.; Lepetit, F.; Reau, F.; Mestdagh, J. -M.; Visticot, J. -P. *Eur. Phys. J. D* **2001**, *14*, 89. d) Dukan, L.; del Fabbro, L.; Pradel, P.; Sunlemontier, O.; Mestdagh, J. -M.; Visticot, J. -P. *Eur. Phys. J. D* **1998**, *3*, 257.
- (12) Harms, A. C.; Khanna, S. N.; Chen, B.; Castleman, A. W., Jr. *J. Chem. Phys.* **1994**, *100*, 3540.
- (13) a) Beyer, M. B. C.; Gorlitzer, H. W.; Schindler, T.; Achatz, U.; Albert, G.; Niedner-Schatteburg, G.; Bondybey, V. E. *J. Am. Chem. Soc.* **1996**, *118*, 7386. b) Beyer, M. A., Achatz, U.; Berg, C.; Joos, S.; Niedner-Schatteburg, G.; Bondybey, V. E. *J. Phys. Chem. A* **1999**, *103*, 671. c) Bondybey, V. E.; Beyer, M. K. *Intl. Rev. Phys. Chem.* **2002**, *21*, 277. d) Fox, B. S.; Balteanu, I.; Balaj, O. P.; Liu, H.; Beyer, M. K.; Bondybey, V. E. *Phys. Chem. Chem. Phys.* **2002**, *4*, 2224. e) Berg, C.; Achatz, U.; Beyer, M. K.; Joos, S.; Albert, G.; Schindler, T.; Niedner-Schatteburg, G.; Bondybey, V. E. *Intl. J. Mass Spectrom.* **1997**, *167/168*, 723. f) Berg, C.; Beyer, M. K.; Achatz, U.; Joos, S.; Niedner-Schatteburg, G.; Bondybey, V. E. *Chem. Phys.* **1998**, *239*, 379. g) Bondybey, V. E.; Beyer, M. K.; Achatz, U.; Fox, B.; Niedner-Schatteburg, G. *Adv. Met. & Semicond. Clusters*, **2001**, *5*, 295.
- (14) a) Klassen, J. S.; Ho, Y.; Blades, A. T.; Kebarle, P. *Adv. Gas Phase Ion Chem.* **1998**, *3*, 255. b) Peschke, M.; Blades, A. T.; Kebarle, P. *J. Phys.*

- Chem. A* **1998**, *102*, 9978. c) Nielsen, S. B.; Masella, M.; Kebarle, P. *J. Phys. Chem. A* **1999**, *103*, 9891. d) Peschke, M.; Blades, A. T.; Kebarle, P. *Intl. J. Mass Spectrom.* **1999**, *185*, 685. e) Peschke, M.; Blades, A. T.; Kebarle, P. *J. Am. Chem. Soc.* **2000**, *122*, 10440. f) Peschke, M.; Blades, A. T.; Kebarle, P. *Adv. Met. Semicond. Clusters* **2001**, *5*, 77.
- (15) a) Stace, A. J.; Walker, N. R.; Firth, S. *J. Am. Chem. Soc.* **1997**, *119*, 10239. b) Walker, N. R.; Firth, S.; Stace, A. J. *Chem. Phys. Lett.* **1998**, *292*, 125. c) Walker, N.; Dobson, M. P.; Wright, R. R.; Barran, P. E.; Murrell, J. N.; Stace, A. J. *J. Am. Chem. Soc.* **2000**, *122*, 11138. d) Stace, A. J. *Adv. Met. Semicond. Clusters* **2001**, *5*, 121. e) Cox, H.; Akibo-Betts, G.; Wright, R. R.; Walker, N. R.; Curtis, S.; Duncombe, B.; Stace, A. J. *J. Am. Chem. Soc.* **2003**, *125*, 233. f) Stace, A. J. *J. Phys. Chem. A* **2002**, *106*, 7993.
- (16) Schroeder, D.; Schwarz, H.; Wu, J.; Desdemiotis, C. *Chem. Phys. Lett.* **2001**, *343*, 258.
- (17) a) Rodriguez-Cruz, S.; Jockusch, R. A.; Williams, E. R. *J. Am. Chem. Soc.* **1998**, *120*, 5842. b) Rodriguez-Cruz, S.; Jockusch, R. A.; Williams, E. R. *J. Am. Chem. Soc.* **1999**, *121*, 1986. c) Rodriguez-Cruz, S.; Jockusch, R. A.; Williams, E. R. *J. Am. Chem. Soc.* **1999**, *121*, 8898. c) Wong, R. L.; Paech, K.; Williams, E. R. *Intl. J. Mass Spectrom.* **2004**, *232*, 59.
- (18) Shvartsburg, A. A.; Siu, K. W. M. *J. Am. Chem. Soc.* **2001**, *123*, 10071-1075.
- (19) a) Hrusak, J.; Stoeckigt, D.; Schwarz, H. *Chem. Phys. Lett.* **1994**, *221*, 518. b) Hrusak, J.; Schroeder, D.; Schwarz, H. *Chem. Phys. Lett.* **1994**, *225*, 416.

- (20) a) Rosi, M.; Bauschlicher, C. W., Jr. *J. Chem. Phys.* **1989**, *90*, 7264. b) Rosi, M.; Bauschlicher, C. W. *J. Chem. Phys.* **1990**, *92*, 1876. c) Bauschlicher, C. W., Jr.; Partridge, H. *J. Phys. Chem.* **1991**, *95*, 3946. d) Bauschlicher, C. W.; Langhoff, S. R.; Partridge, H. *J. Chem. Phys.* **1991**, *94*, 2068. e) Bauschlicher, C. W., Jr.; Sodupe, M.; Partridge, H. *J. Chem. Phys.* **1992**, *96*, 4453. f) Partridge, H.; Bauschlicher, C. W., Jr. *Chem. Phys. Lett.* **1992**, *195*, 494. g) Sodupe, M.; Bauschlicher, C. W., Jr. *Chem. Phys. Lett.* **1993**, *212*, 624. h) Ricca, A.; Bauschlicher, C. W. *J. Phys. Chem. A* **1995**, *99*, 9003. i) Ricca, A.; Bauschlicher, C. W. *J. Phys. Chem. A* **2002**, *106*, 3219. j) Zhou, M.; Andrews, L.; Bauschlicher, C. W., Jr. *Chem. Rev.* **2001**, *101*, 1931.
- (21) a) Watanabe, H.; Iwata, S.; Hashimoto, K.; Misaizu, F.; Fuke, K. *J. Am. Chem. Soc.* **1995**, *117*, 755. b) Watanabe, H.; Iwata, S. *J. Phys. Chem. A* **1997**, *101*, 487. c) Watanabe, H.; Iwata, S. *J. Chem. Phys.* **1998**, *108*, 10078. d) Fuke, K.; Hashimoto, K.; Iwata, S. *Adv. Chem. Phys.* **1999**, *110*, 431. e) Watanabe, H.; Iwata, S. *J. Phys. Chem.* **1996**, *100*, 3377.
- (22) Adamo, C.; Lelj, F. *J. Mol. Struct. THEOCHEM* **1997**, *389*, 8389.
- (23) a) Irigoras, A.; Fowler, J. E.; Ugalde, J. M. *J. Am. Chem. Soc.* **1999**, *121*, 574. b) Irigoras, A.; Fowler, J. E.; Ugalde, J. M. *J. Am. Chem. Soc.* **1999**, *121*, 8549. c) Irigoras, A.; Elizalde, O.; Silanes, I.; Fowler, J. E.; Ugalde, J. M. *J. Am. Chem. Soc.* **2000**, *122*, 114.
- (24) Klippenstein, S. J.; Yang, C. –N. *Intl. J. Mass Spectrom.* **2000**, *201*, 253.
- (25) Feller, D.; Glendenning, E. D.; de Jong, W. A. *J. Chem. Phys.* **1999**, *110*, 1475.

- (26) El-Nahas, A. M. *Chem. Phys. Letters* **2001**, 345, 325.
- (27) a) Reinhard, B. M.; Niedner-Schatteburg, G. *J. Phys. Chem. A*, **2002**, 106, 7988. b) Reinhard, B. M.; Niedner-Schatteburg, G. *Phys. Chem. Chem. Phys.* **2002**, 4, 1471. c) Reinhard, B. M.; Niedner-Schatteburg, G. *J. Chem. Phys.* **2003**, 118, 3571.
- (28) Lee, E. C.; Lee, H. M.; Tarakeshwar, P.; Kim, K. S. *J. Chem. Phys.* **2003**, 119, 7725.
- (29) a) Markham, G. D.; Glusker, J. P.; Bock, C. W. *J. Phys. Chem. B* **2002**, 106, 5118. b) Bock, C. W.; Markham, G. D.; Katz, A. K.; Glusker, J. P. *Inorg. Chem.* **2003**, 42, 1538. c) Trachtman, M.; Markham, G. D.; Glusker, J. P.; George, P.; Bock, C. W. *Inorg. Chem.* **1998**, 37, 4421.
- (30) a) Lessen, D. E.; Brucat, P. J. *Chem. Phys. Lett.* **1988**, 152, 473. b) Lessen, D. E.; Asher, R. L.; Brucat, P. J. *Adv. Metal & Semicon. Clust.* **1993**, 1, 267. c) Lessen, D. E.; Asher, R. L.; Brucat, P. J. *J. Chem. Phys.* **1990**, 93, 6102.
- (31) a) Shen, M. H.; Farrar, J. M. *J. Chem. Phys.* **1991**, 94, 3322. b) Shen, M. H.; Winniczek, J. W.; Farrar, J. M. *J. Phys. Chem.* **1987**, 91, 6447.
- (32) a) Willey, K. F.; Yeh, C. S.; Robbins, D.; Pilgrim, J. S.; Duncan, M. A. *J. Chem. Phys.* **1992**, 97, 8886. b) Scurlock, C. T.; Pullins, S. H.; Reddic, J. E.; Duncan, M. A. *J. Chem. Phys.* **1996**, 104, 4591. c) Duncan, M. A. *Ann. Rev. Phys. Chem.* **1997**, 48, 69.
- (33) a) Sanekata, M.; Misaizu, F.; Fuke, K. *J. Chem. Phys.* **1996**, 104, 9768. b) Misaizu, F.; Sanekata, M.; Tsukamoto, K.; Fuke, K.; Iwata, S. *J. Phys. Chem.* **1992**, 96, 8259. c) Misaizu, F.; Sanekata, M.; Fuke, K.; Iwata, S. *J. Chem.*

- Phys.* **1994**, *100*, 1161. d) Sanekata, M.; Misaizu, F.; Fuke, K.; Iwata, S.; Hashimoto, K. *J. Am. Chem. Soc.* **1995**, *117*, 747. e) Fuke, K.; Hashimoto, K.; Takasu, R. *Adv. Met. Semicond. Clusters*, **2001**, *5*, 1.
- (34) a) Faherty, K. P.; Thompson, C. J.; Aguirre, F.; Michne, J.; Metz, R. B. *J. Phys. Chem.* **2001**, *105*, 10054. b) Thompson, C. J.; Husband, J.; Aguirre, F.; Metz, R. B. *J. Phys. Chem. A* **2000**, *104*, 8155. c) Thompson, C. J.; Aguirre, F.; Husband, J.; Metz, R. B. *J. Phys. Chem. A* **2000**, *104*, 9901. d) Beyer, M. K.; Metz, R. B. *J. Phys. Chem. A* **2003**, *107*, 1760. e) Metz, R. B. *Intl. J. Mass Spectrom.* **2004**, *235*, 131.
- (35) Wang, K.; Rodham, D. A.; McKoy, V.; Blake, G. A. *J. Chem. Phys.* **1998**, *108*, 4817.
- (36) Agreiter, J. K.; Knight, A. M.; Duncan, M. A. *Chem. Phys. Lett.* **1999**, *313*, 162.
- (37) a) Cabarcos, O. M.; Weinheimer, C. J.; Lisy, J. M. *J. Chem. Phys.* **1999**, *110*, 8429. b) Cabarcos, O. M.; Weinheimer, C. J.; Lisy, J. M. *J. Chem. Phys.* **1998**, *108*, 5151. c) Lisy, J. M. *Int. Rev. Phys. Chem.* **1997**, *16*, 267. d) Weinheimer, C. J.; Lisy, J. M. *J. Chem. Phys.* **1996**, *105*, 2938. e) Lisy, J. M. *Cluster Ions* **1993**, 217. f) Vaden, T. D.; Forinash, B.; Lisy, J. M. *J. Chem. Phys.* **2002**, *117*, 46284631. g) Vaden, T. D.; Weinheimer, C. J.; Lisy, J. M. *J. Chem. Phys.* **2004**, *121*, 3102. k) Patwari, G. N.; Lisy, J. M. *J. Chem. Phys.* **2003**, *118*, 8555.

- (38) a) Inokuchi, Y.; Ohshimo, K.; Misaizu, F.; Nishi, N. *Chem. Phys. Lett.* **2004**, 390, 140. b) Inokuchi, Y.; Ohshimo, K.; Misaizu, F.; Nishi, N. *J. Phys. Chem. A*, **2004**, 108, 5034.
- (39) a) Walker, N. R.; Walters, R. S.; Pillai, E. D.; Duncan, M. A. *J. Chem. Phys.* **2003**, 119, 10471. b) Walters, R. S.; Duncan, M. A. *Austr. J. Chem.* **2004**, 57, 1145. c) Walker, N. R.; Walters, R. S.; Tsai, C.-S.; Jordan, K. D.; Duncan, M. A. *J. Phys. Chem. A*, submitted.
- (40) Duncan, M. A. *Intl. Rev. Phys. Chem.* **2003**, 22, 407.
- (41) Shimanouchi, T. *Molecular Vibrational Frequencies*, 69 ed.; Chemistry WebBook, NIST Standard Reference Database (<http://webbook.nist.gov>), 2001.
- (42) a) Pimentel, G. C.; McClellan, A. L. *The Hydrogen Bond*, Freeman, San Francisco, 1960. b) Pimentel, G. C.; McClellan, A. L. *Ann. Rev. Phys. Chem.* **1971**, 22, 347.
- (43) Schuster, P.; Zundel, G.; Sandorfy, C., eds. *The Hydrogen Bond: Recent Developments in Theory and Experiments*, 1976, Vol. 2.
- (44) Jeffrey, G. A. *An Introduction to Hydrogen Bonding*, Oxford University Press, 1997.
- (45) Scheiner, S. *Hydrogen Bonding, A Theoretical Perspective*, Oxford University Press, 1997.
- (46) a) Yeh, L. I.; Okumura, M.; Myers, J. D.; Price, J. M.; Lee, Y. T. *J. Chem. Phys.* **1989**, 91, 7319. b) Yeh, L. I.; Lee, Y. T.; Hougen, J. T. *J. Mol. Spec.* **1994**, 164, 473. c) Crofteon, M. W.; Price, J. M.; Lee, Y. T. *Springer Ser.*

- Chem. Phys.* **1994**, 56 (Clusters of Atoms and Molecules II), 44. d) Wu, C. C.; Jiang, J. C.; Boo, D. W.; Lin, S. H.; Lee, Y. T.; Chang, H. C. *J. Chem. Phys.* **2000**, 112, 176. e) Jiang, J.-C.; Wang, Y.-S.; Chang, H.-C.; Lin, Sheng H.; Lee, Y. T.; Niedner-Schatteburg, G.; Chang, H.-C. *J. Am. Chem. Soc.* **2000**, 122, 1398. f) Chaudhuri, C.; Wang, Y. S.; Jiang, J. C.; Lee, Y. T.; Chang, H. C.; Niedner-Schatteburg, G. *Molecular Physics* **2001**, 99, 1161.
- (47) a) Choi, J. H.; Kuwata, K. T.; Haas, B. M.; Cao, Y.; Johnson, M. S.; Okumura, M. *J. Chem. Phys.* **1994**, 100, 7153. b) Choi, J. H.; Kuwata, K. T.; Cao, Y. B.; Okumura, M. *J. Phys. Chem. A* **1998**, 102, 503. c) Johnson, M. S.; Kuwata, K. T.; Wong, C. K.; Okumura, M. *Chem. Phys. Lett.* **1996**, 260, 551.
- (48) a) Bailey, C. G.; Kim, J.; Dessent, C. E. H.; Johnson, M. A. *Chem. Phys. Lett.* **1997**, 269, 122. b) Ayotte, P.; Weddle, G. H.; Kim, J.; Johnson, M. A. *Chem. Phys.* **1998**, 239, 485. c) Ayotte, P.; Weddle, G. H.; Kim, J.; Johnson, M. A. *J. Am. Chem. Soc.* **1998**, 120, 12361. d) Ayotte, P.; Bailey, C. G.; Kim, J.; Johnson, M. A. *J. Chem. Phys.* **1998**, 108, 444. e) Ayotte, Patrick; Nielsen, Steen B.; Weddle, Gary H.; Johnson, Mark A.; Xantheas, Sotiris S. *J. Phys. Chem. A* **1999**, 103, 10665. f) Price, E. A.; Robertson, W. H.; Diken, E. G.; Weddle, G. H.; Johnson, M. A. *Chem. Phys. Lett.* **2002**, 366, 412. g) Corcelli, S. A.; Kelley, J. A.; Tully, J. C.; Johnson, M. A. *J. Phys. Chem. A* **2002**, 106, 4872. h) Robertson, W. H.; Johnson, M. A. *Ann. Rev. Phys. Chem.* **2003**, 54, 173. i) Robertson, W. H.; Diken, E. G.; Shin, J. -W.; Johnson, M. A. *Science* **2003**, 299, 1367. j) Hammer, N. I.; Shin, J. -W.; Headrick, J. M.; Diken, E.

- G.; Rosciolli, J. R.; Weddle, G. H.; Johnson, M. A. *Science* **2004**, *306*, 675.
- k) Price, E. A.; Hammer, N. I.; Johnson, M. A. *J. Phys. Chem. A* **2004**, *108*, 3910. l) Diken, E. G.; Robertson, W. H.; Johnson, M. A. *J. Phys. Chem. A* **2004**, *108*, 64. m) Headrick, J. M.; Bopp, J. C.; Johnson, M. A. *J. Chem. Phys.* **2004**, *121*, 11523.
- (49) a) Sawamura, T.; Fujii, A.; Sato, S.; Ebata, T.; Mikami, N. *J. Phys. Chem.* **1996**, *100*, 8131. b) Ebata, T.; Fujii, A.; Mikami, N. *Intl. Rev. Phys. Chem.* **1998**, *17*, 331. c) Miyazaki, M.; Fujii, A.; Ebata, T.; Mikami, N. *Science* **2004**, *304*, 1134. d) Miyazaki, M.; Fujii, A.; Ebata, T.; Mikami, N. *J. Phys. Chem. A* **2004**, *108*, 10656. e) Miyazaki, M.; Fujii, A.; Ebata, T.; Mikami, N. *Phys. Chem. Chem. Phys.* **2003**, *5*, 1137.
- (50) a) Bieske, E. J.; Dopfer, O. *Chem. Rev.* **2000**, *100*, 3963. b) Dopfer, O.; Roth, D.; Maier, J. P. *J. Phys. Chem. A* **2000**, *104*, 11702. c) Dopfer, O.; Roth, D.; Maier, J. P. *J. Chem. Phys.* **2001**, *114*, 7081.
- (51) a) Lehr, L.; Zanni, M. T.; Frischkorn, C.; Weinkauff, R.; Neumark, D. M. *Science* **1999**, *284*, 635. b) Asmis, K. R.; Pivonka, N. L.; Santambrogio, G.; Bruemmer, M.; Kaposta, C.; Neumark, D. M.; Woeste, L. *Science* **2003**, *299*, 1375.
- (52) Shin, J. -W.; Hammer, N. I.; Diken, E. G.; Johnson, M. A.; Walters, R. S.; Jaeger, T. D.; Duncan, M. A.; Christie, R. A.; Jordan, K. D. *Science* **2004**, *304*, 1137.
- (53) Fridgen, T. D.; McMahon, T. B.; MacAleese, L.; Lemaire, J.; Maitre, P. J. *J. Phys. Chem. A* **2004**, *108*, 9008.

- (54) Frisch, M. J.; Trucks, G. W.; Schlegel, H. B.; Scuseria, G. E.; Robb, M. A.; Cheeseman, J. R.; Montgomery, J. A.; Vreven, T.; Kudin, K. N.; Burant, J. C.; Millam, J. M.; Iyengar, S. S.; Tomasi, J.; Barone, V.; Mennucci, B.; Cossi, M.; Scalmani, G.; Rega, N.; Petersson, G. A.; Nakatsuji, H.; Hada, M.; Ehara, M.; Toyota, K.; Fukuda, R.; Hasegawa, J.; Ishida, M.; Nakajima, T.; Honda, Y.; Kitao, O.; Nakai, H.; Klene, M.; Li, X.; Knox, J. E.; Hratchian, H. P.; Cross, J. B.; Adamo, C.; Jaramillo, J.; Gomperts, R.; Stratmann, R. E.; Yazyev, O.; Austin, A. J.; Cammi, R.; Pomelli, C.; Ochterski, J. W.; Ayala, P. Y.; Morokuma, K.; Voth, G. A.; Salvador, P.; Dannenberg, J. J.; Zakrzewski, V. G.; Dapprich, S.; Daniels, A. D.; Strain, M. C.; Farkas, O.; Malick, D. K.; Liashenko, A.; Piskorz, P.; Komaromi, I.; Martin, R. L.; Fox, D. J.; Keith, T.; Al-Laham, M. A.; Peng, C. Y.; Nanayakkara, A.; Challacombe, M.; Gill, P. M. W.; Johnson, B.; Chen, W.; Wong, M. W.; Gonzalez, C.; Pople, J. A. *Gaussian 03 (Rev. B.02)*; Gaussian, Inc., Pittsburgh, PA.
- (55) a) Becke, A. D. *J. Chem. Phys.* **1993**, 98, 5648. b) Lee, C.; Yang, W.; Parr, R. G. *Phys. Rev. B* **1988**, 37, 785.
- (56) a) Walters, R. S.; Jaeger, T. D.; Duncan, M. A. *J. Phys. Chem. A* **2002**, 106, 10482. b) Walters, R. S.; Schleyer, P. v. R.; Corminboeuf, C.; Duncan, M. A. *J. Am. Chem. Soc.* **2004**, submitted. c) Walters, R. S.; Schleyer, P. v. R.; Duncan, M. A. *J. Am. Chem. Soc.*, submitted.
- (57) a) Walker, N. R.; Gries, G. A.; Walters, R. S.; Duncan, M. A. *J. Chem. Phys.* **2004**, 121, 10498. b) Walker, N. R.; Gries, G. A.; Walters, R. S.; Duncan, M. A. *Chem. Phys. Lett.* **2003**, 380, 230.

- (58) a) Walters, R. S.; Brinkmann, N. R.; Schaefer, H. F.; Duncan, M. A. *J. of Phys. Chem. A* **2003**, *107*, 7396. b) Gregoire, G.; Brinkmann, N. R.; van Heijnsbergen, D.; Schaefer, H. F.; Duncan, M. A.. *J. Phys. Chem. A* **2003**, *107*, 218.
- (59) Cotton, F. A.; Wilkinson, G. W. *Advanced Inorganic Chemistry*, Wiley, New York, 1988.
- (60) a) Richmond, G. L. *Annu. Rev. Phys. Chem.* **2001**, *52*, 357. b) Richmond, G. L. *Chem. Rev.* **2001**, *102*, 2693.

CHAPTER IV

VIBRATIONAL SPECTROSCOPY OF NICKEL CATION-ACETYLENE
COMPLEXES: A STUDY OF METAL ION- π BONDING¹

¹ Walters, R.S.; Pillai, E.D.; Schleyer, P.v.R.; Duncan, M.A. To be submitted to *J. Am. Chem. Soc.*

Abstract

Nickel ion-acetylene complexes of the form $\text{Ni}^+(\text{C}_2\text{H}_2)_n$, $\text{Ni}^+(\text{C}_2\text{H}_2)\text{Ne}$ and $\text{Ni}^+(\text{C}_2\text{H}_2)_n\text{Ar}_m$, where $n=1-4$, are produced in a laser vaporization pulsed-nozzle cluster source. The ions are size-selected and studied in a reflectron time-of-flight mass spectrometer by infrared photodissociation (IRPD) spectroscopy in the C-H stretch region. The experimental fragmentation patterns are consistent with a coordination of four for this system. The $n = 1 - 4$ complexes both with and without rare gas atoms are also investigated with density functional theory (DFT). The combined IR spectra and theory show that π -complexes are formed for the $n = 1 - 4$ molecules, causing the C-H stretches in the acetylene ligands to shift to lower frequencies. Spectra and theory also reveal that there are two doublet states that are nearly isoenergetic for the $\text{Ni}^+(\text{C}_2\text{H}_2)$ complexes and Jahn-Teller effects are present for $n = 2 - 4$. Attaching rare gas atoms results in only minor perturbations on the structures for all complexes except $n = 3$, where the presence of argon causes the nickel ion to no longer reside in the acetylene center-of-mass plane. This induces a $30\text{-}50\text{ cm}^{-1}$ red shift of its C-H stretches and increases IR intensities significantly. The binding of the fourth acetylene is relatively weak, even though it attaches directly to the metal. The IR spectrum of the $\text{Ni}^+(\text{C}_2\text{H}_2)_4$ complex is consistent with an acetylene arrangement around the nickel cation that is nearly tetrahedral.

Introduction

Transition metal-olefin complexes play an important role in catalysis and have been studied extensively in the past in organometallic chemistry.^{1,2} Gas-phase organometallic clusters serve as convenient models to study the effects of π -bonding and these systems have been investigated with theory.³⁻⁶ Reactions of transition metals with hydrocarbons and the details of their energetics have been observed in gas phase ion chemistry.⁷⁻¹³ Equilibrium mass spectrometry and collision-induced-dissociation (CID) and have been employed to determine bond strengths of metal ion- π complexes,^{14,15} and electronic spectroscopy has been used to probe their excited states.^{16,17} However, information on these complexes in their ground states is somewhat limited. Infrared and Raman spectroscopies are common techniques to study organometallic compounds in the condensed phase,^{1,18-24} but applying these methods to the gas phase is difficult because of the low sample densities inherent to molecular beams. However, recent advances in infrared lasers now enable metal-ligand complexes to be studied via photodissociation,²⁵⁻³⁶ and our group has reported the first infrared photodissociation (IRPD) spectra of transition metal ion complexes.²⁸⁻³⁶ In this paper we report on the IRPD spectroscopy of various $\text{Ni}^+(\text{C}_2\text{H}_2)_{1-4}$ complexes as a study of metal ion π -bonding. The spectra are acquired in the C-H stretch region and compared to harmonic frequencies calculated with density functional theory.

Transition metal-acetylene complexes have been studied since Chatt et al. first synthesized various platinum-acetylene compounds.¹⁹ Maitlis and co-workers studied

nickel-acetylene complexes by IR spectroscopy in the $\text{C}\equiv\text{C}$ stretch stretch region.²⁰ From these and similar studies on metal-ethylene and metal-carbonyl complexes,^{1,18-20} a qualitative picture of the metal-ligand interaction known as the Dewar-Chatt-Duncanson (DCD) π -bonding model was developed. Briefly, there is σ -type forward donation from the filled π orbitals of acetylene into the empty metal d orbitals, and π -type back donation from the filled metal d orbitals into the π^* of acetylene. Both factors weaken the bonding in acetylene, lowering its vibrational frequencies. Most condensed phase metal -acetylene studies have focused on how the π -interaction affects the $\text{C}\equiv\text{C}$ stretch in the olefin, as this mode is commonly the most perturbed.¹⁸⁻²⁰ However, condensed phase spectra are often congested due to overlapping vibronic transitions and solvent effects, precluding absolute assignment of the structures for these transition metal clusters.

Gas phase organometallic complexes are solvent free and IR spectroscopy studies can, in principle, reveal their structural details. Geometric and electronic structures of metal ion π -complexes have been investigated theoretically by a number of groups.³⁻⁶ The driving force behind the theoretical work on transition metal- π complexes is the desire to accurately describe the interplay between electrostatic and covalent forces that are involved in the metal-olefin bond. Bauschlicher was one of the first to investigate the details of the π -interaction in transition metal ion complexes using the modified coupled pair functional (MCPF) methodology.³ Schwarz and coworkers determined that π -backbonding was less important than σ -donation for M^+ -ethylene ($\text{M} = \text{Cu}, \text{Ag}, \text{Au}$) using DFT and HF/DFT hybrid methods.⁴ More recently, Frenking has incorporated an energy partitioning analysis

to DFT and *ab initio* computations to describe which forces dominate in a variety of organometallic clusters.⁵ Of particular interest to this paper, Klippenstein studied various metal ion- π complexes, including Ni^+ -acetylene, with DFT and *ab initio* to determine vibronic shifts caused by π -bonding.⁶

In addition to recent theoretical progress, experimental techniques have advanced to a point where the molecular phenomena of gas phase ions can be probed. Schwarz and coworkers have used mass spectrometry to study reactions of transition metal ions with various hydrocarbon molecules and compare their results to theory.^{4,7} Photodissociation has been employed by a number of groups to observe fragmentation pathways of metal ion- π complexes.⁸⁻¹⁰ Bond energies of transition metal ion- π complexes have been determined with equilibrium mass spectrometry by Bowers¹⁴ and with CID by Armentrout.¹⁵ Our group¹⁶ and Klieber and coworkers¹⁷ have studied metal ion- π complexes by electronic photodissociation spectroscopy, which revealed information on their excited states. However, the studies are limited to single ligand complexes with metal ions that have $\text{P} \leftarrow \text{S}$ transitions accessible with tunable dye lasers. Complexes containing transition metals and molecules with multiple ligands cannot be studied because they often predissociate when excited with ultraviolet or visible photons.

It is clear then that IR spectroscopy, which probes the ground states of these complexes, is necessary to elucidate their structures. Until recently, IR spectroscopy of isolated metal-olefins was limited to rare gas matrices.²²⁻²⁴ Advances in high power infrared lasers now enable us to study organometallic clusters in molecular beams free from matrix effects. IRPD spectroscopy of Group I and II metal ion-

molecule complexes has been reported by the Lisy group²⁵ and by Inokuchi and coworkers.²⁶ Our group was the first to apply this technique to transition metal ion complexes.²⁸⁻³⁶ In collaboration with the Meijer group, we studied metal ion-benzene complexes with a free electron laser (200 – 1600 cm^{-1}) to observe how π -bonding affects the benzene skeletal modes.²⁸ Recently, Maitre and coworkers used a similar free electron laser source to study various Fe^+ -hydrocarbon species.²⁷ We have extended these photodissociation studies to the C-H stretch region using a bench top infrared OPO laser system.²⁹⁻³⁶ In a recent communication, we reported on the IRPD spectroscopy of $\text{M}^+(\text{C}_2\text{H}_2)\text{Ar}_2$ ($\text{M} = \text{V}, \text{Fe}, \text{Co}, \text{Ni}$).³⁰ The spectra clearly show that $\text{Fe}^+(\text{C}_2\text{H}_2)$, $\text{Co}^+(\text{C}_2\text{H}_2)$, and $\text{Ni}^+(\text{C}_2\text{H}_2)$ are π -complexes and their C-H resonances shift in a regular way depending on which metal is involved. The vanadium system, on the other hand, forms a three-membered ring metallacycle and has C-H stretches similar to cyclopropene. In a previous letter, we studied $\text{Ni}^+(\text{C}_2\text{H}_2)_n$ complexes ($n=3-6$) with IRPD spectroscopy, which provided the first preliminary evidence for possible cyclization chemistry for this system in the gas phase.³¹ We continue here with a complete report on the IRPD spectroscopy of $\text{Ni}^+(\text{C}_2\text{H}_2)_{1-4}$ complexes. The spectra are acquired in the acetylene C-H stretch region (3000-3400 cm^{-1}). The complexes are also studied with theory at the B3LYP level. The combined spectra and theory provides detailed information on the ground state structures for these complexes and the effects of π -bonding.

Experimental

Nickel ion-acetylene complexes are produced in a laser vaporization-pulsed nozzle source and analyzed with a reflectron time-of-flight mass spectrometer. The source and molecular beam apparatus have been described previously.³³ The third harmonic of a Nd:YAG (355 nm) is used to vaporize a rotating nickel rod. Ions are produced directly from the laser plasma in our specially designed ‘cutaway’ source that typically produces molecules containing a single metal ion. $\text{Ni}^+(\text{C}_2\text{H}_2)_n$ clusters are made in a 5% acetylene in argon expansion. The mixed complexes, $\text{Ni}^+(\text{C}_2\text{H}_2)_n\text{Ar}_m$ and $\text{Ni}^+(\text{C}_2\text{H}_2)\text{Ne}$, are produced in expansions containing <1% acetylene in argon or 25:75 helium:neon, respectively. The pulsed nozzle is a General Valve Series 9 (1 mm orifice) operating at ~ 50 psi backing pressure and pulse durations near 250 μsec . The ions are skimmed into the differentially pumped mass spectrometer chamber where they are injected into the first drift region of the reflectron by pulsed acceleration voltages. They are then size-selected within the first flight tube by another set of pulsed voltages before entering the reflectron field. Photodissociation is accomplished with the output of an IR Optical Parametric Oscillator/Amplifier (OPO/OPA) at the turning point in the reflectron. Parent and daughter ions are reaccelerated down the second flight tube and detected using an electron multiplier tube (EMT). Data are transferred to a PC by an IEEE interface. Fragmentation is more efficient on resonance, thus monitoring the fragment ion yield as a function of IR laser wavelength produces the IRPD spectrum of the parent ion that has been mass-selected.

The OPO (Laservision) uses two KTP crystals pumped by the second harmonic (532 nm) of a Nd:YAG laser (Continuum 9010) to produce tunable 725 – 872 nm light which is then combined with the delayed fundamental (1064 nm) in the OPA. The OPA consists of four KTA crystals, which generate the tunable IR light (2050 – 4400 cm^{-1}) by difference frequency mixing. This output is then used to generate the IRPD spectra by exciting the ion-molecule complexes near the asymmetric and symmetric C-H stretches of acetylene, 3289 and 3374 cm^{-1} , respectively.³⁷ The IR output of the OPO/OPA is frequency calibrated in the C-H stretch region by acquiring the photo-acoustic spectrum of methane (2800-3200 cm^{-1}). It should be noted that we did not use this method of calibration in our previous paper on the IRPD spectra of $\text{Ni}^+(\text{C}_2\text{H}_2)_n$ ($n=3-6$) complexes.³¹ The energies reported here are accurate and the previous spectra are therefore incorrect by $\sim 14 \text{ cm}^{-1}$.

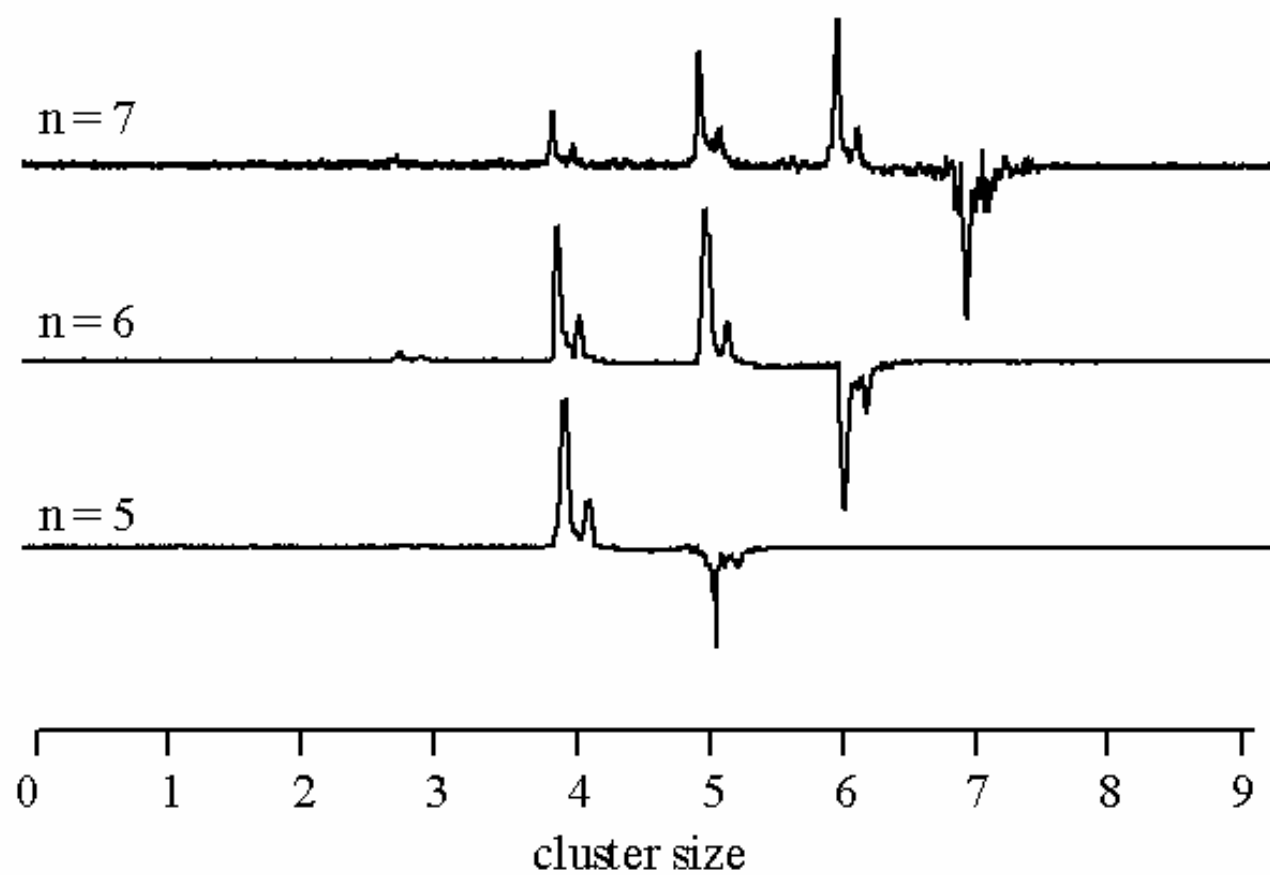
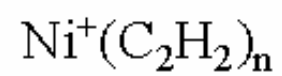
Vibrational spectra are compared to Density Functional Theory (DFT) calculations using the Gaussian '03 package (Windows version)³⁸ at the B3LYP level of theory.³⁹ The 6-311+G** basis set was utilized for the heavy atoms and we allowed for symmetry breaking to occur during the structural optimizations.

Discussion

$\text{Ni}^+(\text{C}_2\text{H}_2)_n$ complexes are size-selected and excited with the IR laser in the C-H stretch region of acetylene ($3000\text{-}3400\text{ cm}^{-1}$) to attempt photodissociation. As stated in our previous letter,²⁷ no photodissociation is observed for the $n = 1\text{-}2$ molecules and the $n = 3$ complex is difficult to fragment producing a broad spectrum with low signal-to-noise. Beginning with the $n = 4$ complex, the fragmentation yield increases and dissociation occurs by the loss of intact acetylene molecules. Figure 4.1 shows the fragmentation mass spectra of the $n = 5\text{-}7$ complexes. The multiplet observed at each cluster size is due to the natural isotopes of nickel. Data are recorded with the IR laser on and off, then subtracted from one another to generate these difference mass spectra. The negative peaks correspond to depletion of the mass-selected parent ions and the positive peaks are the daughter ions that are produced by photodissociation. All of the larger $\text{Ni}^+(\text{C}_2\text{H}_2)_n$ complexes terminate at $n = 4$, suggesting that the nickel cation prefers a coordination of four for acetylene. We also found a coordination of four in our study of $\text{Ni}^+(\text{CO}_2)_n$ clusters.³² Additionally, nickel compounds are known to prefer to be four coordinate in either a tetrahedral or square-planar configuration from traditional inorganic chemistry.⁴⁰

The smaller complexes are harder to dissociate because the IR photons do not impart the clusters with enough energy to break the weakest bond. Energy absorbed in the C-H region is transferred to the $\text{M}^+\text{-L}$ coordinate by intramolecular vibrational redistribution (IVR). If enough energy is absorbed and IVR is fast, then the cluster will dissociate by ligand elimination. The binding energy of the $\text{Ni}^+\text{-C}_2\text{H}_2$ complex has not been measured, but theory predicts it to be about 35.1 kcal/mol ,^{3,6} which

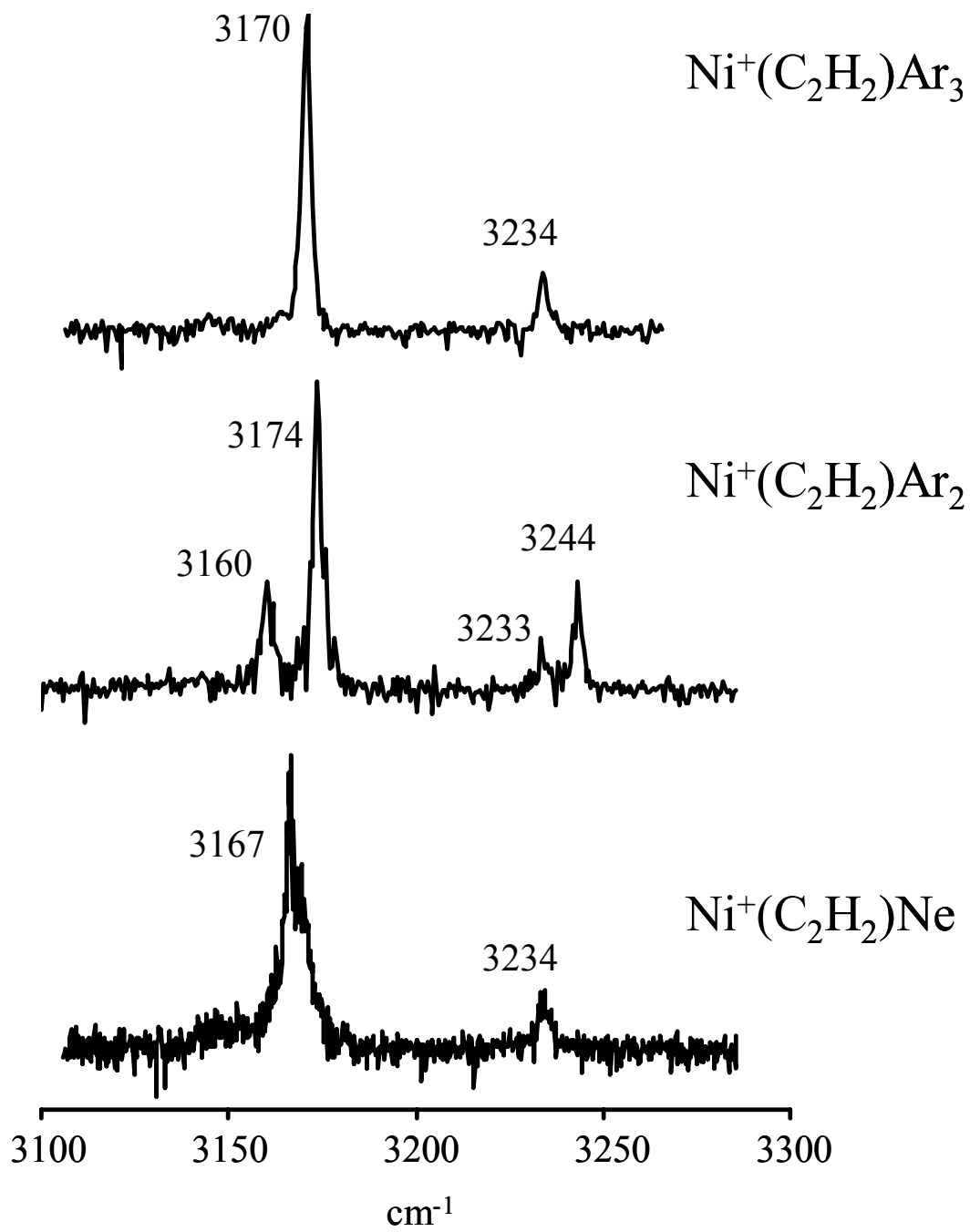
Figure 4.1 The IR photodissociation mass spectra of $\text{Ni}^+(\text{C}_2\text{H}_2)_{5-7}$. The negative peaks are the mass-selected parent ions, the positive peaks are the daughter ions produced by photodissociation. Fragmentation terminates at $n=4$, suggesting that Ni^+ prefers a coordination of four for this system.



corresponds to $\sim 12,300\text{ cm}^{-1}$. A multiphoton process is therefore necessary to dissociate this complex near 3200 cm^{-1} . However, the smaller clusters have lower state densities and multiphoton absorption is inefficient due to the loss of resonance at higher vibrational levels. The $n = 2, 3, 4$ complexes presumably have all ligands attached directly to the metal. Their bond energies are likely to decrease as binding is distributed to multiple acetylenes, but the per-molecule binding energy may still be greater than 3200 cm^{-1} . As the nickel ion is ‘solvated’ by more acetylene molecules, the sites around the metal will eventually fill and additional ligands must attach to existing ‘core’ acetylenes. The molecules in the second solvation layer should have binding energies similar to acetylene dimer ($\sim 400\text{ cm}^{-1}$)^{42,43} resulting from van der Waals forces. Absorption of a single photon should dissociate these complexes by eliminating the weakly bound, second layer ligands. The larger clusters also have higher state densities, increasing the efficiency of the multiphoton process and the rate of IVR. The lack of photodissociation signal observed for the smaller complexes and the increase in fragmentation yield for the larger sizes is therefore consistent with the energetics expected for this system.

Figure 4.2 shows the IRPD spectra of the Ni^+ -monoacetylene complexes with rare gas atoms attached. In order to acquire the spectra of the more strongly bound complexes, we employ a technique known as rare gas ‘tagging’ to improve the fragmentation process. The Y.T. Lee group was one of the first to enhance IR photodissociation by attaching weakly bound ‘messenger’ molecules (H_2 and N_2) to cluster ions.⁴⁴ It is now more common to attach rare gas (RG) atoms and many groups have employed this method to molecular ions.⁴⁵⁻⁴⁹ Our group^{29-30, 33-35} and

Figure 4.2 The IRPD spectra of the $\text{Ni}^+(\text{C}_2\text{H}_2)$ complexes tagged with various rare gas atoms in the $3100 - 3300 \text{ cm}^{-1}$ region. All spectra have bands that correspond to acetylenic C-H stretches. The $\text{Ni}^+(\text{C}_2\text{H}_2)\text{Ar}_2$ IRPD spectrum has four modes in this region due to the presence of a low-lying excited electronic state.



others^{21,22} have used this technique to study the more strongly bound metal ion-molecule complexes. For the small nickel cation-acetylene complexes, the rare gas atoms likely bind to the metal by a charge-induced dipole interaction. The tagged complexes have lower binding energies and higher state densities than the corresponding pure complexes and are therefore easier to dissociate. Excitation into the C-H stretches is transferred to the Ni⁺-RG coordinate via IVR and the tagged complexes dissociate by losing one or more rare gas atoms. Because the tag atoms are bound to the metal ion and do not interact with the ligand, the IRPD action spectra of the mixed complexes provide the best possible approximation to the IR absorption spectra of the corresponding pure complexes.

Each spectrum in Figure 4.2 was acquired in the mass channel that corresponds to the loss of a single rare gas atom. All of the spectra have features to the red of the free acetylene modes (3289 cm⁻¹ and 3374 cm⁻¹), consistent with the DCD model. Ni⁺(C₂H₂)Ar is difficult to dissociate, leading to a broad spectrum with poor signal-to-noise (not shown). The poor fragmentation of this complex is consistent with the marginal energetics for this system. Both theory⁴⁹ and experiment⁵⁰ agree that the Ni⁺-Ar bond is about 12 kcal/mol (~ 4000 cm⁻¹). If the Ni⁺-Ar bond strength in the Ni⁺(C₂H₂)Ar complex is close to this value, one photon cannot dissociate this complex near 3200 cm⁻¹. Attaching a second argon lowers the Ni⁺-Ar per-atom bond strength and increases the photodissociation efficiency. The middle trace shows the IRPD spectrum of the monoacetylene complex tagged with two argons. Two intense bands are observed at 3174/3244 cm⁻¹ and a weak pair of peaks appear at 3160/3233 cm⁻¹. When a third argon is added to this complex, the two doublets collapse to a

single pair of resonances at 3170 cm^{-1} and 3234 cm^{-1} as seen in the upper trace of Figure 4.2. In order to acquire a high quality spectrum of $\text{Ni}^+-\text{C}_2\text{H}_2$ with a single messenger atom we attach neon. The Ni^+-Ne bond is calculated to be 3.4 kcal/mol ($\sim 1190\text{ cm}^{-1}$)⁴⁹ and experiment puts it at 2.4 kcal/mol ($\sim 840\text{ cm}^{-1}$).⁵¹ Absorption of a single photon near 3200 cm^{-1} is then expected to dissociate the $\text{Ni}^+(\text{C}_2\text{H}_2)\text{Ne}$ complex. Consistent with this, the neon-tagged complex dissociates efficiently. The lower trace in Figure 4.2 shows the IRPD spectrum of this complex, which has two features at 3167 cm^{-1} and 3234 cm^{-1} .

Two IR-active bands are expected for the monoacetylene complexes. All of the spectra in Figure 4.2 have resonances near 3170 cm^{-1} and 3240 cm^{-1} . They correspond to the asymmetric and symmetric C-H stretches of the acetylene ligand within the cluster. The symmetric stretch is infrared inactive, but once acetylene is bound to the metal ion, the symmetry of the entire complex must be considered and this mode becomes active. The four bands observed for $\text{Ni}^+(\text{C}_2\text{H}_2)\text{Ar}_2$ present a problem as only two C-H stretches exist for the monoacetylene complex. The weak signals are red-shifted from the intense bands, but are still in the acetylene C-H region. The observation of four C-H modes suggests that another type of isomer might be present in the molecular beam.

Nickel is not known to insert into small hydrocarbons like the early transition metals do,¹¹⁻¹³ and no insertion products are observed in the mass spectrum. Also, such complexes would not have acetylenic C-H stretches ($3200\text{-}3400\text{ cm}^{-1}$), so we can rule out isomers generated from insertion chemistry. Another possibility is the presence of structural isomers with argon attached to acetylene. Similar isomers were

identified in our study of $M^+(H_2O)Ar_n$ ($M = Fe, Mg$), where the OH groups competed with the metal ion for the argon.^{35,36} Argon attached to water causes a significant red-shift of the OH stretching frequencies due to hydrogen bonding. An additional red-shift is possible here if argon binds to an acetylene CH group instead of the nickel cation. This could account for the weaker red-shifted peaks observed in the $Ni^+(C_2H_2)Ar_2$ spectrum. The strong bands might be from isomers where both argon atoms are attached directly to the metal, whereas the weaker signals arise from isomers where at least one argon is attached to acetylene. We therefore turn to theory in order to investigate this possibility and aid us in our interpretation.

Single point calculations were first performed at a lower level of theory using small basis sets before geometry optimizations were performed at the B3LYP level with the 6-311⁺G** basis set. This procedure was carried out on all the $Ni^+(C_2H_2)_{1-4}$ complexes discussed below and their structures are shown in Figure 4.3. DFT finds that the first acetylene binds to the nickel cation to form a 2B_1 π -complex with C_{2v} symmetry consistent with the previous DFT work by Klippenstein.⁶ The 2A_1 complex is calculated to lie ~ 1.5 kcal/mol higher in energy, whereas Modified Coupled Pair (MCP) calculations predict them to be isoenergetic as reported by Bauschlicher.³ Dissociation energies, scaled frequencies, intensities and key parameters for the DFT structures are listed in Table 4.1. The $Ni^+-C_2H_2$ interaction causes two main effects: the $C\equiv C$ bond is weakened and the hydrogen atoms are pushed away from the $C\equiv C$ axis to reduce repulsion from the nickel cation. The weakening of the binding in the acetylene moiety causes its stretching fundamentals to shift to lower energy, and the perturbation on the hydrogen atoms causes the symmetric C-H stretch to become

Figure 4.3 Theoretical structures of the $\text{Ni}^+(\text{C}_2\text{H}_2)_n$ ($n = 1, 2, 3, 4$) complexes computed with B3LYP using the 6-311⁺G** basis set.

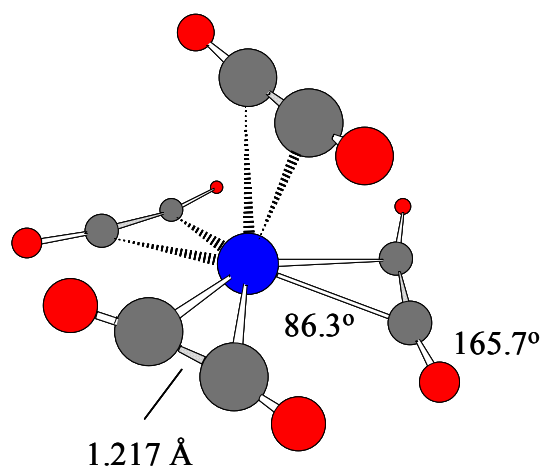
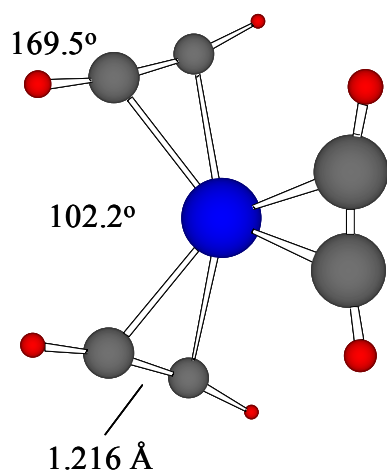
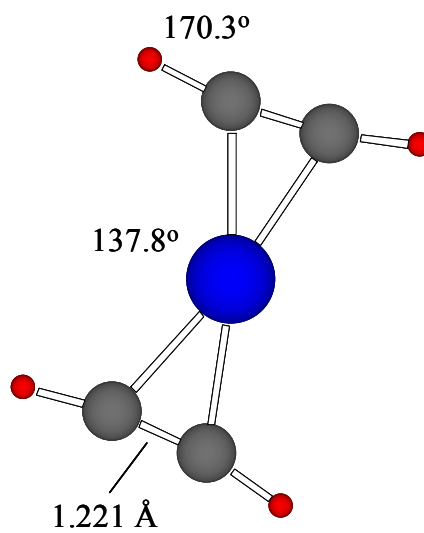
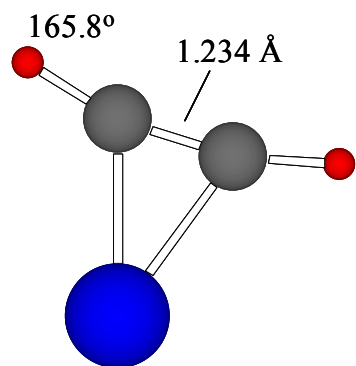


Table 4.1: B3LYP, 6-311⁺G** Energies, Frequencies, IR intensities and Structural information

Ni ⁺ (C ₂ H ₂) _n	Energies*	Frequencies (Ints) [†]	Key Structural Parameters				J-T angle [‡]
			M ⁺ -C (Å)	C≡C (Å)	CCH angle	C ₂ H ₂ Type	
n=1							
² B ₁	47.0	3156(232), 3240(27)	1.996, 1.997	1.234	165.8, 165.8	Core	
² A ₁	46.6	3165(225), 3251(26)	2.042, 2.042	1.228	166.8, 166.8	Core	
n=2							
² A ₂	38.4	3185(4), 3186(426), 3275(84), 3279(1)	2.088, 2.073 2.088, 2.073	1.221 1.221	170.3, 169.3 170.3, 169.3	Core (distorted) Core (distorted)	137.8
n=3							
C _S	16.1	3211(9), 3213(313), 3214(157), 3300(45), 3302(50), 3305(10)	2.177, 2.178 2.177, 2.178 2.113, 2.113	1.216 1.216 1.221	169.4, 170.2 169.4, 170.2 167.7, 167.7	Core (distorted) Core (distorted) Core	102.2
n=4							
C _S	4.9	3229(39), 3235(120), 3237(146), 3258(135), 3314(50), 3320(56), 3324(11), 3356(8)	2.205, 2.220 2.205, 2.220 2.192, 2.192 2.500, 2.510	1.217 1.217 1.219 1.205	166.2, 165.7 166.2, 165.7 165.4, 165.4 174.6, 175.0	Core (distorted) Core (distorted) Core Core	86.3

* Dissociation energies = D_e(Ni⁺(C₂H₂)_n - Ni⁺(C₂H₂)_{n-1} + C₂H₂) in kcal/mol.

[†] Harmonic frequencies scaled by 0.96. Intensities are in km/mol

[‡] Represents the acetylene-Ni+-acetylene angle of the Jahn-Teller distorted pair

infrared active. For the $n = 1$ complex, the acetylenic C-H stretches are predicted to red-shift by $\sim 134\text{ cm}^{-1}$ for both the asymmetric and symmetric modes.

Neon attaches to the nickel cation on the backside, slightly removed from the C_2 axis due to Jahn-Teller effects. It induces only the slightest change on the acetylene moiety as summarized in Table 4.1. DFT predicts that the C-H stretches in the neon-tagged complex are shifted back toward the free acetylene frequencies by only $1\text{-}2\text{ cm}^{-1}$. The experimental peak positions and relative intensities in Figure 4.2 compare favorably to the predicted values at 3157 cm^{-1} and 3241 cm^{-1} . Argon attaches to the $\text{Ni}^+(\text{C}_2\text{H}_2)$ complex in the same way neon does, but induces a greater shift of $\sim 6\text{ cm}^{-1}$ from the $\text{Ni}^+(\text{C}_2\text{H}_2)$ frequencies. The second argon also binds to the backside of the cation with an $\text{Ar-Ni}^+\text{-Ar}$ angle of 95.6° . DFT predicts that the second argon causes an *additional* 8 cm^{-1} spectral-shift away from the $\text{Ni}^+(\text{C}_2\text{H}_2)$ modes and toward the free molecule vibrations. Table 4.2 summarizes the comparison of the DFT scaled harmonic frequencies to the experimental peak positions. As argons are added to the $n = 1$ complex, induction causes the acetylene ligand to become less perturbed within the complex. The acetylene is initially distorted from its free structure by the metal ion- π bond as described above. As rare gas complexation proceeds, the metal- π interaction lessens and the acetylene structure is slowly restored. Therefore, its C-H stretches blue-shift back towards the free acetylene modes. The neat $\text{Ni}^+\text{-C}_2\text{H}_2$ complex is predicted to have the lowest frequency C-H resonances. Attaching neon causes the C-H stretches to shift back to the blue, but only slightly. Adding argon causes a greater blue-shift and adding two

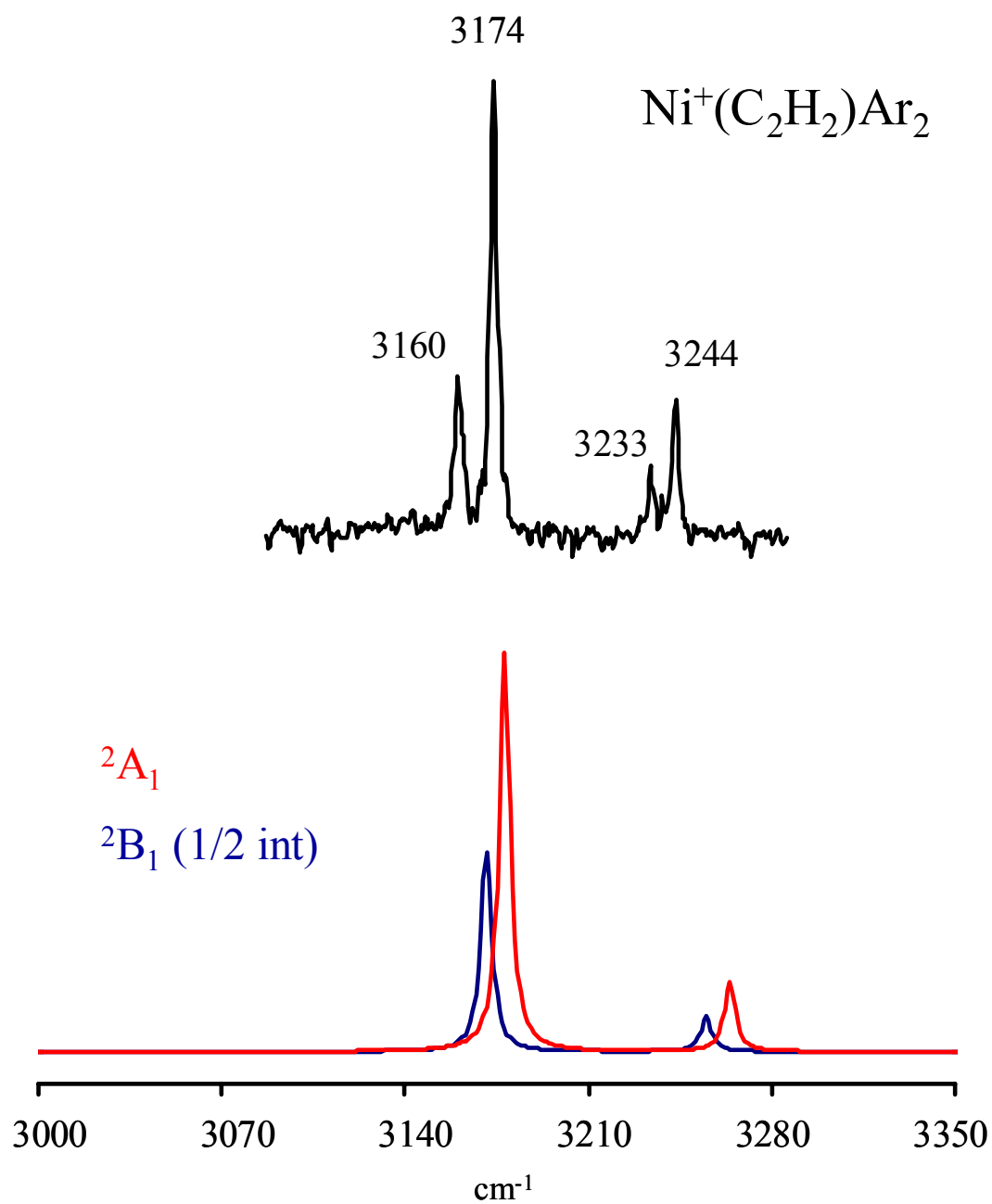
Table 4.2: B3LYP, 6-311⁺G** 0.96 scaled C-H frequencies (km/mol) compared to experiment.

Ni ⁺ (C ₂ H ₂)			-Ne		-Ar		-Ar ₂	
	Theory	Exp.	Theory	Exp.	Theory	Exp.	Theory	Exp.
² B ₁	3156 (232)	-	3157 (226)	3167	3162 (214)	-	3171 (195)	3160
	3240 (27)	-	3241 (29)	3234	3247 (34)	-	3255 (35)	3233
² A ₁	3178 (195)	-			3172 (209)	-	3178 (195)	3174
	3263 (23)	-			3259 (33)	-	3264 (34)	3244
Ni ⁺ (C ₂ H ₂) ₂								
² B ₁	3185 (4)	-			3188 (25)	3185		
	3186 (426)	-			3190 (361)	3194		
	3275 (84)	-			3276 (80)	3262		
	3279 (1)	-			3280 (8)	-		
Ni ⁺ (C ₂ H ₂) ₃								
² B ₁	3190 (7)	-			3217 (97)	3195		
	3199 (10)	-			3230 (47)	3206		
	3199 (7)	-			3232 (197)	3216		
	3249 (1)	-			3288 (54)	3270		
	3259 (3)	-			3309 (72)	3287		
	3259 (5)	-			3312 (25)	-		
Ni ⁺ (C ₂ H ₂) ₄								
² B ₁	3229 (39)							
	3235 (120)	3228						
	3237 (146)							
	3258 (135)	3252						
	3314 (50)							
	3320 (55)	3298						
	3324 (11)							
	3356 (8)	3338						

argons the greatest blue-shift. The IRPD spectrum of $\text{Ni}^+(\text{C}_2\text{H}_2)\text{Ar}_2$ in Figure 4.2 depicts two strong peaks at 3174 cm^{-1} and 3244 cm^{-1} consistent in both position and intensity with the ${}^2\text{B}_1$ calculated asymmetric/symmetric resonances at $3171/3255\text{ cm}^{-1}$. However, the spectrum also shows a weak but reproducible set of bands at 3160 cm^{-1} and 3233 cm^{-1} . They are red-shifted from the intense modes. As stated above, structural isomers where argon binds to the acetylene could account for the additional red-shift. However, DFT calculations failed to identify any structures where argon binds to the CH groups instead of the nickel cation.

The only other reasonable explanation then is that the weaker modes originate from the same complex in a different electronic state. Ni^+ has a low lying ${}^2\text{D}_{3/2}$ state that is 4.3 kcal/mol (1507 cm^{-1}) above the ${}^2\text{D}_{5/2}$ state.⁵² This gives rise to a ${}^2\text{A}_1$ excited state calculated by DFT for the $\text{Ni}^+(\text{C}_2\text{H}_2)$ complex which lies close in energy to the calculated ${}^2\text{B}_1$ ground state ($\sim 1.4\text{ kcal/mol}$). According to the computations, the ${}^2\text{A}_1$ state is stabilized more with respect to the ${}^2\text{B}_1$ as the $\text{Ni}^+(\text{C}_2\text{H}_2)$ ion core is solvated by subsequent argon atoms. Once the second argon atom is attached to the $\text{Ni}^+(\text{C}_2\text{H}_2)$ ion core (i.e. $\text{Ni}^+(\text{C}_2\text{H}_2)\text{Ar}_2$), the ${}^2\text{A}_1$ state becomes the ground state. Figure 4.4 shows the $\text{Ni}^+(\text{C}_2\text{H}_2)\text{Ar}_2$ experimental spectrum as it compares to the harmonic frequencies of the ${}^2\text{A}_1$ and ${}^2\text{B}_1$ states computed at the B3LYP level. Theoretical frequencies have been scaled by 0.96 and plotted at a 2 cm^{-1} resolution to provide a better match to the experiment. The $\text{Ni}^+(\text{C}_2\text{H}_2)\text{Ar}_2\text{ }{}^2\text{A}_1$ ground state has C-H resonances that are $\sim 7\text{ cm}^{-1}$ to the blue of the ${}^2\text{B}_1$ frequencies. The most intense features in the experimental spectrum are also the highest frequency modes and occur $11\text{-}14\text{ cm}^{-1}$ to the blue of the weak features. The strong bands at $3174/3244\text{ cm}^{-1}$ are

Figure 4.4 The IRPD spectrum of $\text{Ni}^+(\text{C}_2\text{H}_2)\text{Ar}_2$ as it compares to the C-H vibrations of the same complex in the $^2\text{A}_1$ and $^2\text{B}_1$ states calculated at the B3LYP level. The harmonic frequencies have been scaled by 0.96 and plotted at a 2 cm^{-1} resolution. The $^2\text{B}_1$ intensities have been reduced by half. The theoretical structure is included in the inset.



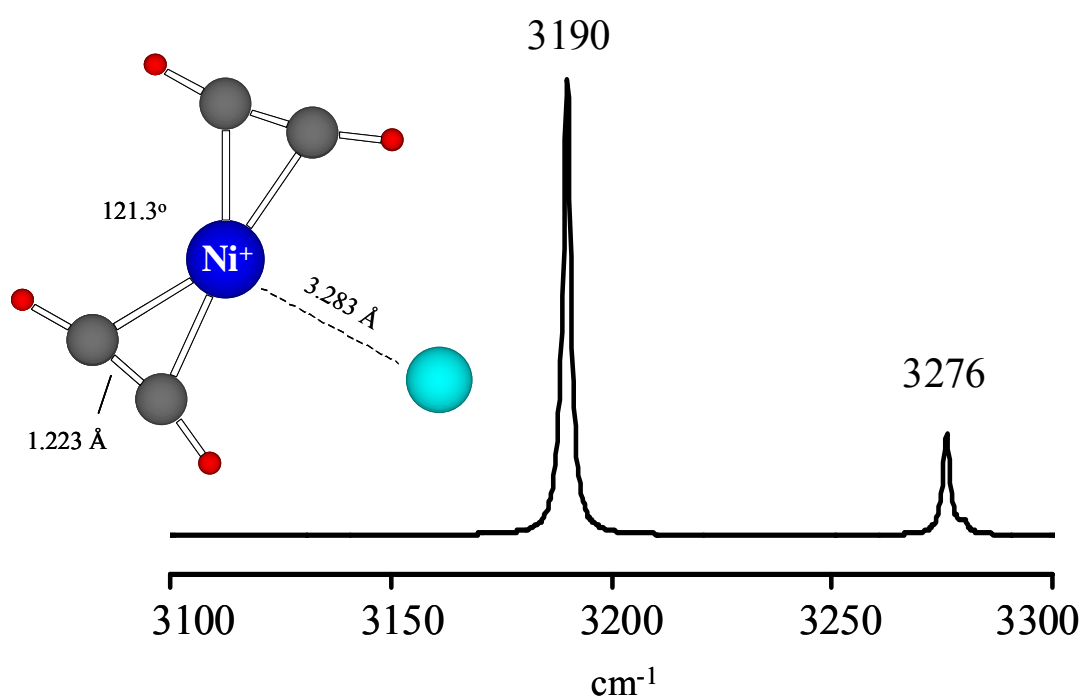
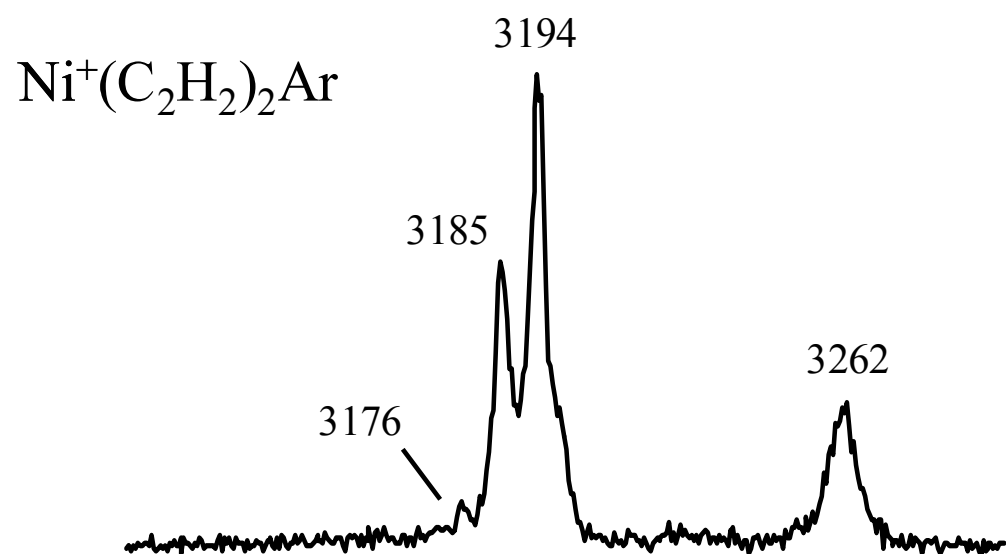
therefore consistent with the asymmetric and symmetric C-H stretches of the 2A_1 ground electronic state calculated for the $Ni^+(C_2H_2)Ar_2$ complex. The weaker bands at $3160/3233\text{ cm}^{-1}$ are likely from a minor population of clusters that are in the 2B_1 electronic state. Therefore the 2B_1 modes (blue trace) have had their intensities reduced by 1/2 to illustrate the point. However, there remains some uncertainty when comparing the experimental and theoretical frequencies for all the monoacetylene complexes shown in Figure 4.2.

As described above, attaching rare gas atoms to the $^2B_1\ Ni^+(C_2H_2)$ complex cause the C-H resonances to shift back towards the free acetylene modes. Looking at the calculated 2B_1 state in Table 4.2, the neat $Ni^+(C_2H_2)$ complex has the lowest frequency modes in the sample set and the resonances blue-shift in a regular way upon rare gas complexation. Neon causes a slight blue-shift, argon induces a greater blue-shift, and attaching two argons produces the largest blue-shift. If the weaker bands in the $Ni^+(C_2H_2)Ar_2$ spectrum are attributed to the 2B_1 state as stated above, then they are *red-shifted* from the modes in $Ni^+(C_2H_2)Ne$. This runs counter to the spectral trend established by the DFT computations. Because of this trend, the intense bands are perhaps more consistent with the 2B_1 state as they occur to the blue of the neon-tagged resonances. The intense features in the $Ni^+(C_2H_2)Ar_2$ can be assigned to either the 2A_1 or the 2B_1 state. We therefore acquired the IRPD spectrum for the mono-acetylene complex tagged with three argon atoms as shown in the upper trace in Figure 4.2. It has two C-H resonances and therefore only a single electronic state is likely present. The resonances are blue-shifted from the weak signals or red-shifted from the intense features in the double argon spectrum. One could come to a

completely different conclusion within the context of the frequency shifts observed in the experimental spectra. The spectra show that only a single electronic state is populated in the $\text{Ni}^+(\text{C}_2\text{H}_2)\text{Ne}$ and $\text{Ni}^+(\text{C}_2\text{H}_2)\text{Ar}_3$ complexes, whereas two states are populated in the $\text{Ni}^+(\text{C}_2\text{H}_2)\text{Ar}_2$ clusters. Because the intense bands in the double argon spectrum are blue-shifted from the neon-tagged resonances, it is likely that they belong to the same electronic state. Likewise, the weak signals in the $\text{Ni}^+(\text{C}_2\text{H}_2)\text{Ar}_2$ spectrum and the bands measured for $\text{Ni}^+(\text{C}_2\text{H}_2)\text{Ar}_3$ (which are blue-shifted from them) belong to the other electronic state. Determining which electronic configuration is the ground state for each complex is problematic for DFT. B3LYP computations are known to overestimate the $\text{Ni}^+-\text{C}_2\text{H}_2$ bond energy with respect to CCSD(T) coupled cluster calculations by as much as 4.0 kcal/mol.⁶ Furthermore, B3LYP predicts that the $^2\text{B}_1$ is the ground state for the $\text{Ni}^+(\text{C}_2\text{H}_2)$ complex, whereas the $^2\text{B}_1$ and $^2\text{A}_1$ states are calculated to be isoenergetic with CCSD(T) for this complex.³ Future theoretical work will be required to resolve this issue. Regardless of which configuration is the ground state for these clusters, it is clear that the four bands observed in the $\text{Ni}^+(\text{C}_2\text{H}_2)\text{Ar}_2$ spectrum are from two electronic states that are nearly isoenergetic and not caused by the presence of structural isomers.

Figure 4.5 shows the IRPD spectrum of $\text{Ni}^+(\text{C}_2\text{H}_2)_2\text{Ar}$ and how it compares to the scaled harmonic frequencies of the same complex calculated with DFT. The experimental spectrum has reproducible bands at 3185, 3194 and 3262 cm^{-1} . The observation of three strong bands in the C-H stretch region is somewhat surprising. If the two acetylenes are coplanar and attached to the cation on opposite sides in a D_{2h} structure, the $\text{Ni}^+(\text{C}_2\text{H}_2)_2$ complex would have four C-H vibrations corresponding to

Figure 4.5 The IRPD spectrum of $\text{Ni}^+(\text{C}_2\text{H}_2)_2\text{Ar}$ as it compares to the C-H vibrations of the same complex in the $^2\text{B}_1$ state calculated with B3LYP. The harmonic frequencies have been scaled by 0.96 and plotted at a 2 cm^{-1} resolution. The theoretical structure is included in the inset.



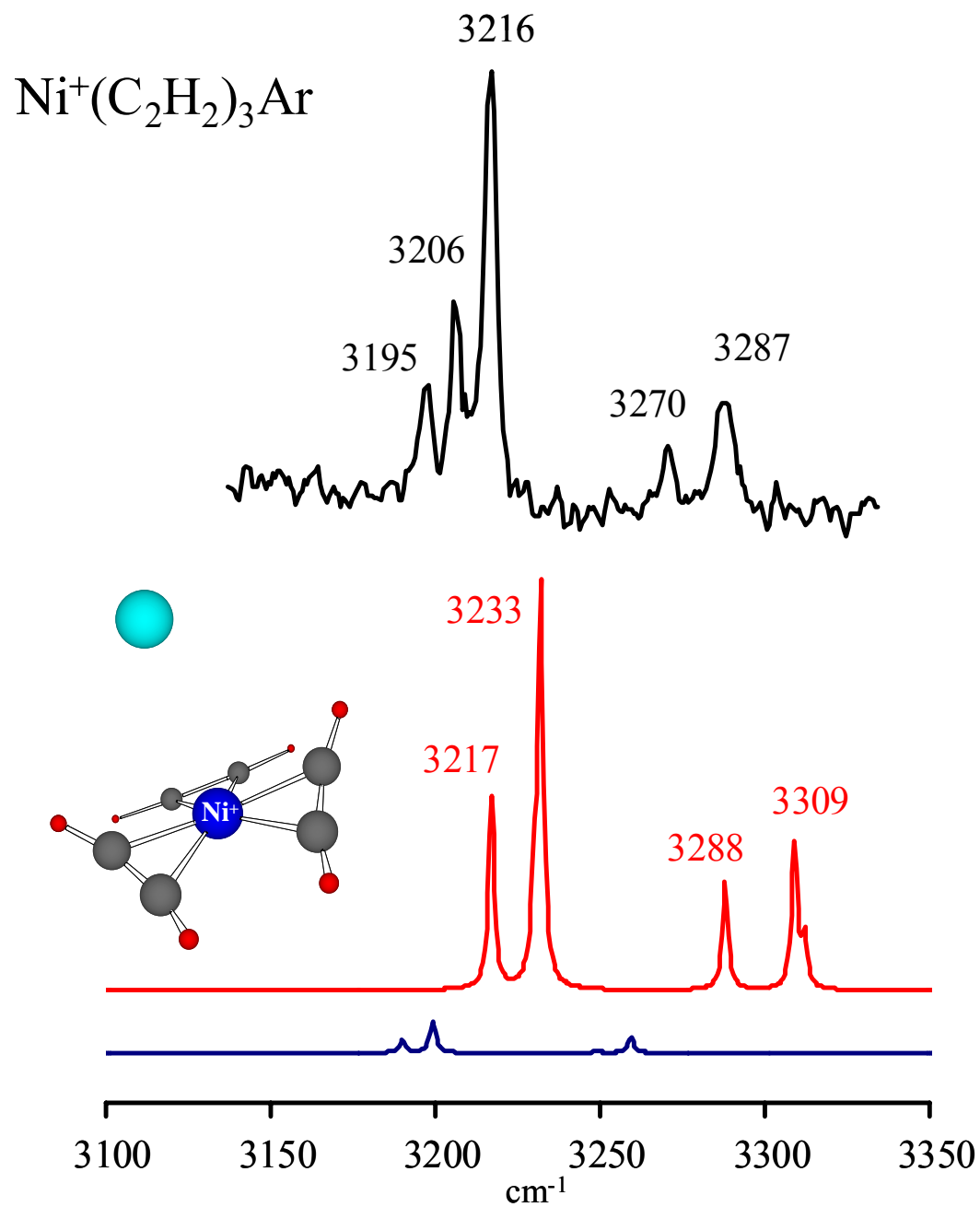
in-phase and out-of-phase motions of the symmetric and asymmetric C-H stretches. Only two of these would be IR active, the out-of-phase symmetric stretch and the in-phase asymmetric stretch. The presence of three intense signals in the C-H stretching region for this complex means that it has adopted a lower symmetry structure or that isomers are present in the molecular beam. Therefore, theory is again required to explain the spectral details.

According to the B3LYP calculations, both acetylenes are π -bonded to the nickel cation side-on but not on opposite sides of the nickel cation. Due to Jahn-Teller distortion, the acetylenes are slightly pinched-in on one side of the metal at an acetylene- Ni^+ -acetylene angle of 137.8° (Table 4.1). Like the monoacetylene complexes, the hydrogens are bent away from linear ($\angle\text{CCH} \sim 170^\circ$) to reduce repulsion from the nickel ion. The overall symmetry of the $\text{Ni}^+(\text{C}_2\text{H}_2)_2$ complex is C_{2v} , which gives rise to a $^2\text{A}_2$ ground state. Argon occupies a site on the backside of the nickel cation as expected and causes only a minor perturbation on the complex. The structure of the $^2\text{A}_2 \text{Ni}^+(\text{C}_2\text{H}_2)_2\text{Ar}$ cluster is shown in the inset of Figure 4.5 and its theoretical IR spectrum is the lower trace in red. All four C-H motions are predicted to have some IR intensity and their fundamental frequencies are predicted at $3188/3190/3276/3280 \text{ cm}^{-1}$. However, the peak at 3188 cm^{-1} is calculated to be much less intense than the nearby 3190 cm^{-1} feature and is not resolved when plotted at a 2 cm^{-1} resolution. Similarly, the weak vibration at 3280 cm^{-1} appears as a shoulder of the more intense 3276 cm^{-1} band. Table 4.2 contains the band positions and their infrared oscillator strengths. Because of the vibrational overlap, the appearance of the theoretical spectrum is dominated by two intense signals in the asymmetric and

symmetric C-H stretching regions. The experimental bands measured at 3194 cm^{-1} and 3262 cm^{-1} compare favorably to the dominant theoretical frequencies at 3190 cm^{-1} and 3276 cm^{-1} . However, the experimental spectrum also contains a relatively intense peak at 3185 cm^{-1} and a weak but reproducible feature at 3176 cm^{-1} . It is possible that the $n = 2$ complex adopts a structure that is less symmetric than the one calculated by DFT. A more distorted geometry might cause the band predicted at 3188 cm^{-1} to gain intensity and shift further away from the intense 3190 cm^{-1} band, which could account for the vibration measured at 3185 cm^{-1} . However, a lower symmetry structure cannot explain both bands measured at 3185 cm^{-1} and 3176 cm^{-1} . Only four C-H stretches are possible for the $n = 2$ complex: two symmetric-like and two asymmetric-like vibrations. Clearly there are three acetylenic asymmetric C-H stretches in the experimental spectrum. Additional modes in the asymmetric region suggest that multiple structural isomers are present in the $n = 2$ cluster distribution or that some of the clusters are in a different electronic state. The latter seems more likely from what was learned from the monoacetylene complexes.

Figure 4.6 displays the IRPD spectrum of $\text{Ni}^+(\text{C}_2\text{H}_2)_3\text{Ar}$ and how it compares to the predicted IR spectrum of the same complex calculated with DFT (red trace) using the 6-31G* basis set. The theoretical spectrum of the neat $\text{Ni}^+(\text{C}_2\text{H}_2)_3$ has also been included for comparison (blue trace). Theoretical frequencies have been scaled by 0.96 and plotted at a 2 cm^{-1} resolution. The predicted IR spectra of the $n = 3$ complexes calculated with the 6-311+G** basis set were less consistent with the experimental IRPD spectrum. As stated before, the $\text{Ni}^+(\text{C}_2\text{H}_2)_3$ complex is difficult to fragment, producing a broad spectrum with poor signal-to-noise.³¹ The argon-tagged

Figure 4.6 The IRPD spectrum of $\text{Ni}^+(\text{C}_2\text{H}_2)_3\text{Ar}$ as it compares to the C-H vibrations of the neat (blue trace) and argon-tagged complex (red trace) calculated with the 6-31G* basis set. The theoretical structure of the $\text{Ni}^+(\text{C}_2\text{H}_2)_3\text{Ar}$ is included in the inset. Harmonic frequencies from the 6-311+G** calculations were less consistent with the experiment.



$n = 3$ complex dissociates efficiently and its spectrum contains a number of resonances at 3195/3206/3216/3270/3287 cm^{-1} . B3LYP (6-31G*) calculations predict that all three acetylene ligands are π -bonded to the nickel. The nickel cation is located near the plane defined by the center-of-mass of the three acetylenes. Similar to the $n = 2$ complex, two of the acetylenes are slightly pinched-in, producing an acetylene- Ni^+ -acetylene angle of 102.2°. The $\text{Ni}^+(\text{C}_2\text{H}_2)_3$ complex belongs to the C_s symmetry group, and its structure is shown in Figure 4.3. Except for the distortion, this structure would be analogous to tris-ethylene platinum, a stable cluster known from traditional organometallic chemistry.¹ The reduced symmetry of the molecule causes more C-H stretches to light up in the infrared. Six IR-active C-H stretches are identified by DFT for $\text{Ni}^+(\text{C}_2\text{H}_2)_3$, though they are calculated to be weak as summarized in Table 2.

Unlike the $n = 1, 2$ complexes, attaching argon to the $n = 3$ complex perturbs its structure significantly. The binding of argon causes the nickel cation to reside above the acetylene center-of-mass plane as can be seen in the inset of Figure 4.6. Because the metal is no longer included in the plane, the C-H resonances shift to higher frequency and their oscillator strengths gain an order of magnitude as can be seen in Table 4.2. There are three asymmetric-like modes at 3217/3230/3232 cm^{-1} and three symmetric-like modes at 3288/3309/3312 cm^{-1} calculated for the $\text{Ni}^+(\text{C}_2\text{H}_2)_3\text{Ar}$ complex in the $^2A'$ electronic state. However, the weak band predicted at 3230 cm^{-1} is not resolved from the intense 3232 cm^{-1} mode when plotted at a 2 cm^{-1} resolution, and the feature at 3312 cm^{-1} appears as a shoulder on the 3309 cm^{-1} band. The theoretical spectrum is then dominated by only four infrared signals at our

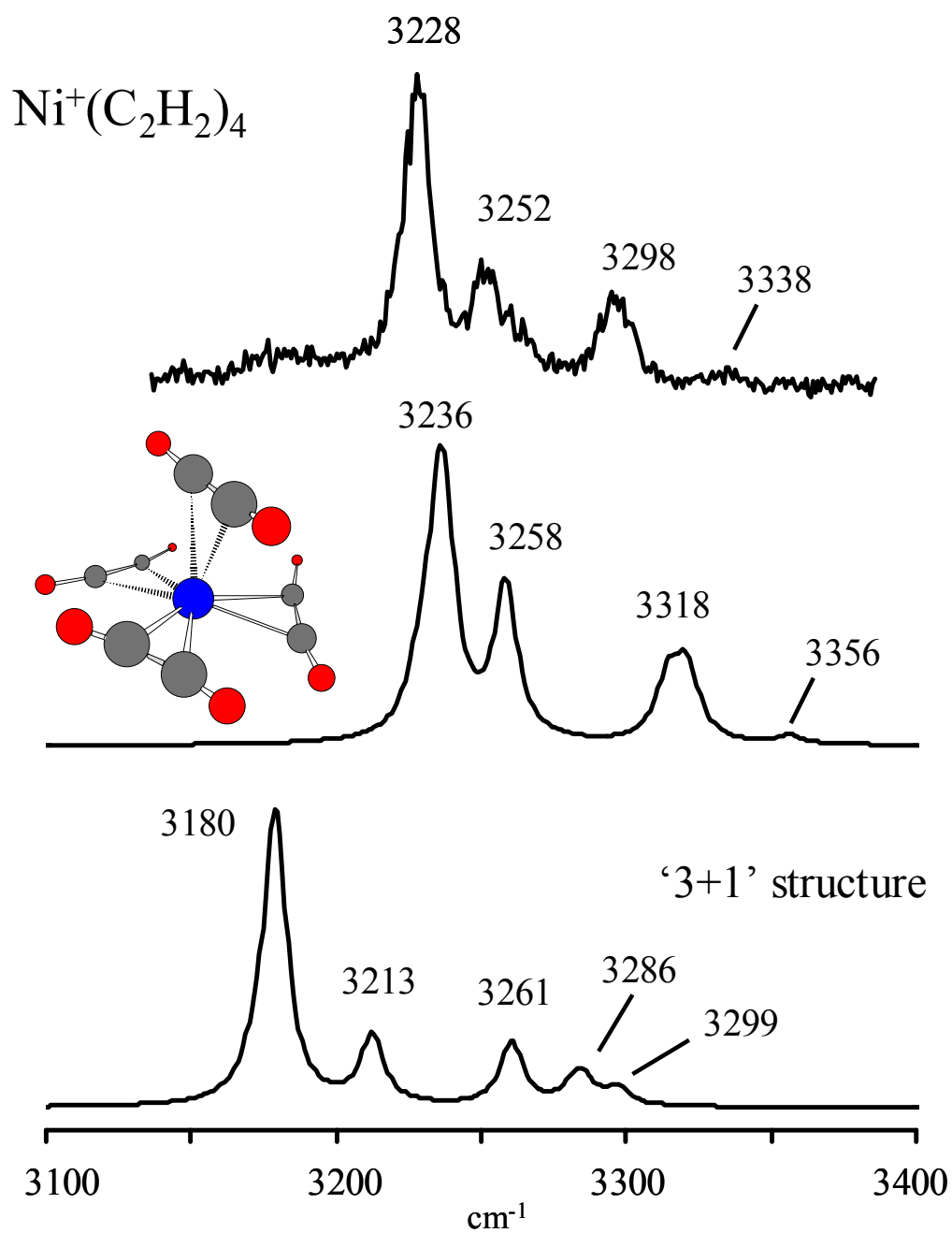
experimental resolution: two in the asymmetric region and two in the symmetric region. The two bands in the symmetric region of the IRPD spectrum at 3270 cm^{-1} and 3287 cm^{-1} compare favorably in both position and intensity to the two theoretical peaks at 3288 cm^{-1} and 3309 cm^{-1} . Additionally, the experimental signal at 3287 cm^{-1} is somewhat broad (7 cm^{-1} FWHM) as compared to the other signals in the spectrum ($\sim 4\text{ cm}^{-1}$ FWHM), and maybe the result of an unresolved doublet.

In the asymmetric region, the match between experiment and theory is not as good. The experimental spectrum has three reproducible bands measured at $3195/3206/3216\text{ cm}^{-1}$. Although theory also calculates three bands in this region at $3217/3230/3232\text{ cm}^{-1}$, the relatively weak band at 3230 cm^{-1} is not resolved. Therefore, the theoretical spectrum displays only two IR bands at 3232 cm^{-1} and 3217 cm^{-1} in the asymmetric stretch region. Both experiment and theory agree that the highest frequency asymmetric-like stretch is the most intense peak. Because of its intensity, the band measured at 3206 cm^{-1} is likely the mode predicted at 3217 cm^{-1} . Theory calculates this mode to be about half as intense as the strongest asymmetric-like vibration, and the experimental band at 3206 cm^{-1} is about half the intensity of the strong band measured at 3216 cm^{-1} . (It is important to note that intensities measured by action spectroscopies do not always track true absorption strengths due to the dynamics of the photofragmentation process. However, theoretical intensities have been fairly reproduced for all IRPD spectra discussed thus far.) The observation of an additional mode at 3195 cm^{-1} presents the same problem as discussed for the $n = 2$ complex. Either the actual structure of the $\text{Ni}^+(\text{C}_2\text{H}_2)_3\text{Ar}$ complex is less symmetric than that calculated at the B3LYP level or isomers and electronic states are present.

If the structure is more distorted, the three calculated asymmetric modes might separate more and their relative intensities might change and could account for the three asymmetric features in the IRPD spectrum. Conversely, the band measured at 3195 cm^{-1} might be an asymmetric-like stretch from a different $n = 3$ isomer or from clusters in a different electronic state. The latter seems more likely from what was learned from the monoacetylene complexes. In general, the overall appearance of the experimental spectrum is reproduced by DFT (6-31G*), which predicts that all three acetylenes are π -bonded to the metal. The 6-311+G** calculations also have all three acetylenes π -bonded to the metal, but the third molecule is not in plane with the other two, as shown in Figure 4.3. Surprisingly, the predicted vibrations for this structure overlap, producing a simpler IR spectrum dominated by just two bands (not shown), and attaching argon does not change its IR spectrum much. More theoretical work will be required to resolve the issue.

Figure 4.7 shows the IRPD spectrum of $\text{Ni}^+(\text{C}_2\text{H}_2)_4$ as it compares to the predicted spectra of two theoretical structures. Harmonic frequencies have been scaled by 0.96 and plotted at a 10 cm^{-1} resolution for better comparison to the experiment. Two relevant isomeric structures were calculated with DFT for the $n = 4$ complex: a “3+1” complex, where the fourth acetylene is attached to an existing core acetylene, and a complex with all four acetylenes attached directly to the metal ion in a pseudo-tetrahedral arrangement. A square-planar structure was also considered, but the calculations failed to converge. Significant structural changes are not observed when calculating these structures with either the small or large basis sets, therefore the results presented here are from the 6-311+G** calculations. According to the

Figure 4.7 The IRPD spectrum of $\text{Ni}^+(\text{C}_2\text{H}_2)_4$ as it compares to the two isomers calculated at the B3LYP level. The harmonic frequencies have been scaled by 0.96 and plotted at a 10 cm^{-1} resolution. The predicted structure where all four acetylenes are π -bonded to the nickel cation is shown in the inset.



computations, the isomers are nearly isoenergetic with the ‘3+1’ structure being more stable by only 1.0 kcal/mol. However, the IRPD spectrum is more consistent with the structure where all four acetylenes are attached directly to the nickel cation, as shown in Figure 4.7. This is not surprising, as density functional theory is known to overestimate hydrogen bonding. Of the isomeric structures computed for the $n = 4$ complex, only the ‘3+1’ structure contains a hydrogen bond. Therefore, comparing the total energies of these two structures does not provide reliable information on their relative structural stability. The fragmentation patterns observed in Figure 4.1 and the match between experiment and theory in the vibrational spectra of the $n = 4$ complex both indicate that the fourth acetylene is attached directly to the nickel cation and completes its coordination.

The $n = 4$ theoretical structure belongs to the C_s symmetry group because two of the four acetylenes are pinched-in on one side of the nickel. This structure is included in the Figure 4.7 inset and also shown in Figure 4.3. The $Ni^+(C_2H_2)_4$ IRPD spectrum has three intense C-H bands at 3228/3252/3298 cm^{-1} and a weak but reproducible mode at 3338 cm^{-1} . DFT predicts eight infrared active C-H vibrations for $Ni^+(C_2H_2)_4$ due to its lower symmetry and their frequencies and intensities are summarized in Table 4.2. However, many of these vibrations overlap when plotted at a resolution similar to the experiment. For example, the asymmetric-like C-H resonances at 3229/3235/3237 cm^{-1} appear as a single strong infrared band at 3236 cm^{-1} as seen in the middle trace of Figure 4.7. Likewise, overlapping symmetric features at 3314/3320/3324 cm^{-1} produce a rather broad, irregularly shaped band centered near 3322 cm^{-1} . Therefore only four bands, three relatively intense at

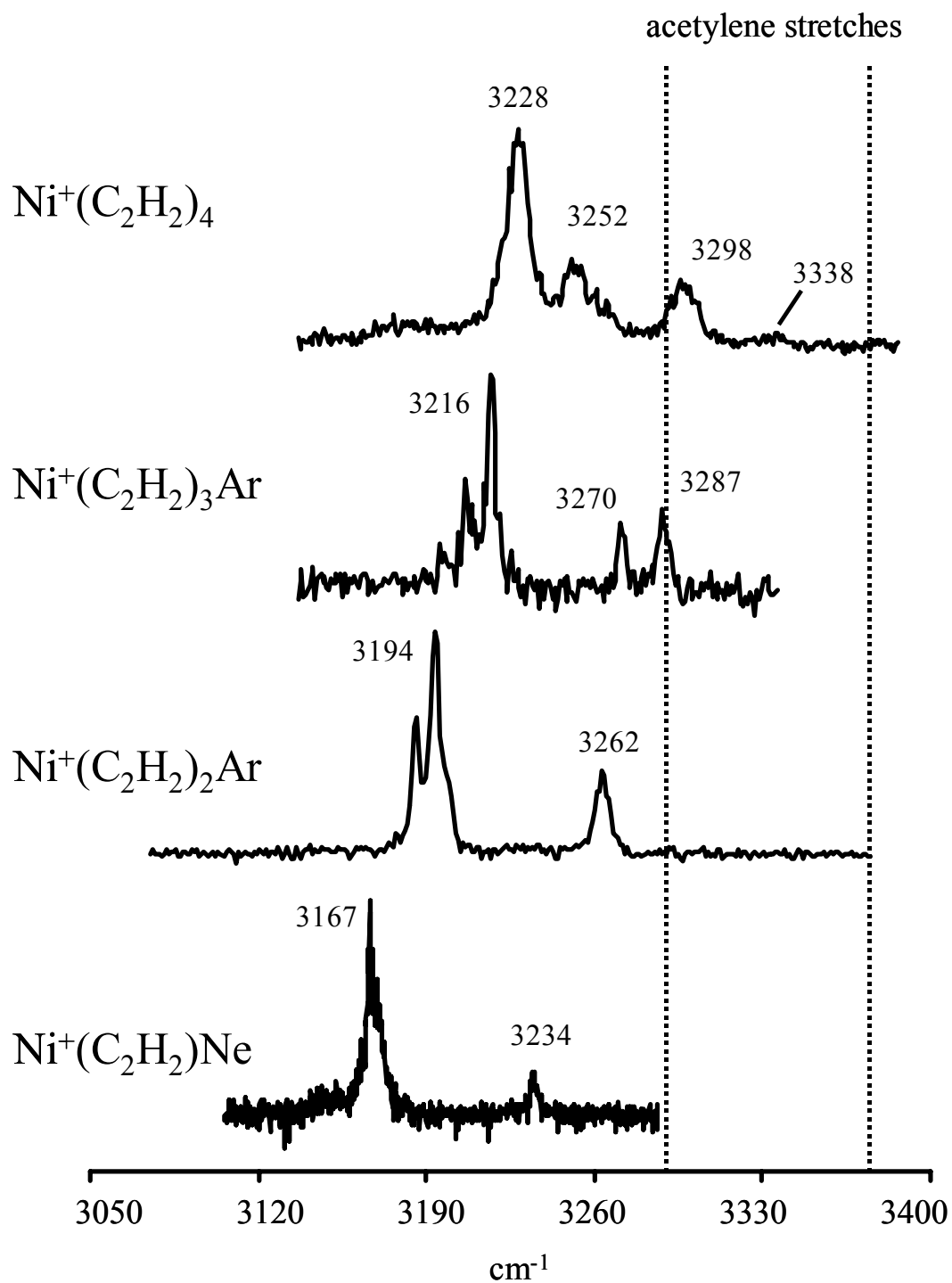
3236/3258/3322 cm^{-1} and a weak feature at 3356 cm^{-1} , are observed in the theoretical spectrum. The match between experiment and theory is quite good for both band positions and intensities. The lower frequency band is the most intense in both spectra and even the weak, highest frequency feature is reproduced. According to the calculations, the two most intense resonances at 3235 cm^{-1} and 3237 cm^{-1} involve asymmetric C-H motions of the two pinched-in acetylenes. The structural asymmetry caused by Jahn-Teller effects produces a permanent dipole for this complex. Stretches involving the two acetylene moieties that are bound on the same side of the nickel cation are more intense due to their larger amplitude dynamic dipole moments. Of course symmetric C-H stretches are weaker than the asymmetric motions, but of the four symmetric-like modes, the two intense bands predicted at 3314 cm^{-1} and 3320 cm^{-1} also involve the distorted acetylene pair. This is true for the $n = 2, 3$ complexes as well. The most intense asymmetric and symmetric C-H vibrations are from the two acetylenes that are bound to the nickel cation on the same side.

According to the calculations, the third and fourth acetylene molecules are predicted to be weakly bound to the nickel cation. For example, the sequential dissociation energies for the detachment of a single C_2H_2 ligand can be estimated from the B3LYP results. As seen in Table 4.1, the bond dissociation energies (BDE) of $\text{Ni}^+(\text{C}_2\text{H}_2)_n$ (ie: $\text{Ni}^+(\text{C}_2\text{H}_2)_{n-1} + \text{C}_2\text{H}_2 \leftrightarrow \text{Ni}^+(\text{C}_2\text{H}_2)_n$) are 47.0, 38.4, 16.1, and 4.9 kcal/mol for $n = 1-4$ complexes, respectively. There is a significant drop in BDE when going from $n = 2$ to $n = 3$. This is consistent with dissociation energies measured for similar complexes. Bowers and coworkers measured the BDEs of $\text{Ag}^+(\text{C}_2\text{H}_4)_n$ complexes with equilibrium mass spectrometry and compared their

results to theory.¹⁴ They determined that this system was also four-coordinate and observed a significant drop in BDE after $n = 2$. In this case, detachment of acetylene from the $\text{Ni}^+(\text{C}_2\text{H}_2)_3$ complex requires $\sim 5600 \text{ cm}^{-1}$ of energy, which is still greater than the energy of a single photon near 3300 cm^{-1} . However, only 1700 cm^{-1} is calculated to dissociate the $n = 4$ complex, therefore this complex should photodissociate via a single photon process. The inefficient fragmentation observed for $\text{Ni}^+(\text{C}_2\text{H}_2)_3$ and the increase in photodissociation yield beginning with the $n = 4$ complex is consistent with the BDEs estimated from the DFT calculations.

Figure 4.8 shows the IRPD spectra of $\text{Ni}^+(\text{C}_2\text{H}_2)\text{Ne}$, $\text{Ni}^+(\text{C}_2\text{H}_2)_{2,3}\text{Ar}$ and $\text{Ni}^+(\text{C}_2\text{H}_2)_4$ to illustrate how the C-H stretches evolve as more acetylenes are π -bonded to the nickel cation. The spectra and theory for the $n = 1$ -4 complexes show that the metal ion- π interaction distorts the geometry of the acetylene moieties by weakening the $\text{C}\equiv\text{C}$ bond and pushing the hydrogens away from linear. This causes two effects: the symmetric stretches become IR active and all the C-H resonances occur at lower frequency than the pure acetylene modes. As more ligands are added, the individual Ni^+ -acetylene bonds weaken. Therefore, the bands should shift back towards the free acetylene modes as cluster size increases. The IRPD spectra of the $n = 1$ -4 complexes are consistent with this expected trend as shown in Figure 4.8. The asymmetric C-H stretch for the $\text{Ni}^+(\text{C}_2\text{H}_2)\text{Ne}$ complex occurs at 3167 cm^{-1} , while the most intense asymmetric features are 3194 cm^{-1} , 3216 cm^{-1} and 3228 cm^{-1} for the $\text{Ni}^+(\text{C}_2\text{H}_2)_{2,3}\text{Ar}$ and $\text{Ni}^+(\text{C}_2\text{H}_2)_4$ complexes, respectively. Thus, the C-H resonances for the $n=1$ cluster are red-shifted from the free modes the most and the magnitude of the red-shift decreases as cluster size increases.

Figure 4.8 The IRPD spectra of the $n = 1-4$ complexes from $3100 - 3400 \text{ cm}^{-1}$. The vertical dashed lines represent the free acetylene C-H stretches at 3289 cm^{-1} and 3374 cm^{-1} . As subsequent acetylenes are added to the nickel cation, the C-H resonances blue-shift back towards the free acetylene modes.



Conclusions

Nickel cation-acetylene complexes are studied with infrared photodissociation spectroscopy and density functional theory. Both experiment and theory agree that π -complexes are formed for all molecules studied. The metal ion-ligand interaction distorts the acetylene geometry, weakening the $\text{C}\equiv\text{C}$ bond and pushing the hydrogens off the $\text{C}\equiv\text{C}$ axis. This distortion activates the symmetric C-H stretch in the infrared and shifts both C-H resonances to lower frequency. The four bands observed in the $\text{Ni}^+(\text{C}_2\text{H}_2)\text{Ar}_2$ spectrum arise from two electronic states that are nearly isoenergetic. DFT calculations predict that the $^2\text{A}_1$ state is the ground electronic state for this complex, but the experimental trends suggest that it might be the $^2\text{B}_1$ state. The structure of the $\text{Ni}^+(\text{C}_2\text{H}_2)_2$ complex is Jahn-Teller distorted with the acetylene ligands adsorbed on one side of the nickel cation. This distortion is maintained in the structures of the larger complexes and accounts for the most intense bands in their IRPD spectra. The presence of rare gas atoms produce only minor perturbations on the structures, and therefore the infrared spectra, of all complexes studied except for $\text{Ni}^+(\text{C}_2\text{H}_2)_3$. According to the computations, attaching argon to the $n = 3$ complex causes the nickel to be pulled out of the acetylene center-of-mass plane. This increases the intensity of the C-H stretches and shifts their band positions to higher frequency. For $\text{Ni}^+(\text{C}_2\text{H}_2)_4$, the fragmentation patterns, unique IR spectrum and the close comparison to DFT results all indicate that the fourth acetylene is also π -bonded to the nickel cation and completes its coordination.

References

- (1) Heck, R. F. *Organotransition Metal Chemistry*; Academic Press: New York, 1974.
- (2) Jolly, P. W.; Wilke, G. *The Organic Chemistry of Nickel*; John Wiley: New York, 1974.
- (3) a) Sodupe, M.; Bauschlicher, C. W. Jr. *J. Phys. Chem.* **1991**, 95, 8640. b) Sodupe, M.; Bauschlicher, C. W. Jr.; Langhoff, S. R.; Partridge, H. *J. Phys. Chem.* **1992**, 96, 2118.
- (4) a) Hertwig, R. H.; Koch, W.; Schroeder, D.; Schwarz, H.; Hrusak, J.; Schwerdtfeger, P. *J. Phys. Chem.* **1996**, 100, 12253. b) Holthausen, M. C.; Fiedler, A.; Schwarz, H.; Koch, W. *J. Phys. Chem.* **1996**, 100, 6236.
- (5) a) Frenking, G.; Frohlich, N. *Chem. Rev.* **2000**, 100, 717. b) Nechaev, M. S.; Rayon, V. M.; Frenking, G. *J. Phys. Chem. A* **2004**, 108, 3134.
- (6) Klippenstein, S. J.; Yang, C.-N. *Int. J. Mass Spectrom.* **2000**, 201, 253.
- (7) a) Eller, K.; Schwarz, H. *Chem. Rev.* **1991**, 91, 1121. b) Wesendrup, R.; Schwarz, H. *Organometallics* **1997**, 16, 461. c) Harvey, J. N.; Diefenbach, M.; Schroder, D.; Schwarz, H. *Int. J. Mass Spectrom.* **1999**, 182, 85.
- (8) a) Freiser, B. S., ed., *Organometallic Ion Chemistry*; Kluwer: Dordrecht, The Netherlands, 1996. b) Ranatunga, D. R. A.; Freiser, B. S. *Chem. Phys. Lett.* **1995**, 233, 319. c) Chen, Q.; Auberry, K. J.; Freiser, B. S. *Int. J. Mass Spectrom. Ion Proc.* **1998**, 175, 1.
- (9) a) Metz, R. B.; *Int. Rev. Chem.* **2004**, 23, 79. b) Aguirre, F.; Husband, J.; Thompson, C. J.; Metz, R. B. *Chem. Phys. Lett.* **2000**, 318, 466. c) Husband,

- J.; Aguirre, F.; Thompson, C. J.; Laperle, C. M.; Metz, R. B. *J. Phys. Chem. A* **2000**, *104*, 2020.
- (10) Gibson, J. K. *J. Organomet. Chem.* **1998**, *558*, 51.
- (11) a) Armentrout, P. B.; Beauchamp, J. L. *J. Am. Chem. Soc.* **1981**, *103*, 784. b) Elkind, J. L.; Armentrout, P. B. *J. Am. Chem. Soc.* **1986**, *108*, 2765. c) van Koppen, P. A. M.; Bowers, M. T.; Haynes, C. L.; Armentrout, P. B. *J. Am. Chem. Soc.* **1998**, *120*, 5704.
- (12) Tonkyn, R.; Ronan, M.; Weisshaar, J.C. *J. Phys. Chem.* **1988**, *92*, 92.
- (13) a) van Koppen, P. A. M.; Kemper, P. R.; Bushnell, J. E.; Bowers, M. T. *J. Am. Chem. Soc.* **1995**, *117*, 2098. b) van Koppen, P. A. M.; Perry, J. K.; Kemper, P. R.; Bushnell, J. E.; Bowers, M. T. *Int. J. Mass Spectrom.* **1999**, *185*, 989.
- (14) a) Manard, M. J.; Kemper, P. R.; Carpenter, C. J.; Bowers, M. T. *Int. J. Mass Spectrom.* **2005**, *241*, 99. b) Manard, M. J.; Kemper, P. R.; Bowers, M. T. *Int. J. Mass Spectrom.* **2005**, *241*, 109.
- (15) a) Aristov, N.; Armentrout, P. B. *J. Am. Chem. Soc.* **1986**, *108*, 1806. b) Georgiadis, R.; Armentrout, P. B. *Int. J. Mass Spectrom. Ion Proc.* **1989**, *89*, 227. c) Fisher, E. R.; Armentrout, P. B. *J. Phys. Chem.* **1990**, *94*, 1674. d) Meyer, F.; Khan, F. A.; Armentrout, P. B. *J. Am. Chem. Soc.* **1995**, *117*, 9740. e) Sievers, M. R.; Jarvis, L. M.; Armentrout, P. B. *J. Am. Chem. Soc.* **1998**, *120*, 1891. f) Sievers, M. R.; Chen, Y.-M.; Haynes, C. L.; Armentrout, P. B. *Int. J. Mass Spectrom.* **2000**, *195*, 149.
- (16) a) France, M. R.; Pullins, S. H.; Duncan, M. A. *J. Chem. Phys.* **1998**, *109*, 8842. b) Reddic, J. E.; Duncan, M.A. *Chem. Phys. Lett.* **1999**, *312*, 96. c) Weslowski,

- S. S.; King, R. A.; Schaefer, H. F.; Duncan, M. A. *J. Chem. Phys.* **2000**, *113*, 701.
- (17) a) Kleiber, P. D. in *Adv. Metal Semicond. Clusters*, **2001**, *5*, 267. b) Lu, W.-Y.; Liu, R.-G.; Wong, T.-H.; Chen, J.; Kleiber, P. D. *J. Phys. Chem. A* **2002**, *106*, 725.
- (18) Nakamoto, K. *Infrared and Raman Spectra of Inorganic and Coordinated Compounds*, 5th ed.; John Wiley: New York, 1997; Vols. A&B.
- (19) a) Chatt, J.; Rowe, G. A.; Williams, A. A. *Proc. Chem. Soc.* **1957**, 208. b) Chatt, J.; Duncanson, L. A.; Guy, R. G. *J. Chem. Soc.* **1961**, 827. c) Chatt, J.; Duncanson, L. A.; Guy, R. G.; Thompson, D. T. *J. Chem. Soc.* **1963**, 5170.
- (20) Greaves, E. O.; Lock, C. J. L.; Maitlis, P. M. *Can. J. Chem.* **1968**, *46*, 3879.
- (21) a) Colborn, R. E.; Vollhardt, K. P. C. *J. Am. Chem. Soc.* **1986**, *108*, 5470. b) Colborn, R. E.; Vollhardt, K. P. C. *J. Am. Chem. Soc.* **1981**, *103*, 6259.
- (22) Ozin, G. A.; McIntosh, D. F.; Power, W. J.; Messmer, R.P. *Inorg. Chem.* **1981**, *20*, 1782.
- (23) Kline, E. S.; Kafafi, Z. H.; Hauge, R. H.; Margrave, J. L. *J. Am. Chem. Soc.* **1987**, *109*, 2402.
- (24) a) Manceron, L.; Andrews, L. *J. Phys. Chem.* **1989**, *93*, 2964. b) Burkholder, T. R.; Andrews, L. *Inorg. Chem.* 1993, *32*, 2491. c) Thompson, C. A.; Andrews, L. *J. Am. Chem. Soc.* **1996**, *118*, 10242.
- (25) a) Cabarcos, O. M.; Weinheimer, C. J.; Lisy, J. M. *J. Chem. Phys.* **1999**, *110*, 8429. b) Cabarcos, O. M.; Weinheimer, C.J.; Lisy, J. M. *J. Chem. Phys.* **1998**, *108*, 5151. c) Lisy, J. M. *Int. Rev. Phys. Chem.* **1997**, *16*, 267. d) Weinheimer,

- C. J.; Lisy, J. M. *J. Chem. Phys.* **1996**, *105*, 2938. e) Lisy, J. M. *Cluster Ions* **1993**, 217. f) Vaden, T. D.; Forinash, B.; Lisy, J. M. *J. Chem. Phys.* **2002**, *117*, 46284631. g) Vaden, T. D.; Weinheimer, C. J.; Lisy, J. M. *J. Chem. Phys.* **2004**, *121*, 3102. k) Patwari, G. N.; Lisy, J. M. *J. Chem. Phys.* **2003**, *118*, 8555.
- (26) a) Inokuchi, Y.; Ohshimo, K.; Misaizu, F.; Nishi, N. *J. Phys. Chem. A* **2004**, *108*, 5034. b) Inokuchi, Y.; Ohshimo, K.; Misaizu, F.; Nishi, N. *Chem. Phys. Lett.* **2004**, *390*, 140.
- (27) Simon, A.; Jones, W.; Ortega, J.-M.; Boissel, P.; Lemaire, J.; Maitre, P. *J. Am. Chem. Soc.* **2004**, *126*, 11666.
- (28) Jaeger, T. D.; van Heijnsbergen, D.; Klippenstein, S. J.; von Helden, G.; Meijer, G.; Duncan, M. A. *J. Am. Chem. Soc.* **2004**, *126*, 10981.
- (29) Jaeger, T. D.; Pillai, E. D.; Duncan, M. A. *J. Phys. Chem. A* **2004**, *108*, 6605.
- (30) Walters, R. S.; Schleyer, P. v. R.; Corminboeuf, C.; Duncan, M. A. *J. Am. Chem. Soc.* **2005**, *127*, 1100.
- (31) Walters, R. S.; Jaeger, T. D.; Duncan, M. A. *J. Phys. Chem. A* **2002**, *106*, 10482.
- (32) Walker, N. R.; Greives, G. A.; Walters, R. S. *Chem. Phys. Lett.* **2003**, *380*, 230.
- (33) Duncan, M. A. *Int. Rev. Phys. Chem.* **2003**, *22*, 407.
- (34) Walker, N. R.; Walters, R. S.; Pillai, E. D.; Duncan, M. A. *J. Chem. Phys.* **2003**, *119*, 10471.
- (35) Walters, R. S.; Duncan, M. A. *Austral. J. Chem.* **2004**, *57*, 1145.

- (36) Walker, N. R.; Walters, R. S.; Jordan, K. D.; Duncan, M. A. *J. Phys. Chem. A* submitted.
- (37) Shimanouchi, T. *Molecular Vibrational Frequencies*; 69th ed.; Chemistry WebBook, NIST Standard Reference Database (<http://webbook.nist.gov>), 2001.
- (38) Frisch, M. J.; Trucks, G. W.; Schlegel, H. B.; Scuseria, G. E.; Robb, M. A.; Cheeseman, J. R.; Montgomery, J. A. Jr.; Vreven, T.; Kudin, K. N.; Burant, J. C.; Millam, J. M.; Iyengar, S. S.; Tomasi, J.; Barone, V.; Mennucci, B.; Cossi, M.; Scalmani, G.; Rega, N.; Petersson, G. A.; Nakatsuji, H.; Hada, M.; Ehara, M.; Toyota, K.; Fukuda, R.; Hasegawa, J.; Ishida, M.; Nakajima, T.; Honda, Y.; Kitao, O.; Nakai, H.; Klene, M.; Li, X.; Knox, J. E.; Hratchian, H. P.; Cross, J. B.; Adamo, C.; Jaramillo, J.; Gomperts, R.; Stratmann, R. E.; Yazyev, O.; Austin, A. J.; Cammi, R.; Pomelli, C.; Ochterski, J. W.; Ayala, P. Y.; Morokuma, K.; Voth, G. A.; Salvador, P.; Dannenberg, J. J.; Zakrzewski, V. G.; Dapprich, S.; Daniels, A. D.; Strain, M. C.; Farkas, O.; Malick, D. K.; Rabuck, A. D.; Raghavachari, K.; Foresman, J. B.; Ortiz, J. V.; Cui, Q.; Baboul, A. G.; Clifford, S.; Cioslowski, J.; Stefanov, B. B.; Liu, G.; Liashenko, A.; Piskorz, P.; Komaromi, I.; Martin, R. L.; Fox, D. J.; Keith, T.; Al-Laham, M. A.; Peng, C. Y.; Nanayakkara, A.; Challacombe, M.; Gill, P. M. W.; Johnson, B.; Chen, W.; Wong, M. W.; Gonzalez, C.; Pople, J. A. *Gaussian 03 (Revision B.02)*; Gaussian, Inc.: Pittsburgh, PA, 2003.
- (39) a) Becke, A. D. *J. Chem. Phys.* **1993**, 98, 5648 b) Lee, C.; Yang, W.; Parr, R. G. *Phys. Rev. B* **1988**, 37, 785.

- (40) Cotton, F. A.; Wilkinson, G. *Advanced Inorganic Chemistry*, 6th ed., John Wiley & Sons: New York, 1999.
- (41) MacBeth, C. E.; Thomas, J. C.; Betley, T. A.; Peters, J. C. *Inorg. Chem.* **2004**, *43*, 4645.
- (42) Alberts, I. L.; Rowlands, T. W.; Handy, N. C. *J. Chem. Phys.* **1988**, *88*, 3811.
- (43) a) Fischer, G.; Miller, R. E.; Vohralik, P. F.; Watts, R. O. *J. Chem. Phys.* **1985**, *83*, 1471. b) Miller, R. E.; Vohralik, P. F.; Watts, R. O. *J. Chem. Phys.* **1984**, *80*, 5453.
- (44) a) Okumura, M.; Yeh, L. I.; Lee, Y. T. *J. Chem. Phys.* **1985**, *83*, 3705. b) Okumura, M.; Yeh, L. I.; Lee, Y. T. *J. Chem. Phys.* **1988**, *88*, 79. c) Okumura, M.; Yeh, L. I.; Myers, J. D.; Lee, Y. T. *J. Phys. Chem.* **1990**, *94*, 3416.
- (45) a) Meuwly, M.; Nizkorodov, S. A.; Maier, J. P.; Bieske, E. J. *J. Chem. Phys.* **1996**, *104*, 3876. b) Dopfer, O.; Roth, D.; Maier, J. P. *J. Phys. Chem. A* **2000**, *104*, 11702. c) Bieske, E. J.; Dopfer, O. *Chem. Rev.* **2000**, *100*, 3963.
- (46) a) Bailey, C. G.; Kim, J.; Dessent, C. E. H.; Johnson, M. A. *Chem. Phys. Lett.* **1997**, *269*, 122. b) Ayotte, P.; Weddle, G. H.; Kim, J.; Johnson, M. A. *J. Am. Chem. Soc.* **1998**, *120*, 12361. c) Corcelli, S. A.; Kelley, J. A.; Tully, J. C.; Johnson, M. A. *J. Phys. Chem. A* **2002**, *106*, 4872. d) Robertson, W. H.; Johnson, M. A. *Ann. Rev. Phys. Chem.* **2003**, *54*, 173.
- (47) Pino, T.; Boudin, N.; Brechignac, P. *J. Chem. Phys.* **1999**, *111*, 7337.
- (48) Satink, R. G.; Piest, H.; von Helden, G.; Meijer, G. *J. Chem. Phys.* **1999**, *111*, 10750.

- (49) Partridge, H.; Bauschlicher, C. W.; Langhoff, S. R. *J. Phys. Chem.* **1992**, 96, 5350.
- (50) a) Lessen, D. E.; Asher, R. L.; Brucat, P. J. *Advances in Metal & Semiconductor Clusters* **1993**, 1, 267. b) Lessen, D. E.; Brucat, P. J. *Chem. Phys. Lett.* **1988**, 152, 473.
- (51) Kemper, P. R.; Hsu, M.-T.; Bowers, M. T. *J. Phys. Chem.* **1991**, 95, 10600.
- (52) Sugar, J.; Corliss, C. *J. Phys. Chem. Ref. Data* 14 Supplement, **1985**, 14, 1.

CHAPTER V

INVESTIGATIONS OF INTRACLUSTER CHEMISTRY IN NICKEL CATION-
ACETYLENE COMPLEXES¹

¹ Walters, R.S.; Pillai, E.D.; Duncan, M.A. To be submitted to *J. Am. Chem. Soc.*

Abstract

Nickel ion-acetylene complexes of the form $\text{Ni}^+(\text{C}_2\text{H}_2)_n$, where $n = 4 - 6$, are produced in a laser vaporization pulsed-nozzle cluster source, size-selected and studied by infrared photodissociation spectroscopy in the C-H stretch region. Experimental spectra are compared to theoretical results calculated with density functional theory at the B3LYP level. For the $n = 4$ complex, theory finds that various reaction products containing π -benzene, π -cyclobutadiene and a metallacycle are more stable than the unreacted $\text{Ni}^+(\text{C}_2\text{H}_2)_4$ cluster. However, the best match between experiment and theory is the unreacted isomer which has all four intact acetylenes π -bonded to the nickel cation. New intense features are observed in the experimental spectra beginning with the $n = 5$ complex, and attributed to the formation of the second solvation layer. Multiple isomeric structures are considered for the $n = 5$ molecule to explore the possible role of condensation chemistry that might occur for this system. Like the $n = 4$ cluster, structures containing reaction products are found to be more stable with respect to the unreacted isomers. Although the IRPD spectrum of this complex seems to be more consistent with two unreacted isomers of C_s and C_1 symmetry, condensation products cannot be completely ruled out due to spectral congestion in the C-H region.

Introduction

The study of transition metals complexed to unsaturated hydrocarbon molecules has been of long-standing interest in organometallic chemistry as these compounds are important in heterogeneous catalysis.^{1,2} However, detailed information on the structures of these complexes is often obscured in the condensed phase. Isolated gas-phase organometallic complexes are solvent free and can be used as tractable models to study the metal-ligand interaction. Geometric and electronic structures of metal-olefin complexes have been investigated with theory by a number of groups.³⁻⁷ The reactions of transition metals with small hydrocarbon molecules have been observed in gas phase ion chemistry,⁸⁻¹⁴ and metal ion- π complex bond energies have been measured by equilibrium mass spectrometry¹⁵ and collision induced dissociation.¹⁶ Electronic photodissociation spectroscopy has been employed in the past to probe excited states,^{17,18} but direct spectroscopic measurements of these complexes in their ground states is limited. Infrared and Raman spectroscopies are common techniques used in condensed phase studies,¹⁹⁻²⁵ but applying them to the gas phase is problematic due to low sample densities. However, recent advances in high-power pulsed infrared lasers now enable geometric structures of metal-ligand complexes in their electronic ground states to be investigated by photodissociation.²⁶⁻³⁶ In this paper, we report on the infrared photodissociation (IRPD) spectroscopy of $\text{Ni}^+(\text{C}_2\text{H}_2)_{4-6}$ complexes. The spectra are acquired in the C-H stretch region and compared to harmonic frequencies of theoretical structures calculated with density functional theory (DFT) at the B3LYP level.

From the early work on metal-ethylene complexes and metal-carbonyls, the Dewar-Chatt-Duncanson π -bonding model was developed to interpret the structure of metal-olefin compounds.^{1,2,19-21} The model proposes that electron density is σ -donated from the filled π -orbitals of the ligand to the unoccupied metal orbitals coupled with back-donation from the filled metal d orbitals into the unoccupied π^* orbital. Both factors weaken the bonding in the ligand, shifting its vibrations to lower frequency. Understanding the details of the metal- π interaction is important as these compounds are possibly involved in a number of catalytic reactions.^{1,2} The cracking of hydrocarbons as well as olefin polymerization and cyclization reactions are common to the petroleum, natural gas and chemical industries. Catalysts made from Group VIII transition metals are traditionally used to carry out these processes. Of particular interest to this work, acetylene cyclizes to form cyclooctatetraene (COT) via a nickel catalyst in what is known as the Reppe reaction.^{1,2} Although this reaction and similar ones have been studied for decades, the details are difficult to observe at the metal-molecule interface. Spectral congestion produced by overlapping optical excitation and solvent effects often preclude *in situ* condensed phase measurements. Therefore, energy pathways and transition state structures in many catalytic reactions remain speculative.

Gas phase organometallic complexes are solvent free and are therefore convenient models to study the effects of the metal- π interaction and the possible chemistry that can occur in these systems. Bauschlicher was one of the first to study metal- π bonding with modern theoretical methods using the modified coupled pair functional (MCPF).³ Schwarz and coworkers used DFT to study noble metal ion-

ethylene complexes and determined that π -backbonding was less important than σ -donation.⁴ More recently, Frenking has incorporated an energy partitioning analysis to DFT and *ab initio* methods to determine the extent of electrostatic and covalent bonding in a variety of organometallic complexes.⁵ There are two theoretical papers of particular importance to this study. Klippenstein studied the first row transition metal ions complexed to acetylene with DFT to observe how the acetylene stretches would be affected by the metal ion- π interaction.⁶ The other paper by Straub and coworkers reported on various theoretical mechanisms for the Reppe reaction.⁷ They studied possible low energy pathways that involve metallacycle transition state structures for neutral nickel and nickel dimer reactions with acetylene.

In addition to theoretical advances, experiments have evolved to the point where molecular phenomena can be studied in detail. Reactions of transition metals with small hydrocarbons have been observed and, in some cases, their energetics measured in gas phase ion chemistry.⁸⁻¹⁴ Armentrout has used collision-induced dissociation to determine bond strengths in a variety of metal ion- π complexes,¹⁶ and other groups have studied similar molecules with photodissociation.⁹⁻¹¹ There are no accurate bond measurements reported in the literature on Ni^+ -acetylene complexes however. Bowers and coworkers recently reported on bond energies for Ag^+ -ethylene clusters which are analogous to the molecules reported in this work.¹⁵ Using equilibrium mass spectrometry, they determined that the Ag^+ is four-coordinate, but that the third and fourth ethylenes are more weakly bound than the first two. Electronic photodissociation spectroscopy of metal ion- π complexes has been employed in the past to probe excited states,^{17,18} but these studies are limited to

metals that have optical transitions accessible with tunable dye lasers. Information on transition metal clusters as well as multiple ligand complexes cannot be obtained because they predissociate during electronic excitation. Additionally, excited state structures and energies of metal ion radical complexes are difficult to handle with theory, making direct comparisons to experiment problematic.

Infrared spectroscopy is therefore necessary to determine ground state geometric structures which can then be compared to current quantum chemical calculations. Until recently, IR measurements of isolated metal-olefin complexes were only available using matrix isolation.²³⁻²⁵ New infrared laser systems now provide a way to study organometallic complexes in a molecular beam environment, free from matrix effects. IRPD spectroscopy of alkali and alkali-earth metal ion complexes was first reported by the Lisy group.²⁶ Inokuchi and coworkers have also employed this method to study similar molecules,²⁷ and our group was the first to apply this technique to transition metal complexes.²⁹⁻³⁶ Using a free electron laser, we studied metal ion-benzene clusters to determine how π -bonding affected the benzene C=C stretches.²⁹ Maitre and coworkers used a similar laser to study various Fe^+ -hydrocarbon molecules.²⁸ We have extended these IR studies to higher frequencies using a bench top OPO laser system.³⁰⁻³⁶ In a communication, we reported on the IRPD spectroscopy of $\text{M}^+(\text{C}_2\text{H}_2)\text{Ar}_2$ ($\text{M} = \text{V}, \text{Fe}, \text{Co}, \text{Ni}$) in the C-H stretch region.³¹ The spectra show that π -complexes are formed for the Group VIII metal cations, whereas $\text{V}^+(\text{C}_2\text{H}_2)$ is a three-member ring metallacycle. More recently, we studied $\text{Ni}^+(\text{C}_2\text{H}_2)_{1-4}$ complexes in the C-H stretch region and compared our results to B3LYP structures.³² The combined experiment and theory indicate that the

$n = 2 - 4$ complexes are Jahn-Teller distorted and that four acetylenes complete the Ni^+ coordination. In an earlier letter, we reported on the vibrational spectroscopy of the $n = 3 - 6$ complexes which suggested that condensation chemistry might have occurred after the second solvation layer was formed.³³ We continue here with a more thorough investigation of the larger $\text{Ni}^+(\text{acetylene})_n$ complexes. The IRPD spectra of $\text{Ni}^+(\text{C}_2\text{H}_2)_{4-6}$ are acquired in the C-H stretch region and compared to B3LYP results. Multiple theoretical structures are considered, including π -bonded benzene, π -bonded cyclobutadiene and metallacycle complexes.

Experimental Spectra

Nickel ion-acetylene complexes are produced in a laser vaporization pulsed nozzle source and analyzed with a reflectron time-of-flight mass spectrometer. The source and molecular beam apparatus have been described previously.³⁴ The third harmonic of a Nd:YAG (355 nm) is used to vaporize a rotating nickel rod. Ions are produced directly from the laser plasma in our specially designed cutaway source that typically produces clusters containing a single metal ion. $\text{Ni}^+(\text{C}_2\text{H}_2)_n$ clusters are made in an argon expansion that contains ~5% acetylene. The pulsed nozzle is a General Valve Series 9 (1 mm orifice) operating at ~50 psi backing pressure and pulse durations near 250 μsec . The metal ion-molecule complexes are skimmed into the mass spectrometer chamber and injected into the reflectron by pulsed acceleration voltages. The ions are size-selected within the first flight tube by another set of pulsed voltages before entering the reflectron field. They are then intersected at the turning point with the output of an IR Optical Parametric Oscillator/Amplifier

(OPO/OPA) laser. If photodissociation occurs, fragment ions separate from the mass-selected parent ions when reaccelerated in the second stage of the reflectron. Parent and daughter ions are detected using an electron multiplier tube (EMT) and their signals are transferred to a PC by an IEEE interface. Photodissociation is more efficient on resonance, thus monitoring the fragment ion yield as a function of IR laser wavelength produces the IRPD spectra of the parent ion that was mass-selected.

The OPO (Laservision) uses two KTP crystals pumped by the second harmonic (532 nm) of a Nd:YAG laser (Continuum 9010) to produce tunable 725 – 872 nm light. This radiation is then combined with the delayed fundamental (1064 nm) in the optical parametric amplifier (OPA). The OPA generates the near IR light (2050 – 4400 cm^{-1}) by difference frequency mixing in four KTA crystals. This output is then used to excite the ion-molecule complexes near the asymmetric (3289 cm^{-1}) and symmetric (3374 cm^{-1}) C-H stretches of acetylene,³⁷ and produce their IRPD spectra. We frequency calibrated the OPO/OPA in the C-H stretch region by acquiring the photo-acoustic spectrum of methane (2800-3200 cm^{-1}). It should be noted that we did not use this method of calibration in our previous paper on the IRPD spectra of $\text{Ni}^+(\text{C}_2\text{H}_2)_n$ ($n=3-6$) complexes.³³ The wavenumbers reported here are accurate and the previous spectra are therefore incorrect by $\sim 14 \text{ cm}^{-1}$.

Theoretical Methods

The structures, energies, vibrational frequencies and IR oscillator strengths for the $\text{Ni}^+(\text{C}_2\text{H}_2)_{4-5}$ complexes are calculated using density functional theory (DFT). The B3LYP (Becke-3-Lee-Yang-Parr)³⁸ functional available on the Gaussian 03W

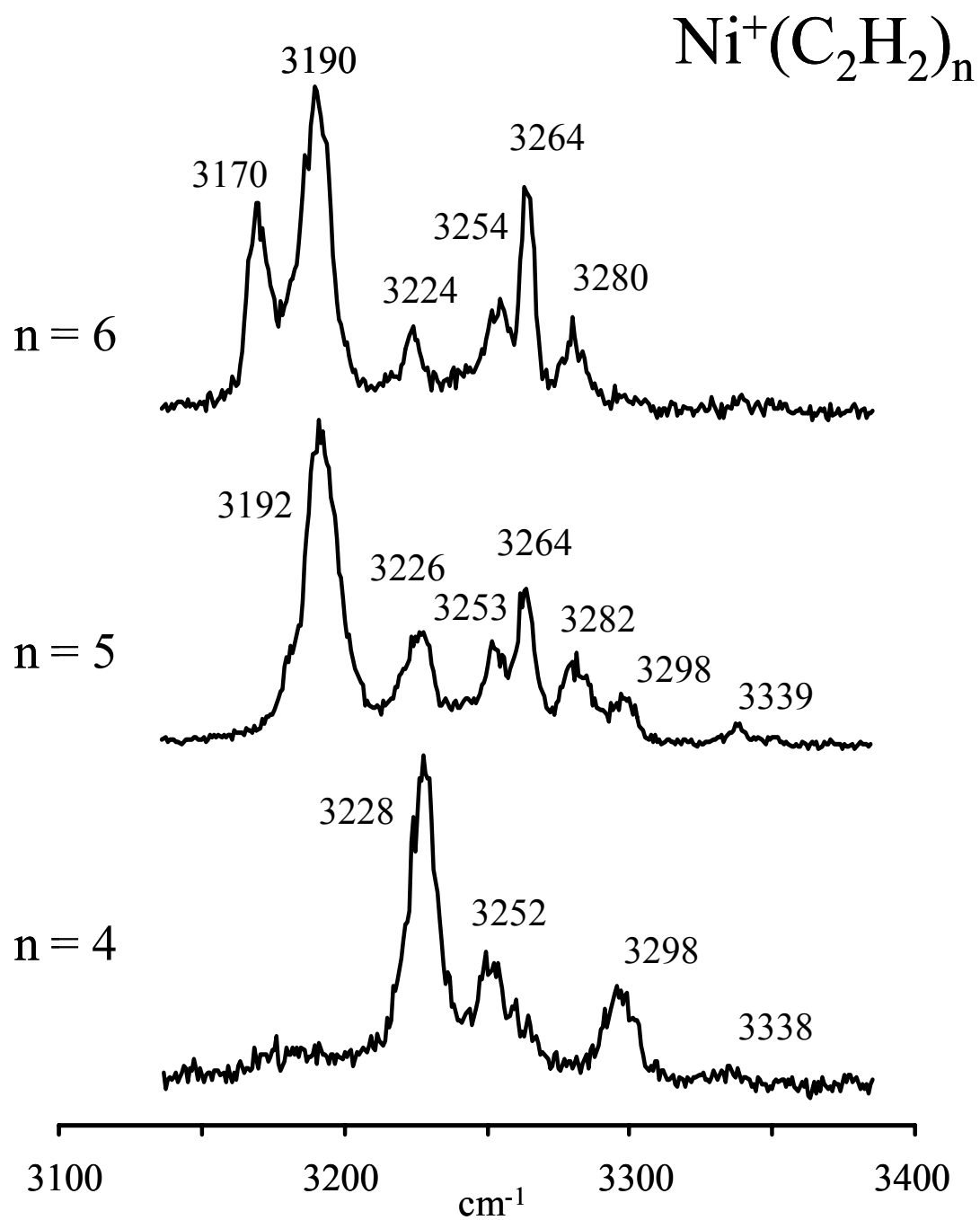
package³⁹ is utilized with an all-electron triple zeta basis set employing polarization functions on all atoms and diffuse functions only on the heavy atoms (6-311⁺G**). For the unsaturated molecules, the nickel cation is presumed to bind to the π -electrons, but we allow the calculations to break symmetry to obtain all possible geometries. The energies are not zero-point corrected and we employ the 0.96 empirical scaling factor for the harmonic frequencies as suggested in the literature.⁴⁰

All possible isomeric structures were considered for the unreacted $n = 4$ complex, including square-planar arrangements and a “3+1” structure as reported earlier.³² For the reacted systems however, we chose the most likely candidates that are known from studies on transition metal surfaces and organometallic chemistry.^{1,2,43-48} The experimental spectra for all cluster sizes show intense bands in the 3150 – 3350 cm^{-1} region that arise from C-H stretches of perturbed but intact acetylene molecules as discussed below. Hence, the theoretical work presented here is for the subset of isomers containing at least one unreacted acetylene. For example, we did not consider cyclooctatetraene π -bonded to the nickel cation for the $n = 4$ complex, as this cluster would not contain an acetylene ligand. One intact acetylene would remain for this cluster in the $n = 5$ complex, but its IR spectrum is expected to be similar to the π -benzene $n = 4$ molecule and was therefore not studied. Similar reasoning was used to disregard other reacted species such as clusters containing two π -bonded cyclobutadienes, one π -cyclobutadiene and one metallacyclopentadiene, larger metallacycle species, etc.

Discussion

Previously, we reported on the IRPD spectra of the smaller Ni^+ -acetylene complexes as they compared to B3LYP theoretical structures.³² The spectra and theory revealed that $\text{Ni}^+(\text{C}_2\text{H}_2)_{1-4}$ formed π -complexes, that Jahn-Teller effects are present in the $n = 2-4$ complexes, and that this system is four-coordinate. Additionally, the CH stretches are observed to shift back towards the free acetylene vibrations as cluster size increases. As more acetylenes are added to the $n = 4$ core complex, we expect to see signature IR peaks that correspond to surface-bound acetylene (i.e. second sphere) in addition to the metal-bonded acetylene modes observed for the $n = 4$ cluster. Our previous IR studies on $\text{M}^+(\text{CO}_2)_n$ complexes showed a significant new vibrational band for the second sphere ligand, and its frequency was close to that in the free CO_2 molecule.^{34,35} We therefore expect to see similar unshifted bands for this system corresponding to solvent acetylene. Figure 5.1 shows the IRPD spectra for $\text{Ni}^+(\text{C}_2\text{H}_2)_{4-6}$ complexes. Careful inspection reveals that the four resonances, three intense and one weak, for the $n = 4$ complex are still present in the larger complexes. They correspond to C-H stretches of core acetylenes that are attached directly to the nickel cation. The 3228 cm^{-1} band measured for the $n = 4$ complex red-shifts slightly to 3226 cm^{-1} and 3224 cm^{-1} for the $\text{Ni}^+(\text{C}_2\text{H}_2)_5$ and $\text{Ni}^+(\text{C}_2\text{H}_2)_6$ complexes respectively. On the other hand, the 3252 cm^{-1} mode blue-shifts to 3253 cm^{-1} and 3254 cm^{-1} , while the $n = 4$ feature at 3298 cm^{-1} doesn't change much in its position, but gradually diminishes in intensity as cluster size increases. Larger clusters also have additional modes that are more intense than the 'core' modes. Three new bands at 3192 , 3264 and 3282 cm^{-1} are observed for the $n = 5$

Figure 5.1 The IRPD spectra of the $\text{Ni}^+(\text{C}_2\text{H}_2)_{4-6}$ complexes. The bands in the $\text{Ni}^+(\text{C}_2\text{H}_2)_4$ spectrum are reproduced in the spectra of the larger complexes. Additional modes are observed near 3170 cm^{-1} , $\sim 3190\text{ cm}^{-1}$, 3264 cm^{-1} and $\sim 3280\text{ cm}^{-1}$ in the spectra of the $\text{Ni}^+(\text{C}_2\text{H}_2)_{5,6}$ complexes



complex and are reproduced in the $n = 6$ spectrum at 3190, 3264 and 3280 cm^{-1} . The $n = 6$ spectrum also displays an additional feature at 3170 cm^{-1} . The new peaks observed between 3260-3285 cm^{-1} are somewhat expected as acetylene dimers and trimers have C-H stretches in this region.^{41,42} The features that occur to the red of the core modes are completely unexpected however. The IR spectra reported previously for the smaller Ni^+ -acetylene complexes showed that the C-H stretches blue-shift back toward the free acetylene modes as binding is distributed to multiple acetylenes.³² The appearance of new intense modes that are red-shifted from the core modes suggests that something quite different is occurring for the larger clusters beginning with $n = 5$. In our previous paper on these complexes, we assigned the red-shifted resonances to an intracuster reaction product that forms once the second solvation layer begins.³³

Reactions of acetylene on transition metal surfaces are known to produce benzene⁴³ and the formation of benzene has been observed in gas-phase ion chemistry.^{7b} Additionally, COT is formed from the cyclization of acetylene using a nickel catalyst via the Reppe reaction.^{1,2} Acetylene is also known to isomerize to form metal-vinylidene structures.^{23a,43} However, all of these possible reaction products have C-H stretches below 3100 cm^{-1} . Because no signals were detected in this region for any of the $\text{Ni}^+(\text{C}_2\text{H}_2)_n$ cluster sizes studied, we initially ruled out benzene, COT and vinylidene as possible reaction products.³³ We have recently studied $\text{Ni}^+(\text{benzene})\text{Ar}_2$ with IRPD spectroscopy and its C-H resonances occur near 3096 cm^{-1} .³⁰ However, fragmentation signals of this cluster in the C-H stretch region were somewhat weak. Action spectroscopies are not only dependent on optical transition

strengths, but also on the dynamics of the photodissociation process. In this case, we are detecting the loss of acetylene, which is more strongly bound than argon.

Photofragmentation of a weakly bound rare gas atom is more efficient than that of an acetylene ligand, therefore detecting the loss of acetylene is less sensitive. If benzene is formed in the $\text{Ni}^+(\text{C}_2\text{H}_2)_5$ complex, its weak C-H resonances might not be detected in the acetylene-loss channel. Therefore, benzene formation cannot be completely ruled out. As we discuss below, the C-H transitions of the other reaction products are also relatively weak and cannot be ruled out either.

Another possibility is the reaction of two acetylenes to form butadiene-like complexes. There are two types of species known from organometallic chemistry and surface science: the di- σ bonded metallacyclopentadienyl complex^{23b,43-45} and the η^4 π -bonded metal-cyclobutadiene structure.^{1,2,46-48} Cyclobutadiene is unstable, but once π -bonded to a metal it can make an overall stable complex. From IR studies on transition metal surfaces and in matrices, the C-H stretches for metallacycles occur near 3040 cm^{-1} .^{23b,43} The limited IR data on metal-cyclobutadiene indicate that its C-H vibration is around 3140 cm^{-1} ,⁴⁸ which is near the value measured for the isolated molecule.³⁹ From this information alone, we tentatively concluded that the observed peaks at 3170 cm^{-1} and 3190 cm^{-1} were C-H stretches from π -bonded cyclobutadiene formed from an intracuster cyclization reaction of two acetylenes.³³

The proposed reaction is reasonable because iron, cobalt and nickel form stable metal-cyclobutadiene complexes in conventional organometallic chemistry.^{46,47} Unsaturated hydrocarbons can undergo Woodward-Hoffman cycloaddition reactions if their molecular orbitals have the proper symmetry. The reaction of two isolated

acetylenes to form cyclobutadiene (2+2 cycloaddition) is symmetry forbidden,⁴⁹ and has been observed only under high pressure conditions.⁵⁰ However, acetylene π -bonded to a metal changes its orbital symmetries and cyclization might be possible if another acetylene aligns itself parallel to the first. It is unlikely that two core acetylenes react to form cyclobutadiene, as they bind tightly to the nickel cation and cannot achieve the proper configuration. However, acetylenes in the second solvation layer should have binding strengths similar to acetylene dimer ($\sim 400 \text{ cm}^{-1}$)^{41,42} and might therefore move more easily into alignment. A core + surface acetylene pair could then react, producing cyclobutadiene π -bonded to the metal cation. Such a rearrangement would have to overcome some unknown reaction barrier, but the fact that the new spectral bands appear after the Ni^+ coordination sites are filled ($n > 4$) supports this hypothesis. In order to test this mechanism we have also studied Co^+ -acetylene complexes with IRPD spectroscopy.³⁶ The fragmentation patterns and the IR spectra of the $\text{Co}^+(\text{C}_2\text{H}_2)_n$ complexes indicate that this system prefers a coordination of three, as opposed to four for the Ni^+ system. New red-shifted features are also observed for the $\text{Co}^+(\text{C}_2\text{H}_2)_n$ clusters, but they begin with the $n = 4$ complex. The fact that both $\text{Ni}^+(\text{C}_2\text{H}_2)_n$ and $\text{Co}^+(\text{C}_2\text{H}_2)_n$ complexes exhibit the same intense features only when acetylene is added to the second solvation layer is consistent with our proposed mechanism.

Because this chemistry is unexpected, a more rigorous test is required to prove that cyclobutadiene is formed. We therefore turned to DFT computations for this investigation. A number of different isomeric structures were considered for the $\text{Ni}^+(\text{C}_2\text{H}_2)_4$ complex. There is the unreacted cluster reported previously, where the

four acetylenes attach to the nickel cation to form a pseudotetrahedral structure.³² Calculations on an unreacted isomer where the intact acetylenes attach to the nickel cation in a square-planar arrangement did not converge. The remaining structures include reaction products known from surface science and organometallic chemistry. The three reacted isomers contain π -benzene, π -cyclobutadiene and metallacyclopentadiene. If two acetylenes have reacted to form either π -cyclobutadiene or the metallacycle complex, then two acetylenes would remain in the $\text{Ni}^+(\text{C}_2\text{H}_2)_4$ complex. Likewise, if three acetylenes have reacted to form π -benzene, then one acetylene would remain. As stated previously, acetylene is known to cyclize to form cyclooctatetraene via the Reppe reaction.^{1,2} However, if COT is formed in the $n = 4$ complex, no acetylenes would remain and this complex would not absorb and fragment in the acetylenic C-H stretch region. Therefore, we can rule out COT as a possible reaction product for the $\text{Ni}^+(\text{C}_2\text{H}_2)_4$ complex. The DFT structures and relative energies of the possible $n = 4$ complexes are shown in Figure 5.2 and key structural parameters, dissociation energies, frequencies and IR intensities are listed in Table 5.1. As stated before, scaled harmonic frequencies calculated for the unreacted isomer matched the $n = 4$ experimental spectrum almost perfectly.³² However, B3LYP predicts that this is not the global minimum structure for this molecule, and all three isomers containing reaction products were found to be more stable. The π -benzene complex was determined to be the lowest energy structure with the π -cyclobutadiene, metallacyclopentadienyl, and unreacted species lying higher in energy by 123.1, 133.2, 146.4 kcal/mol, respectively.

Figure 5.2 B3LYP theoretical structures and relative energy levels for the $n = 4$ complexes. Structures containing the reaction products were found to be significantly more stable than the unreacted isomer with all four acetylenes intact.

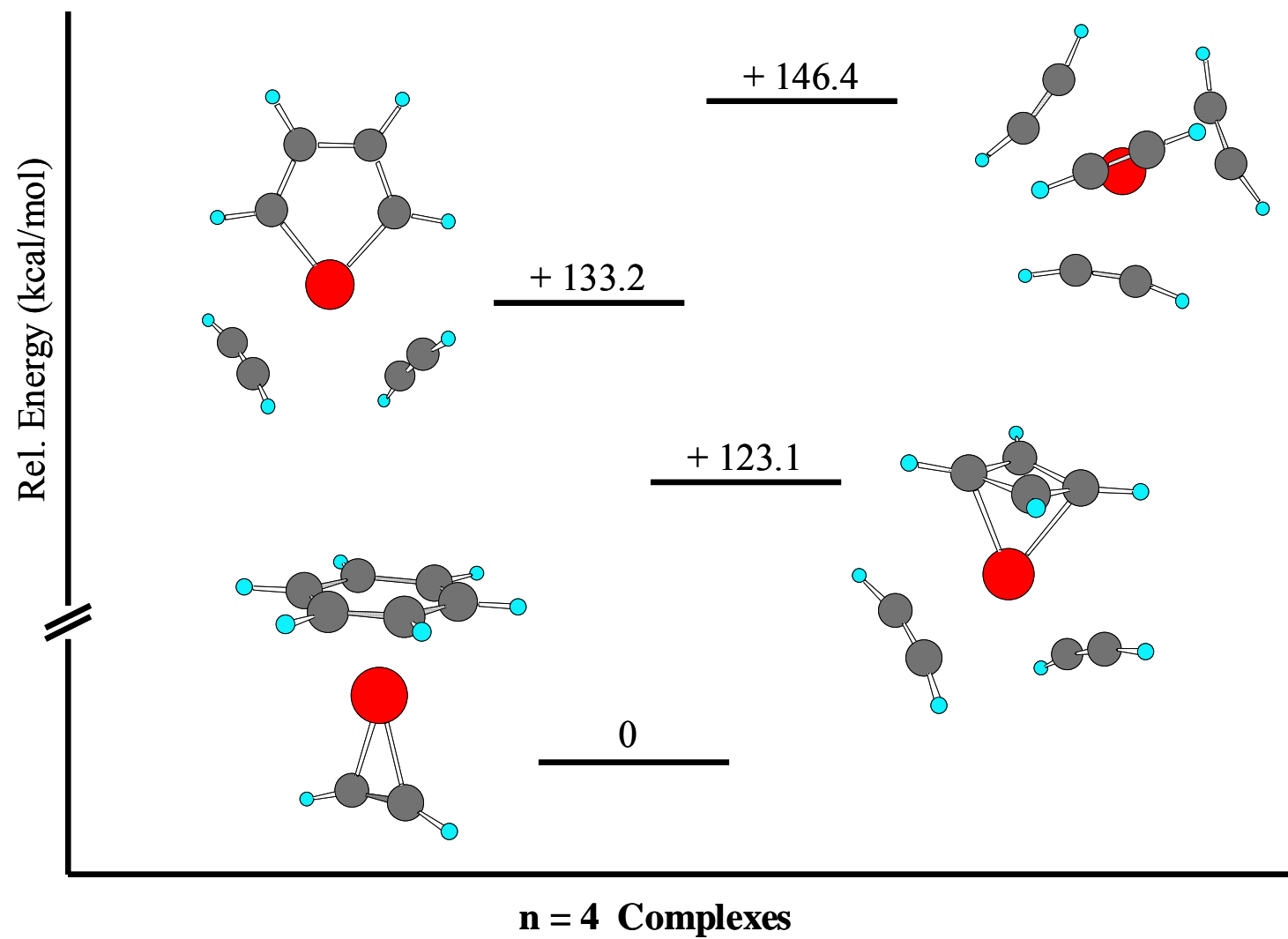


Table 5.1 B3LYP, 6-311+G** Energies, Frequencies, IR intensities, Structural information for the n = 4 isomers.

Ni ⁺ (C ₂ H ₂) ₄	Energies*	Frequencies (Ints) †	Key Structural Parameters				J-T angle‡
			M ⁺ -C (Å)	C≡C (Å)	CCH angle	C ₂ H ₂ Type	
unreacted Cs	4.9	1875(5), 1885(4), 1887(1), 1952(7),	2.205, 2.220	1.217	166.2, 165.7	J-T distorted	86.3
		3229(39), 3235(120), 3237(146),	2.205, 2.220	1.217	166.2, 165.7	J-T distorted	
		3258(135), 3314(50), 3320(56),	2.192, 2.192	1.219	165.4, 165.4	Backside	
		3324(11), 3356(8)	2.500, 2.510	1.205	174.6, 175.0	On-top	
metallacycle		1064(2), 1070(0), 1209(14), 1299(3),					
		1414(46), 1439(0), 1925(3), 3037(0),	2.293, 2.319	1.210	172.8, 173.5	Core	
		3050(0), 3234(57), 3235(268),	2.293, 2.319	1.210	172.8, 173.5	Core	
		3330(20), 3330(30)					
π-cyclobutadiene	30.3	1070(0), 1152(0), 1215(0), 1275(19),					
		1308(12), 1877(6), 1878(2), 3099(1),	2.170, 2.159	1.219	167.5, 169.1	Core	
		3108(4), 3125(18), 3135(5), 3221(49),	2.170, 2.159	1.219	167.4, 169.1	Core	
		3222(234), 3309(43), 3310(50)					
π-benzene	40.2	1433(22), 1437(22), 1523(0), 1526(0),					
		1777(22), 3066(0), 3071(0), 3073(0),	1.973, 1.973	1.239	161.4, 161.4	Core	
		3080(6), 3082(5), 3087(0),					
		3175(114), 3249(59)					

* Dissociation energies = D_e(Ni⁺(C₂H₂)_n – Ni⁺(C₂H₂)_{n-1} + C₂H₂) in kcal/mol.

† Harmonic frequencies scaled by 0.96. Intensities are in km/mol

‡ Represents the acetylene-Ni+-acetylene angle of the Jahn-Teller distorted pair

Figure 5.3 shows the IR absorption spectra predicted for the $n = 4$ theoretical structures in the C-H region. The spectra have been frequency scaled by 0.96 and plotted at a 10 cm^{-1} resolution to provide a better comparison to the experiment. Intensities have also been scaled so that the most intense features in each spectrum are roughly equal. The theoretical spectra of the reaction products are quite similar. They are dominated by two intense peaks that correspond to asymmetric and symmetric C-H stretches of the remaining intact acetylenes. For example, if three acetylenes have reacted to form benzene in the $n = 4$ cluster, then one acetylene would be left over. This remaining acetylene is responsible for the intense modes predicted at 3175 cm^{-1} and 3249 cm^{-1} in the π -benzene theoretical spectrum. The cyclobutadiene and metallacyclopentadienyl complexes have two unreacted equivalent acetylenes, which account for their two intense acetylenic C-H resonances in the $3200 - 3350\text{ cm}^{-1}$ region. The C-H stretches of the product moieties are predicted to be relatively weak and occur at 3080 cm^{-1} for π -benzene, $3099 - 3135\text{ cm}^{-1}$ for π -cyclobutadiene and 3037 cm^{-1} and 3050 cm^{-1} for the metallacycle complex. The structure of the unreacted $n = 4$ isomer has four intact acetylenes π -bonded to the nickel cation with two of them distorted due to Jahn-Teller effects. Its predicted spectrum has more features in the $3200 - 3350\text{ cm}^{-1}$ region because of its lower symmetry structure. As described previously, all eight C-H motions in the unreacted isomer are predicted to be infrared active due to Jahn-Teller effects.³² However, its theoretical spectrum has only four main features when plotted at our experimental resolution because some of these vibrations overlap.

Figure 5.3 The theoretical spectra of the $n = 4$ isomeric structures calculated with B3LYP. Harmonic frequencies have been scaled by 0.96 and plotted at a 10 cm^{-1} resolution. Intensities have been scaled so that the most intense features are equal. All spectra are expected to have intense acetylenic C-H stretches. The C-H vibrations of the product moieties are predicted to be weak.

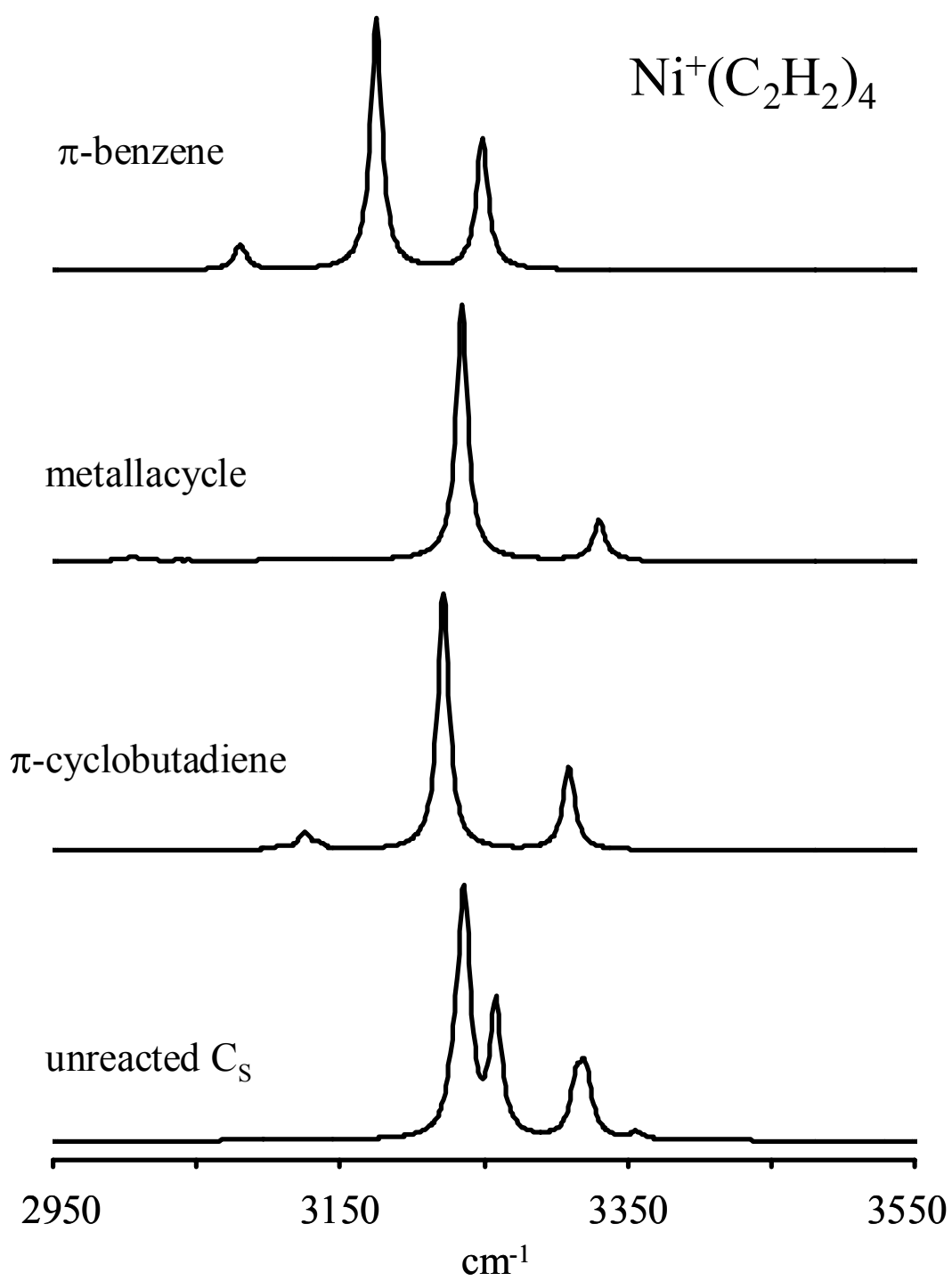
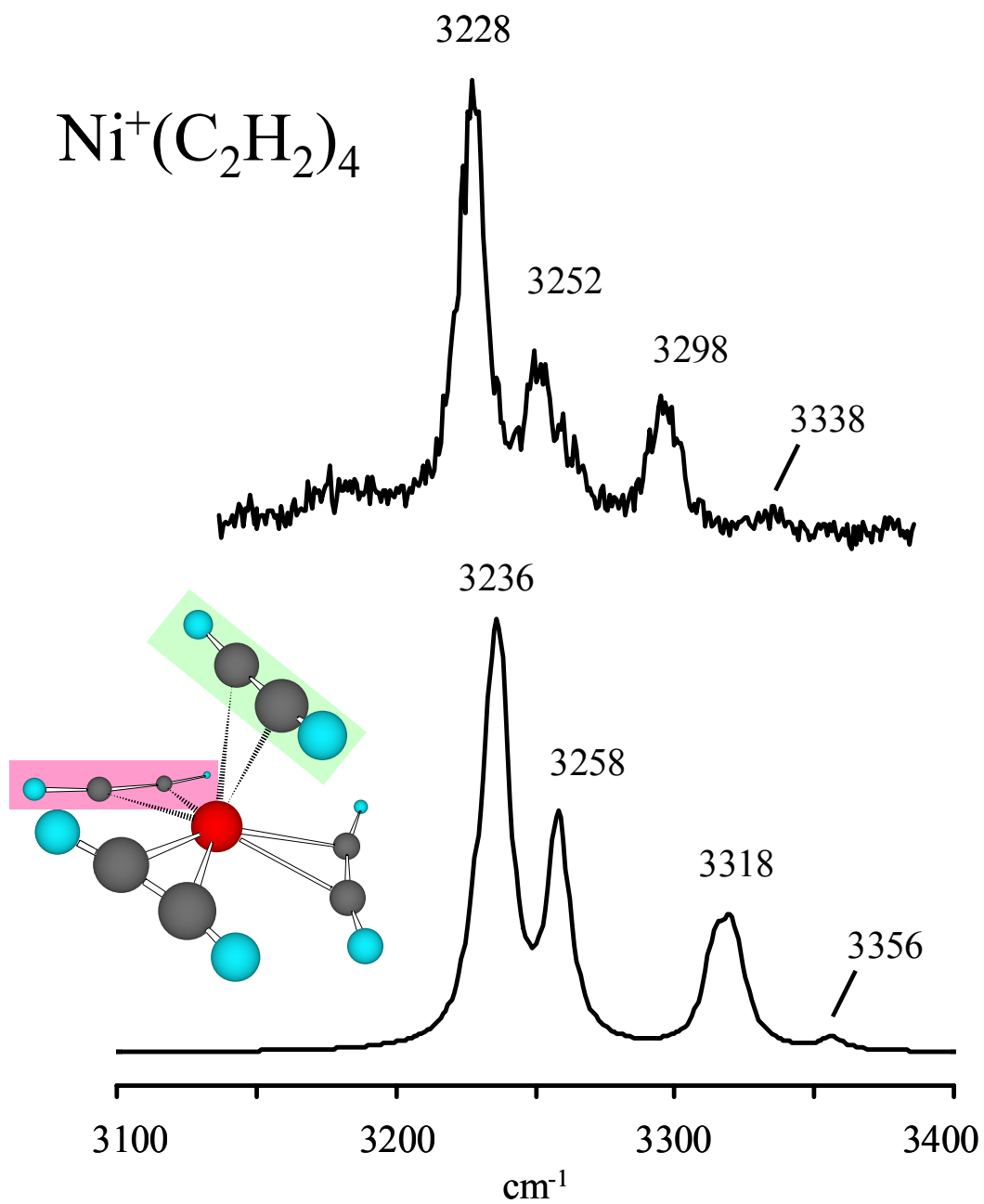
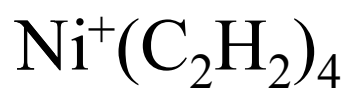


Figure 5.4 shows the comparison between the IRPD spectrum of $\text{Ni}^+(\text{C}_2\text{H}_2)_4$ and the theoretical spectrum of the unreacted $n = 4$ isomer. The structure of the $n = 4$ complex has three acetylenes whose centers-of-mass are near-planar with the Ni^+ and a fourth acetylene in an ‘on-top’ position. Of the three planar acetylenes, two of these are slightly pinched-in on one side of the cation due to Jahn-Teller effects. Because of this, we refer to them as the ‘distorted pair’ and the third planar acetylene as the ‘backside’ ligand. According to DFT, the in-phase and out-of-phase asymmetric stretches of the distorted acetylene pair are very close in energy (3235 cm^{-1} and 3237 cm^{-1}) and account for the intense peak at 3236 cm^{-1} . This intense feature also masks the weaker asymmetric stretch of the backside acetylene predicted at 3229 cm^{-1} . The band at 3258 cm^{-1} corresponds to the asymmetric stretch of the on-top acetylene. Therefore, the four asymmetric vibrations appear as two infrared features when plotted at the experimental resolution. Like the asymmetric features, the distorted pair and backside symmetric stretches overlap to produce the band centered at 3318 cm^{-1} . The weak transition at 3356 cm^{-1} is the symmetric stretch of the on-top acetylene. The unreacted isomer’s DFT spectrum reproduces the experimental spectrum quite well.

The only experimental detail not accurately reproduced by theory is the separation between the asymmetric and symmetric modes. This is because we are comparing the IRPD bands to B3LYP harmonic frequencies. When pure acetylene is calculated at the same level of theory, its vibrations occur at 3420 cm^{-1} and 3523 cm^{-1} (3283 cm^{-1} , 3382 cm^{-1} scaled) for the asymmetric and symmetric C-H stretches respectively. As expected, the harmonic values are higher than the well-known

Figure 5.4 The IRPD spectrum of the $\text{Ni}^+(\text{C}_2\text{H}_2)_4$ complex as it compares to the predicted spectrum of the B3LYP unreacted isomer. Harmonic frequencies have been scaled by 0.96 and plotted at a 10 cm^{-1} resolution. All band labels represent the center of the peak positions. The theoretical structure is shown in the inset. The ligands highlighted in pink and green are the ‘backside’ and ‘on-top’ acetylenes, respectively. The other two ligands are slightly pinched-in due to Jahn-Teller effects and referred to as the ‘distorted pair’ in the text.



experimental values, 3289 cm^{-1} and 3374 cm^{-1} .³⁹ However, the theoretical spacing between the modes is 12 cm^{-1} greater than the true separation. It is likely that this spectral separation is also overestimated in the Ni^+ -acetylene complexes. The asymmetric-like bands in the IRPD spectrum of $\text{Ni}^+(\text{C}_2\text{H}_2)_4$ at 3228 cm^{-1} and 3252 cm^{-1} are separated by 24 cm^{-1} . The center of the theoretical bands at 3236 cm^{-1} and 3258 cm^{-1} are also separated by approximately this amount (22 cm^{-1}). In the symmetric region, the 38 cm^{-1} spacing between the theoretical band centers at 3318 cm^{-1} and 3356 cm^{-1} is comparable to the 40 cm^{-1} experimental separation. However, when comparing the difference between the most intense asymmetric and symmetric features, the theoretical spacing of 82 cm^{-1} is significantly greater than the 70 cm^{-1} experimental measurement. This suggests that anharmonicity effects for the symmetric acetylene stretches are greater than the asymmetric vibrations, an important point when discussing the spectra of the $\text{Ni}^+(\text{C}_2\text{H}_2)_5$ complexes.

Figure 5.5 shows the B3LYP isomeric structures and relative energies calculated for the $n = 5$ complex. Dissociation energies, fundamental vibrations, IR intensities and structural parameters are included in Table 5.2. The same reaction product species calculated for the $n = 4$ complex were considered for $\text{Ni}^+(\text{C}_2\text{H}_2)_5$: π -benzene, π -cyclobutadiene and a metallacyclopentadienyl complex. If three acetylenes react to form benzene, two would remain for the $n = 5$ complex. DFT finds a stable structure where benzene and the remaining acetylenes are all π -bonded to the metal. Similarly, if two acetylenes react to form the butadiene complexes, three acetylenes would be left over. DFT finds stable structures for the π -cyclobutadiene and metallacycle complexes where the fifth acetylene attaches as a

Figure 5.5 B3LYP theoretical structures and relative energy levels for the $n = 5$ complexes. Like the $n = 4$ system, structures containing the reaction products are more stable than the unreacted isomers for $n = 5$. The π -benzene complex has both acetylenes attached to the metal. All other isomers have the fifth acetylene attached as a solven.

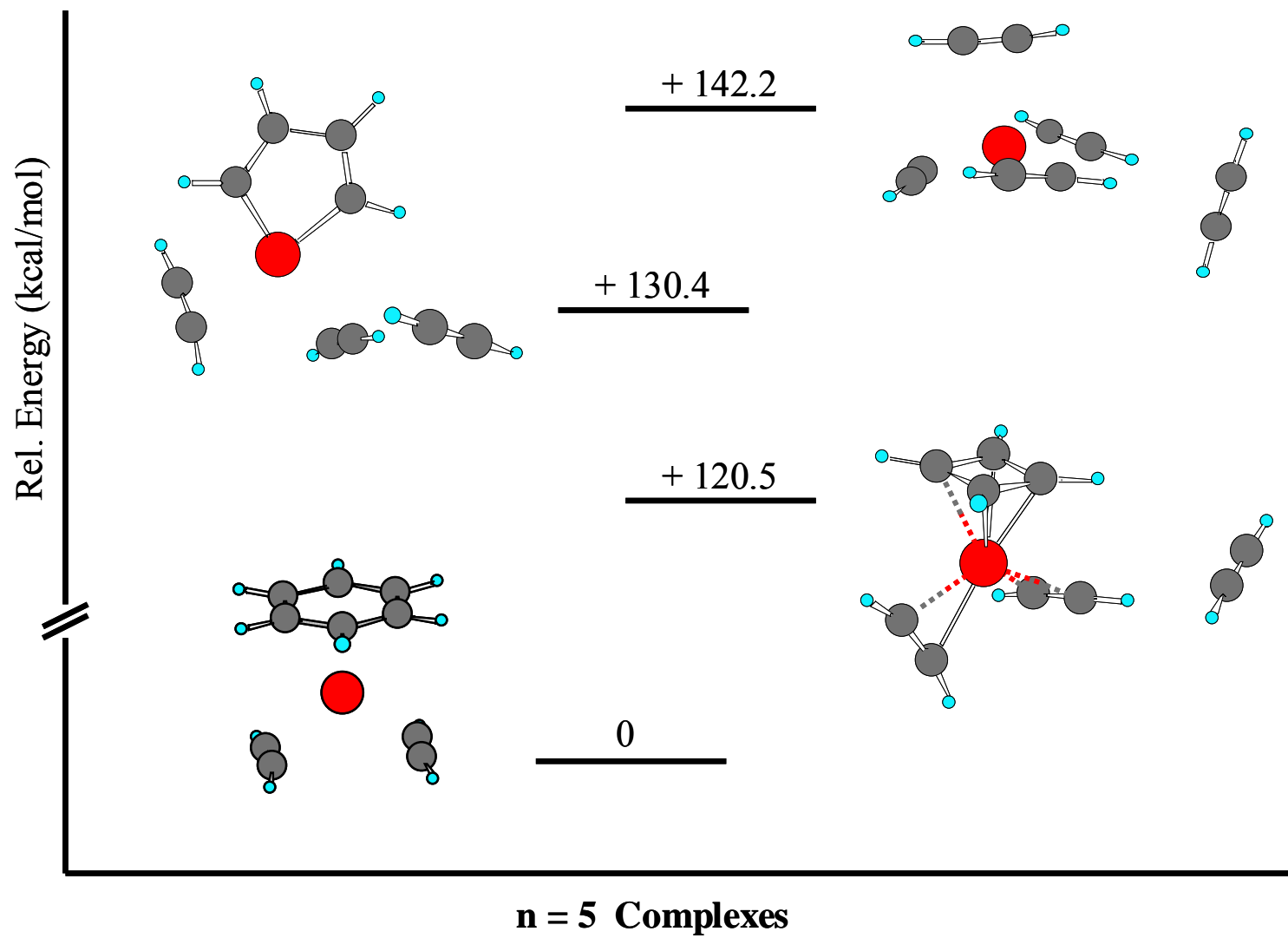


Table 5.2 B3LYP, 6-311+G** Energies, Frequencies, IR intensities, Structural information for the n = 5 isomers.

Ni ⁺ (C ₂ H ₂) ₅	Energies*	Frequencies (Ints) [†]	Key Structural Parameters			
			M ⁺ -C (Å)	C≡C (Å)	CCH angle	C ₂ H ₂ Type
unreacted Cs	4.6	3190(51), 3202(498), 3228(105), 3261(119), 3263(133), 3304(62), 3306(49), 3313(19), 3358(7), 3363(1)	2.215, 2.240	1.216	166.4, 167.3	J-T distorted
			2.215, 2.240	1.217	166.4, 167.3	J-T distorted
			2.176, 2.176	1.220	165.1, 165.1	Backside
			2.490, 2.498	1.205	174.7, 175.0	On-top
			-	1.201	177.2, 177.6	Solvent
unreacted C ₁	4.7	3184(67), 3194(466), 3241(118), 3258(131), 3263(121), 3293(61), 3296(35), 3331(29), 3356(9), 3363(1)	2.268, 2.282	1.213	168.8, 169.3	J-T distorted
			2.189, 2.194	1.219	164.9, 167.1	J-T distorted
			2.183, 2.194	1.219	165.7, 167.2	Backside
			2.471, 2.475	1.205	174.5, 174.8	On-top
			-	1.201	177.4, 177.7	Solvent
metallacycle	2.9	3003(3), 3011(2), 3038(1), 3050(0), 3163(422), 3236(159), 3269(109), 3306(38), 3331(26), 3368(1)	2.279, 2.307	1.210	172.5, 173.3	Core
			2.293, 2.314	1.211	172.9, 173.0	Core
			-	1.201	177.5, 177.9	Solvent
π-cyclobutadiene	2.9	3094(1), 3109(13), 3118(9), 3129(4), 3176(351), 3222(113), 3266(113), 3289(47), 3307(41), 3366(1)	2.199, 2.229	1.218	168.0, 170.6	Core
			2.111, 2.122	1.222	165.4, 166.9	Core
			-	1.201	177.1, 177.6	Solvent
π-benzene	2.8	3059(0), 3065(0), 3066(0), 3076(1), 3076(1), 3083(0), 3229(0), 3231(254), 3319(37), 3321(39)	2.216, 2.217	1.214	170.0, 170.0	Core
			2.216, 2.217	1.214	170.0, 170.0	Core

* Dissociation energies = D_e(Ni⁺(C₂H₂)_n – Ni⁺(C₂H₂)_{n-1} + C₂H₂) in kcal/mol.

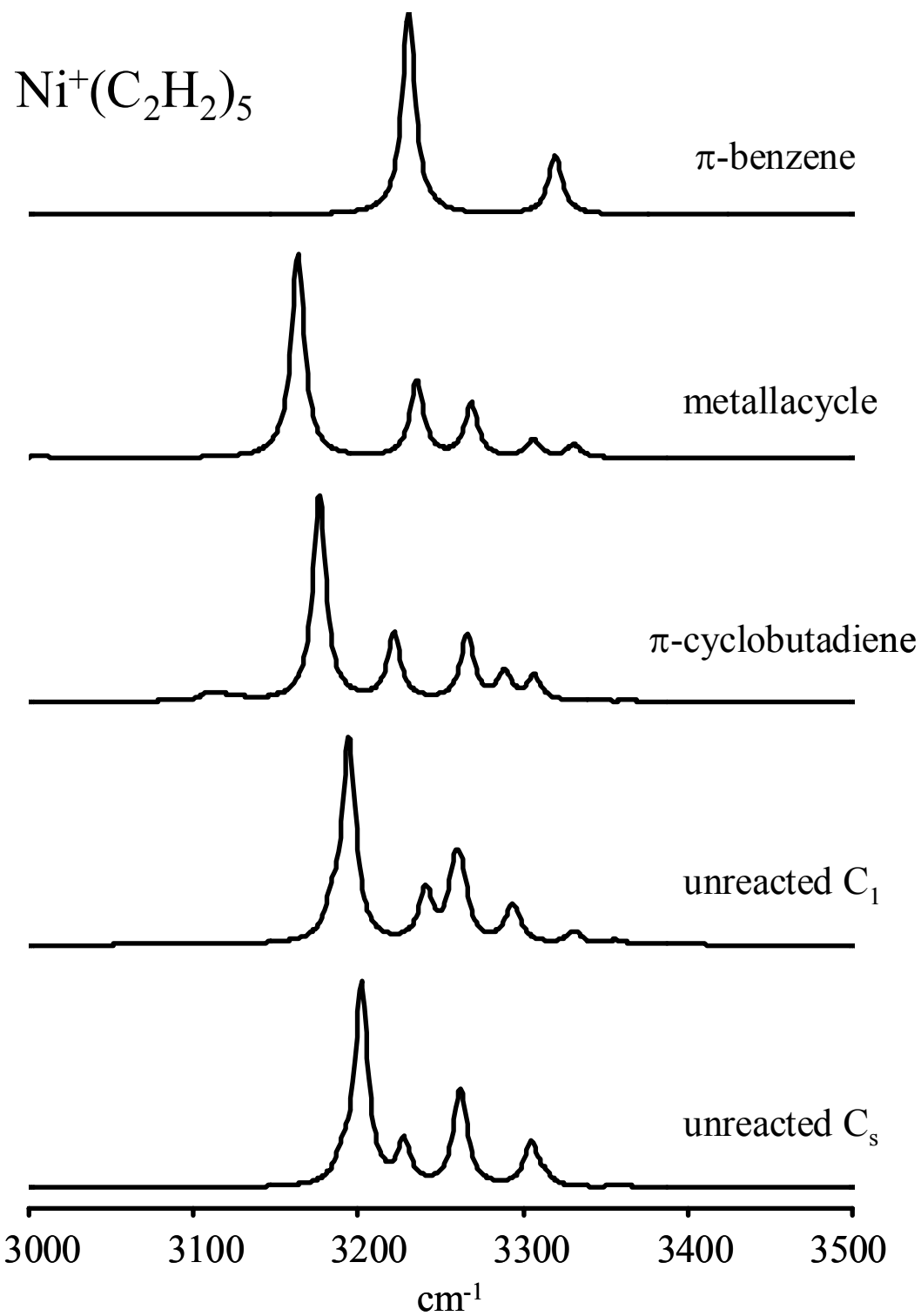
‡ Represents the acetylene-Ni+-acetylene angle of the Jahn-Teller distorted pair

[†] Harmonic frequencies scaled by 0.96. Intensities are in km/mol

solvent to an existing core acetylene. The calculations also find that the fifth molecule binds as a solvent acetylene to the unreacted $n = 4$ core complex. However, there are two structures for the $n = 5$ unreacted complex predicted by DFT. The solvent acetylene can occupy two different positions near the three planar core acetylenes. Because two of these core acetylenes are distorted, the binding sites are not equivalent and give rise to structures with different symmetries. The C_s symmetry structure is produced if the fifth acetylene binds to the distorted acetylene pair. The other two possible binding sites in this plane are degenerate and produce a structure whose symmetry is C_1 . They involve the interaction of the solvent molecule with the backside acetylene and one of the distorted acetylenes. Attempts to find a stable structure where the fifth acetylene attaches near the on-top acetylene in the $n = 4$ core complex were unsuccessful. The C_s symmetry structure was found to be more stable than the C_1 structure, but only by 0.1 kcal/mol. In all cases where the fifth acetylene binds in the second solvation layer, its π -electrons interact with at least one hydrogen in a core acetylene to form a ‘T-shaped’ configuration. This is consistent with the structures observed for pure acetylene clusters, which can adopt either the ‘T-shaped’ or the ‘slipped-parallel’ geometries.^{41,42} In the case of the unreacted $n = 5$ isomers, the solvent molecule interacts with two core acetylenes instead of one. The different structures (C_1 , C_s) for the $n = 5$ unreacted complex give rise to two slightly different infrared spectra as discussed below.

Figure 5.6 shows the infrared absorption spectra in the C-H region for all the $n = 5$ theoretical structures considered. The predicted spectra have been frequency scaled by 0.96 and plotted at a 10 cm^{-1} resolution to provide a better comparison to

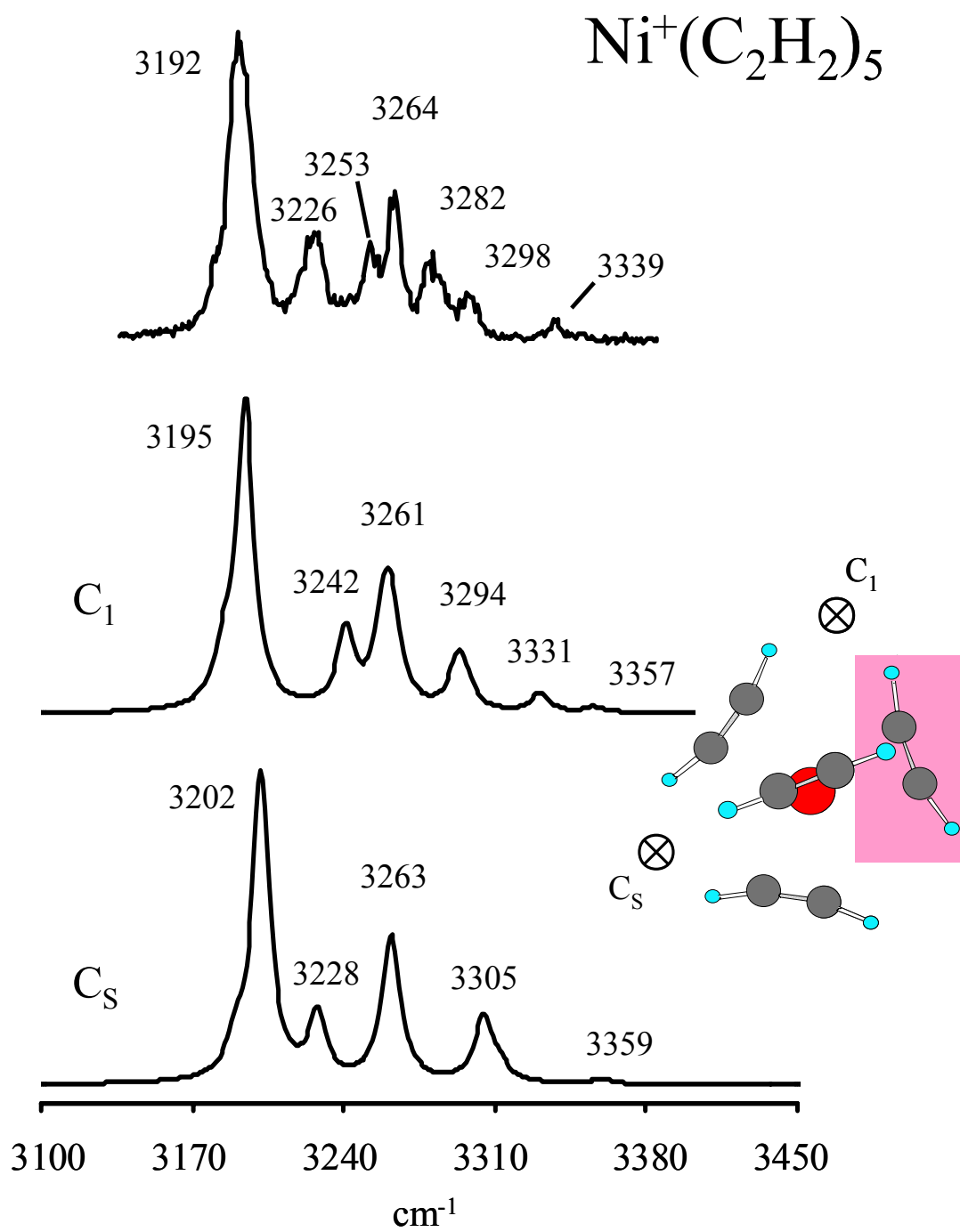
Figure 5.6 The theoretical spectra of the $n = 5$ isomeric structures calculated with B3LYP. Theoretical frequencies have been scaled by 0.96 and plotted at a 10 cm^{-1} resolution. Intensities have been scaled so that the most intense features are equal. The C-H vibrations of the product moieties are predicted to be weak.



the experiment. Intensities have been scaled so that the most intense features in each spectrum are equal. Like the $n = 4$ complexes, the C-H stretches for all of the product moieties, π -benzene, π -cyclobutadiene and the metallacycle, are predicted to be extremely weak. Because the reaction products contain intact acetylene ligands however, their infrared spectra have intense C-H bands in the region of the signals detected in the experiment. The π -benzene complex has two equivalent core acetylenes which give rise to the infrared bands at 3231 cm^{-1} and 3320 cm^{-1} in its spectrum. They correspond to asymmetric and symmetric acetylene C-H resonances, respectively. For the other complexes, one acetylene is bound as a solvent, resulting in multiple infrared active bands in the C-H region. All of the isomers, both reacted and unreacted species, have acetylene-like resonances near $3200\text{--}3350\text{ cm}^{-1}$, making absolute assignment of the IRPD spectrum of $\text{Ni}^+(\text{C}_2\text{H}_2)_5$ difficult at best.

Figure 5.7 compares the IRPD spectrum of the $\text{Ni}^+(\text{C}_2\text{H}_2)_5$ complex to the predicted IR absorption spectra of the unreacted isomers. As stated previously, the appearance of new intense features that are red-shifted from the $n = 4$ core modes in the spectra of the larger complexes are unexpected. Our previous work on $\text{M}^+(\text{CO}_2)_n$ complexes also observed new modes once the second solvation layer was reached, but these occurred near the vibration of free CO_2 .³⁴ For the $\text{Ni}^+(\text{C}_2\text{H}_2)_5$ complex however, the intense new feature at 3190 cm^{-1} is $\sim 100\text{ cm}^{-1}$ to the red of the asymmetric stretch of free acetylene. Because of this, we concluded that the 3190 cm^{-1} band in the $n = 5$ IRPD spectrum was likely a C-H stretch from an intracuster reaction product and not an acetylene vibration.³³ However, the current DFT results indicate that this may not be the case. Unlike solvation in the metal ion- CO_2

Figure 5.7 The IRPD spectrum of $\text{Ni}^+(\text{C}_2\text{H}_2)_5$ compared to the predicted spectra of two unreacted isomers calculated with B3LYP. The theoretical frequencies have been scaled by 0.96 and plotted at a 10 cm^{-1} resolution. All band labels represent the center of the peak positions. The theoretical structure of the $n = 4$ unreacted isomer is included and the marks represent the two possible binding sites for the solvent acetylene. The ligand highlighted in pink is the ‘backside’ core acetylene.



complexes, formation of the second layer in $\text{Ni}^+(\text{C}_2\text{H}_2)_n$ causes some of the core acetylene vibrations to shift away from their free values due to hydrogen bonding. It is worth mentioning that acetylene dimers and trimers also have vibrations that are shifted to lower energy than the free molecule because of hydrogen bonding.^{41,42} However, we did not consider that this would be an additive effect in the Ni^+ -(acetylene)_n clusters.³³ For example, we have recently studied $\text{Ni}^+(\text{H}_2\text{O})_n$ complexes with IRPD spectroscopy and it too shows red-shifted OH features due to hydrogen bonding.³⁶ However, the $\text{Ni}^+(\text{H}_2\text{O})_n$ modes occurred in the same region as hydrogen-bonded OH stretches in pure water clusters, and we expected to see something similar in the $\text{Ni}^+(\text{C}_2\text{H}_2)_n$ system. In this case, hydrogen atoms from core acetylenes vibrate into the π -bonding electron density of the solvent molecule. The electrostatic interaction with the electron cloud slows the hydrogen motions, lowering the frequencies of the core acetylenes' C-H stretches. The solvated core acetylenes, whose frequencies are already red-shifted due to the interaction with the metal cation, vibrate at even lower energy once solvated. Which two core acetylenes are affected depends on where the fifth acetylene binds to the $n = 4$ cluster. As shown in Figure 5.7, two unequivalent binding sites result in two different symmetry structures and, therefore, two different infrared spectra. If the fifth acetylene binds to the distorted pair (C_s structure), their in-phase and out-of-phase C-H stretches shift to lower energy producing the intense features predicted at 3202 cm^{-1} and 3263 cm^{-1} . The backside and on-top acetylenes are largely unperturbed and vibrate near their $n = 4$ frequencies. Conversely, if the fifth acetylene interacts with the backside ligand and one of the distorted acetylenes (C_1 symmetry), their vibrations are shifted to lower frequency

and account for the 3195 cm^{-1} and 3261 cm^{-1} predicted bands. The vibrations of the on-top acetylene and remaining Jahn-Teller distorted acetylene are largely unpreturbed.

The IR bands observed in the experimental spectrum of $\text{Ni}^+(\text{C}_2\text{H}_2)_5$ are not reproduced by either unreacted isomers when considered separately. The C_s theoretical spectrum is missing the IRPD asymmetric feature at 3253 cm^{-1} and is short one of the symmetric bands. Likewise, the C_1 theoretical spectrum is missing the 3226 cm^{-1} IRPD band and its three symmetric features are too widely spaced. The main point is that a single unreacted structure cannot account for the 3226 cm^{-1} and the 3253 cm^{-1} feature in the $n = 5$ experimental spectrum. However, if we consider that the C_s and C_1 structures are nearly isoenergetic, both isomers are likely present in the molecular beam and all the IRPD features can then be accurately reproduced. The most intense bands in the C_s and C_1 structures near 3200 cm^{-1} and 3262 cm^{-1} might overlap and account for the 3192 cm^{-1} and 3264 cm^{-1} intense signals in the experiment. The C_s asymmetric stretch at 3228 cm^{-1} and the C_1 asymmetric stretch at 3242 cm^{-1} match the experimental signals at 3226 cm^{-1} and 3253 cm^{-1} . Likewise, the number of symmetric modes is reproduced if both isomers are present. The spacing between the asymmetric and symmetric features are not correct, but this can be explained by anharmonicity as discussed above. If anharmonicity is greater for the symmetric stretches, then the theoretical bands in the symmetric region should actually occur further to the red and can account for the 3282 cm^{-1} , 3298 cm^{-1} and 3339 cm^{-1} bands observed in the experiment.

Because we did not find a single theoretical structure whose spectrum accurately reproduces the experiment, other isomeric structures including the reaction products cannot be completely ruled out. Intracuster reactions might still be possible for the Ni^+ -acetylene complexes as the products are found to be more stable. Such isomers might be present in the experiment and contribute to the IRPD spectrum of the $n = 5$ complex. For example, the theoretical spectrum for the π -cyclobutadiene complex in Figure 5.6 reproduces all of the experimental signals except the shoulder band at 3253 cm^{-1} . We could then invoke the presence of the C_1 unreacted structure to account for the missing mode and their remaining bands might overlap. However, the simplest interpretation is probably the correct one: the new features observed in the $n = 5$ spectrum are caused by the solvation of the $n = 4$ core complex. When a core acetylene interacts with the solvent acetylene, its vibrations are shifted to lower frequency. The low symmetry structure of the $n = 4$ cluster provides unequivalent binding sites for the fifth molecule, leading to two unreacted isomeric structures that are nearly isoenergetic. Both structures are likely present in the experiment which accounts for the complexity observed in the $\text{Ni}^+(\text{C}_2\text{H}_2)_5$ IRPD spectrum.

Using the insight gained from the DFT calculations on the $n = 5$ complex, an interpretation of the $\text{Ni}^+(\text{C}_2\text{H}_2)_6$ IRPD spectrum in Figure 5.1 can be made. The only major difference between the $n = 5$ and $n = 6$ spectra is the appearance of the new feature at 3170 cm^{-1} . All other $n = 5$ bands are reproduced in the spectrum of the $\text{Ni}^+(\text{C}_2\text{H}_2)_6$ complex with only minor changes in positions and intensities. The sixth acetylene likely binds to one of the two open sites near the planar core acetylenes in the $n = 5$ complex. Because there are only three planar sites, occupation of two of

these by solvent molecules means that one of the core ligands is interacting with both second sphere acetylenes (see the inset in Figure 5.7). An additional solvent interaction would produce an additional red-shift of this core acetylene's vibrations. Therefore, it is likely that the band measured at 3170 cm^{-1} in the $n = 6$ spectrum is the asymmetric stretch of the core acetylene that is 'caged' by both solvent molecules. The caged symmetric stretch should also be more perturbed and lie to the red of the 3264 cm^{-1} experimental band. It is likely that the small intensity increase in the 3254 cm^{-1} band is the symmetric stretch partner of the 3170 cm^{-1} signal, which overlaps with the 3252 cm^{-1} core mode. Like the $n = 5$ spectrum, assigning the IRPD spectrum of the $n = 6$ cluster cannot be made with absolute certainty.

Although DFT predicts that reaction products are substantially more stable than the unreacted species, the IRPD spectra of $\text{Ni}^+(\text{C}_2\text{H}_2)_{5,6}$ seem more consistent with the simple solvation of the $n = 4$ core complex. If this is true, it is likely that reaction barriers prevent acetylene condensation. However, due to congestion in the CH region and the weak CH stretches expected for the product species, condensation reactions cannot be completely ruled out. The spectroscopy of gas-phase organometallic clusters is similar to condensed phase measurements in that both are congested in the CH region. Acquiring the IRPD spectra of these complexes in the fingerprint region to observe their C=C stretches will provide more accurate information on their structures and additional insight on reaction products that might be present in the larger complexes. Future experiments using a free electron laser ($200 - 1800\text{ cm}^{-1}$) or an OPO laser equipped with a AgGaSe₂ crystal ($600 - 1800\text{ cm}^{-1}$) should detect these signals and hopefully resolve these issues.

Conclusions

Nickel cation-acetylene complexes, $\text{Ni}^+(\text{C}_2\text{H}_2)_{4-6}$, are studied with infrared photodissociation spectroscopy and density functional theory. Theory finds that reaction products containing π -benzene, π -cyclobutadiene and a metallacycle cluster are more stable structures than the unreacted $n = 4$ complex. However, the IRPD spectrum of $\text{Ni}^+(\text{C}_2\text{H}_2)_4$ is consistent with a structure where all four acetylenes remain intact. The match between experiment and theory suggests that this cluster is a Jahn-Teller distorted π -complex. New intense features are observed beginning with the $n = 5$ complex and attributed to the formation of the second solvation layer. The spectra of $\text{Ni}^+(\text{C}_2\text{H}_2)_5$ and $\text{Ni}^+(\text{C}_2\text{H}_2)_6$ can be explained if the fifth and sixth acetylene ligands attach as solvent molecules to the $n = 4$ core complex. The presence of solvent acetylene molecules induce additional red-shifts of the core acetylene vibrations due to hydrogen bonding. A single unreacted structure cannot account for all the modes in the $n = 5, 6$ complexes, indicating isomers are present in the molecular beam. Although there is no need to invoke intracuster reactions to explained the experimental details, reaction products cannot be completely ruled out. B3LYP predicts that the CH vibrations of the products are relatively weak and might be undetected at our sensitivity. Future experiments using IR lasers that cover the C=C stretch region should prove whether intracuster chemistry is possible for this gas phase organometallic system.

References

- (1) Heck, R. F. *Organotransition Metal Chemistry*; Academic Press: New York, 1974.
- (2) Jolly, P. W.; Wilke, G. *The Organic Chemistry of Nickel*; John Wiley: New York, 1974.
- (3) a) Sodupe, M.; Bauschlicher, C. W. Jr. *J. Phys. Chem.* **1991**, *95*, 8640. b) Sodupe, M.; Bauschlicher, C. W. Jr.; Langhoff, S. R.; Partridge, H. *J. Phys. Chem.* **1992**, *96*, 2118.
- (4) a) Hertwig, R. H.; Koch, W.; Schroeder, D.; Schwarz, H.; Hrusak, J.; Schwerdtfeger, P. *J. Phys. Chem.* **1996**, *100*, 12253. b) Holthausen, M. C.; Fiedler, A.; Schwarz, H.; Koch, W. *J. Phys. Chem.* **1996**, *100*, 6236.
- (5) a) Frenking, G.; Frohlich, N. *Chem. Rev.* **2000**, *100*, 717. b) Nechaev, M. S.; Rayon, V. M.; Frenking, G. *J. Phys. Chem. A.* **2004**, *108*, 3134.
- (6) Klippenstein, S. J.; Yang, C.-N. *Int. J. Mass Spectrom.* **2000**, *201*, 253.
- (7) Straub, B. F.; Gollub, C. *Chem. Eur. J.* **2004**, *10*, 3081.
- (8) a) Eller, K.; Schwarz, H. *Chem. Rev.* **1991**, *91*, 1121. b) Wesendrup, R.; Schwarz, H. *Organometallics* **1997**, *16*, 461. c) Harvey, J. N.; Diefenbach, M.; Schroder, D.; Schwarz, H. *Int. J. Mass Spectrom.* **1999**, *182*, 85.
- (9) a) Freiser, B. S., ed., *Organometallic Ion Chemistry*; Kluwer: Dordrecht, The Netherlands, 1996. b) Ranatunga, D. R. A.; Freiser, B. S. *Chem. Phys. Lett.* **1995**, *233*, 319. c) Chen, Q.; Auberry, K. J.; Freiser, B. S. *Int. J. Mass Spectrom. Ion Proc.* **1998**, *175*, 1.

- (10) a) Metz, R. B.; *Int. Rev. Chem.* **2004**, 23, 79. b) Aguirre, F.; Husband, J.; Thompson, C. J.; Metz, R. B. *Chem. Phys. Lett.* **2000**, 318, 466. c) Husband, J.; Aguirre, F.; Thompson, C. J.; Laperle, C. M.; Metz, R. B. *J. Phys. Chem. A.* **2000**, 104, 2020.
- (11) Gibson, J. K. *J. Organomet. Chem.* **1998**, 558, 51.
- (12) a) Armentrout, P. B.; Beauchamp, J. L. *J. Am. Chem. Soc.* **1981**, 103, 784. b) Elkind, J. L.; Armentrout, P. B. *J. Am. Chem. Soc.* **1986**, 108, 2765. c) van Koppen, P. A. M.; Bowers, M. T.; Haynes, C. L.; Armentrout, P. B. *J. Am. Chem. Soc.* **1998**, 120, 5704.
- (13) Tonkyn, R.; Ronan, M.; Weisshaar, J.C. *J. Phys. Chem.* **1988**, 92, 92.
- (14) a) Koppen, P. A. M.; Kemper, P. R.; Bushnell, J. E.; Bowers, M. T. *J. Am. Chem. Soc.* **1995**, 117, 2098. b) Koppen, P. A. M.; Perry, J. K.; Kemper, P. R.; Bushnell, J. E.; Bowers, M. T. *Int. J. Mass Spectrom.* **1999**, 185, 989.
- (15) a) Manard, M. J.; Kemper, P. R.; Carpenter, C. J.; Bowers, M. T. *Int. J. Mass Spectrom.* **2005**, 241, 99. b) Manard, M. J.; Kemper, P. R.; Bowers, M. T. *Int. J. Mass Spectrom.* **2005**, 241, 109.
- (16) a) Aristov, N.; Armentrout, P. B. *J. Am. Chem. Soc.* **1986**, 108, 1806. b) Georgiadis, R.; Armentrout, P. B. *Int. J. Mass Spectrom. Ion Proc.* **1989**, 89, 227. c) Fisher, E. R.; Armentrout, P. B. *J. Phys. Chem.* **1990**, 94, 1674. d) Meyer, F.; Khan, F. A.; Armentrout, P. B. *J. Am. Chem. Soc.* **1995**, 117, 9740. e) Sievers, M. R.; Jarvis, L. M.; Armentrout, P. B. *J. Am. Chem. Soc.* **1998**, 120, 1891. f) Sievers, M. R.; Chen, Y.-M.; Haynes, C. L.; Armentrout, P. B. *Int. J. Mass Spectrom.* **2000**, 195, 149.

- (17) a) France, M. R.; Pullins, S. H.; Duncan, M. A. *J. Chem. Phys.* **1998**, *109*, 8842. b) Reddic, J. E.; Duncan, M.A. *Chem. Phys. Lett.* **1999**, *312*, 96. c) Weslowski, S. S.; King, R. A.; Schaefer, H. F.; Duncan, M. A. *J. Chem. Phys.* **2000**, *113*, 701.
- (18) a) Kleiber, P. D. in *Adv. Metal Semicond. Clusters*, **2001**, *5*, 267. b) Lu, W.-Y.; Liu, R.-G.; Wong, T.-H.; Chen, J.; Kleiber, P. D. *J. Phys. Chem. A.* **2002**, *106*, 725.
- (19) Nakamoto, K. *Infrared and Raman Spectra of Inorganic and Coordinated Compounds*, 5th ed.; John Wiley: New York, 1997; Vols. A&B.
- (20) a) Chatt, J.; Rowe, G. A.; Williams, A. A. *Proc. Chem. Soc.* **1957**, 208. b) Chatt, J.; Duncanson, L. A.; Guy, R. G. *J. Chem. Soc.* **1961**, 827. c) Chatt, J.; Duncanson, L. A.; Guy, R. G.; Thompson, D. T. *J. Chem. Soc.* **1963**, 5170.
- (21) Greaves, E. O.; Lock, C. J. L.; Maitlis, P. M. *Can. J. Chem.* **1968**, *46*, 3879.
- (22) a) Colborn, R. E.; Vollhardt, K. P. C. *J. Am. Chem. Soc.* **1986**, *108*, 5470. b) Colborn, R. E.; Vollhardt, K. P. C. *J. Am. Chem. Soc.* **1981**, *103*, 6259.
- (23) Ozin, G. A.; McIntosh, D. F.; Power, W. J.; Messmer, R.P. *Inorg. Chem.* **1981**, *20*, 1782.
- (24) Kline, E. S.; Kafafi, Z. H.; Hauge, R. H.; Margrave, J. L. *J. Am. Chem. Soc.* **1987**, *109*, 2402.
- (25) a) Manceron, L.; Andrews, L. *J. Phys. Chem.* **1989**, *93*, 2964. b) Burkholder, T. R.; Andrews, L. *Inorg. Chem.* **1993**, *32*, 2491. c) Thompson, C. A.; Andrews, L. *J. Am. Chem. Soc.* **1996**, *118*, 10242.

- (26) a) Cabarcos, O. M.; Weinheimer, C. J.; Lisy, J. M. *J. Chem. Phys.* **1999**, *110*, 8429. b) Cabarcos, O. M.; Weinheimer, C.J.; Lisy, J. M. *J. Chem. Phys.* **1998**, *108*, 5151. c) Lisy, J. M. *Int. Rev. Phys. Chem.* **1997**, *16*, 267. d) Weinheimer, C. J.; Lisy, J. M. *J. Chem. Phys.* **1996**, *105*, 2938. e) Lisy, J. M. *Cluster Ions* **1993**, 217. f) Vaden, T. D.; Forinash, B.; Lisy, J. M. *J. Chem. Phys.* **2002**, *117*, 46284631. g) Vaden, T. D.; Weinheimer, C. J.; Lisy, J. M. *J. Chem. Phys.* **2004**, *121*, 3102. k) Patwari, G. N.; Lisy, J. M. *J. Chem. Phys.* **2003**, *118*, 8555.
- (27) a) Inokuchi, Y.; Ohshimo, K.; Misaizu, F.; Nishi, N. *J. Phys. Chem. A* **2004**, *108*, 5034. b) Inokuchi, Y.; Ohshimo, K.; Misaizu, F.; Nishi, N. *Chem. Phys. Lett.* **2004**, *390*, 140.
- (28) Simon, A.; Jones, W.; Ortega, J.-M.; Boissel, P.; Lemaire, J.; Maitre, P. *J. Am. Chem. Soc.* **2004**, *126*, 11666.
- (29) Jaeger, T. D.; van Heijnsbergen, D.; Klippenstein, S. J.; von Helden, G.; Meijer, G.; Duncan, M. A. *J. Am. Chem. Soc.* **2004**, *126*, 10981.
- (30) Jaeger, T.D.; Pillai, E.D.; Duncan, M.A. *J. Phys. Chem. A* **2004**, *108*, 6605.
- (31) Walters, R. S.; Schleyer, P. v. R.; Corminboeuf, C.; Duncan, M. A. *J. Am. Chem. Soc.* **2005**, *127*, 1100.
- (32) Walters, R. S.; Pillai, E. D.; Schleyer, P.v.R.; Duncan, M. A. *J. Am. Chem. Soc.* to be submitted.
- (33) Walters, R. S.; Jaeger, T. D.; Duncan, M. A. *J. Phys. Chem. A* **2002**, *106*, 10482.
- (34) Duncan, M. A. *Int. Rev. Phys. Chem.* **2003**, *22*, 407.

- (35) a) Walker, N. R.; Greives, G. A.; Walters, R. S.; Duncan, M. A. *Chem. Phys. Lett.* **2003**, *380*, 230. b) Walker, N. R.; Walters, R. S.; Greives, G. A.; Duncan, M. A. *J. Chem. Phys.* **2004**, *121*, 10498.
- (36) Walters, R. S.; Pillai, E. D.; Duncan, M. A. *J. Am. Chem. Soc.*, to be submitted.
- (37) Shimanouchi, T. *Molecular Vibrational Frequencies*; 69th ed.; Chemistry WebBook, NIST Standard Reference Database (<http://webbook.nist.gov>), 2001
- (38) a) Becke, A. D. *J. Chem. Phys.* **1993**, *98*, 5648. b) Lee, C.; Yang, W.; Parr, R. G. *Phys. Rev. B* **1988**, *37*, 785.
- (39) Frisch, M. J.; Trucks, G. W.; . Schlegel, H. B.; Scuseria, G. E.; Robb, M. A.; Cheeseman, J. R.; Montgomery, J. A. Jr.; Vreven, T.; Kudin, K. N.; Burant, J. C.; Millam, J. M.; Iyengar, S. S.; Tomasi, J.; Barone, V.; Mennucci, B.; Cossi, M.; Scalmani, G.; Rega, N.; Petersson, G. A.; Nakatsuji, H. Hada, M.; Ehara, M.; Toyota, K.; Fukuda, R.; Hasegawa, J.; Ishida, M.; Nakajima, T.; Honda, Y.; Kitao, O.; Nakai, H.; Klene, M.; Li, X.; Knox, J. E.; Hratchian, H. P.; Cross, J. B.; Adamo, C.; Jaramillo, J.; Gomperts, R.; Stratmann, R. E.; Yazyev, O.; Austin, A. J.; Cammi, R.; Pomelli, C.; Ochterski, J. W.; Ayala, P. Y.; Morokuma, K.; Voth, G. A.; Salvador, P.; Dannenberg, J. J.; Zakrzewski, V. G.; Dapprich, S.; Daniels, A. D.; Strain, M. C.; Farkas, O.; Malick, D. K.; Rabuck, A. D.; Raghavachari, K.; Foresman, J. B.; Ortiz, J. V.; Cui, Q.; Baboul, A. G.; Clifford, S.; Cioslowski, J.; Stefanov, B. B.; Liu, G.; Liashenko, A.; Piskorz, P.; Komaromi, I.; Martin, R. L.; Fox, D. J.; Keith, T.;

- Al-Laham, M. A.; Peng, C. Y.; Nanayakkara, A.; Challacombe, M.; Gill, P. M. W.; Johnson, B.; Chen, W.; Wong, M. W.; Gonzalez, C.; Pople, J. A. Gaussian 03 (Revision B.02); Gaussian, Inc.: Pittsburgh, PA, 2003.
- (40) Scott, A. P.; Radom, L. *J. Phys. Chem.* **1996**, *100*, 16502.
- (41) Alberts, I. L.; Rowlands, T. W.; Handy, N. C. *J. Chem. Phys.* **1988**, *88*, 3811.
- (42) a) Fischer, G.; Miller, R. E.; Vohralik, P. F.; Watts, R. O. *J. Chem. Phys.* **1985**, *83*, 1471. b) Miller, R. E.; Vohralik, P. F.; Watts, R. O. *J. Chem. Phys.* **1984**, *80*, 5453.
- (43) Somorjai, G. A. *Introduction to Surface Chemistry and Catalysis*; John Wiley: New York, 1994.
- (44) Weiss, M. J.; Hagedorn, C. J.; Weinberg, W. H. *J. Vac. Sci. Technol.* **2000**, *18*, 1443.
- (45) Teplyakov, A. V.; Kong, M. J.; Bent, S. F. *J. Chem. Phys.* **1998**, *108*, 4599.
- (46) Maitlis, P. M. Cyclobutadiene-Metal Complexes. In *Advances in Organometallic Chemistry*; Stone, F. G. A.; West, R., Eds.; Academic Press: New York, 1966; Vol. 4, p. 95.
- (47) Efraty, A. *Chem. Rev.* **1977**, *77*, 691.
- (48) Andrews, D. C.; Davidson, G. *J. Organomet. Chem.* **1972**, *36*, 349.
- (49) Longuet-Higgins, H. C.; Orgel, L. E. *J. Chem. Soc. London* **1956**, 1969.
- (50) Buehler, R.; Geist, R.; Meundnich, R.; Pleininger, H. *Tetrahedron Lett.* **1973**, 1919.

CHAPTER VI

CONCLUSIONS

Nickel cation-water and -acetylene complexes, $\text{Ni}^+(\text{H}_2\text{O})_n$ and $\text{Ni}^+(\text{C}_2\text{H}_2)_n$, are generated in a laser vaporization pulsed-nozzle cluster source and investigated with infrared photodissociation spectroscopy and Density Functional Theory. The combined experiments and theoretical studies have provided significant insight into the nature of the nickel ion-ligand interactions. In some cases, structural geometries of the smaller complexes have been determined as well as gas phase coordination numbers. Also, the ability to size-select these ion-molecule complexes has allowed their solvation dynamics to be examined from a ‘bottoms-up’ approach. Vibrational spectroscopy of these prototypical systems has revealed information vital to our understanding of metal ion- π bonding and metal ion solvation.

Infrared photodissociation spectroscopy of the hydrated nickel ions, $\text{Ni}^+(\text{H}_2\text{O})_n$, presented here is the first of its kind, providing detailed information on how the nickel cation perturbs the structure of the water moieties. Comparison of the IRPD spectrum of $\text{Ni}^+(\text{H}_2\text{O})\text{Ar}_2$ to theoretical results confirms that bonding electron density is polarized toward the Ni^+ , causing the water ligand’s OH stretches to shift to lower energy. Inconsistent with earlier experiments, the onset of hydrogen-bonding was observed to occur at $n = 4$, indicating that isomers are present for this cluster size. The IR spectra simplify in the OH region by $n = 7$ and are attributed to

formation of complex hydrogen-bonding networks. This result is somewhat surprising as the symmetric and asymmetric OH stretches are observed for the neutral water and protonated water clusters up to $n = 10$. However, this maybe somewhat misleading due to the vibrational overlap near 3700 cm^{-1} in the hydrated nickel ions. The IRPD spectra of the larger complexes reveal that dodecahedron structures are not formed for the $\text{Ni}^+(\text{H}_2\text{O})_n$ complexes. Apparently, the symmetric clustering of water is prevented by the presence of the nickel cation. AD/AAD line spacings suggest that the nickel ion continues to influence the hydrogen-bonding network even at the largest cluster size studied ($n = 30$).

The first vibrational spectroscopy of gas phase nickel cation-acetylene complexes, $\text{Ni}^+(\text{C}_2\text{H}_2)_n$, is reported in the C-H region. IR bands are observed at lower frequency than the free acetylene modes for all cluster sizes, consistent with the Dewar-Chatt-Duncanson π -bonding model. The IRPD spectra of the smaller complexes ($n = 1-3$) are acquired with the aid of the rare gas tagging technique. A comparison of their spectra to theoretical results reveal that the $n > 2$ complexes are Jahn-Teller distorted. According to the fragmentation patterns of the larger complexes and the match between theory and experiment, the $n = 4$ complex is determined to have all four acetylenes π -bonded directly to the nickel cation, which completes its coordination. New features appear beginning with the $n = 5$ complex and attributed to formation of the second solvent layer. Multiple reaction products are investigated with theory for the $n = 4$ and $n = 5$ complexes and found to be significantly more stable than the unreacted species. However, the vibrational spectra are more consistent with the simple solvation of the $n = 4$ unreacted core complex,

but only if more than one isomeric structure is contributing to the $\text{Ni}^+(\text{C}_2\text{H}_2)_5$ IRPD spectrum. Because isomers are likely present in the ion distribution, intracuster reactions cannot be completely ruled out as the spectra of the larger complexes are congested in the C-H region.

The laser vaporization, pulsed-nozzle cluster source coupled with a tunable, high-powered, pulsed infrared laser has proven to be a powerful technique to study novel gas phase metal-ion complexes in their ground electronic states. Furthermore, it has opened the door to examine a variety of materials and substances including, but not limited to, semiconductor and carbon clusters, pure molecular clusters, molecules adsorbed onto clusters of pure metals and metal aggregates, as well as multiple ligand species like the ones presented here. New advances in infrared laser technology, such as difference frequency mixing in AgGaSe_2 crystals, continue to push the envelope and now provide tunable infrared light in the fingerprint region ($600 - 1800 \text{ cm}^{-1}$) from a benchtop laser system. Future experiments utilizing this new light source will provide more detailed information at the metal-molecule interface and hopefully answer the questions that remain in these prototypical metal ion-molecular systems.